MICROSPORIDIAN DIVERSITY OF THE PACIFIC NORTHWEST: MICROSPORIDIOSIS IN A MARINE NEMATODE

by

ALEX MAURICIO ARDILA GARCIA

B. Sc., The University of Guelph, 2006
M. Sc., The University of Guelph, 2008

A THESIS SUBMITTED IN PARTIAL FULFILLMENT OF

THE REQUIREMENTS FOR THE DEGREE OF

DOCTOR OF PHILOSOPHY

in

THE FACULTY OF GRADUATE AND POSTDOCTORAL STUDIES

(Botany)

THE UNIVERSITY OF BRITISH COLUMBIA

(Vancouver)

July 2015

Abstract

Microsporidia are a diverse group of spore-forming obligate endoparasitic fungi that have over 1,300 named species. Microsporidian spores are ubiquitous in the environment, but species diversity remains vastly unexplored, as the total number of species is suspected to equal that of their hosts. Microsporidian parasites are also model organisms for the study of genome reduction since they possess some of the smallest eukaryotic genomes known to date.

To examine the diversity of microsporidian parasites in the environment, I screened for the presence of microsporidian parasites in poorly sampled reservoirs: soil, sand, and compost. I amplified ribosomal DNA (rDNA) sequences for 23 undescribed and three described microsporidian species that were highly diverse phylogenetically, including representatives from four of the five major microsporidian clades. Molecular screening for the hosts revealed that one undescribed microsporidian infected a free-living marine nematode (*Odontophora rectangula*). I characterized the infection and ultrastructure of the parasite by transmission electron microscopy and fluorescent *in situ* hybridization. It is a novel microsporidian that I named *Sporanauta perivermis* ("marine spore of roundworms"). *S. perivermis* infects the hypodermal, muscle, and reproductive tissues of adult *O. rectangula*. However, the infection pattern differed between genders where only reproductive tissues were infected in adult females (uteri and eggs), suggesting that *S. perivermis* is transmitted vertically. Juvenile hosts showed similar infection patterns to adults, and infection pattern allowed prediction of host gender prior to adulthood.

Phylogenetic analyses revealed that *S. perivermis* is sister to a clade containing the *Daphnia*-infecting microsporidian *Ordospora colligata* and the *Encephalitozoon* lineage (five species), which contains three species that infect humans. A genomic survey of *S. perivermis* indicated high levels of similarity in gene content (over 90%), gene length, and synteny between *S. perivermis, O. colligata* and *Encephalitozoon*. *S. perivermis* and *O. colligata* shared chromosomal arrangements that were not present in *Encephalitozoon* genomes, including chromosomal rearrangements that could be linked to genome reduction mechanisms. The genome size of *S. perivermis* is at least 2.2 Mbp, but is likely larger since its intergenic regions were longer, on average, than those of relatives with genome sizes of 2.3-3.0 Mbp.

Preface

A version of Chapter 2 has been published. Ardila-Garcia, A.M., Raghuram, N., Sihota, P., and Fast, N.M. 2013. Microsporidian diversity in soil, sand, and compost of the Pacific Northwest. J Eukaryot Microbio. 60(6):601-8. doi: 10.1111/jeu.12066. NMF and I designed this project. I selected the sampling sites, collected all samples, performed the DNA extractions, screened the samples for microsporidia using microsporidian-specific primers, and performed the phylogenetic analysis. NR and PS assisted in the collection of samples and DNA extractions. NMF and I analyzed the data and I wrote the first draft of the manuscript. NMF and I edited the final version of the published manuscript.

A version of Chapter 3 has been published. Ardila-Garcia, A.M. and Fast, N.M. 2012. Microsporidian infection in a free-living marine nematode. Eukaryot Cell. 11-12: 1544-1551. doi:10.1128/EC.00300-12. NMF and I designed this project. I collected the sand and nematode samples, screened the infection in the nematodes using microscopy and molecular techniques, conducted the DNA extractions, performed transmission electron microscopy and fluorescent *in situ* hybridization, and imaged the samples using an electron microscope and a confocal microscope. NMF and I analyzed the data and named the species. I wrote the first draft of the manuscript. NMF and I edited the final version of the published manuscript.

Chapter 4 is a version of a manuscript in preparation. Ardila-Garcia, A.M. and Fast, N.M. (in preparation). *Sporanauta perivermis* infection in juvenile *Odontophora rectangula*. NMF and I designed this project. I collected the sand and nematode samples based on their morphology,

screened the infection in the nematodes using microscopy and molecular techniques, conducted the DNA extractions, performed fluorescent *in situ* hybridization, and imaged the samples using a confocal microscope. NMF and I analyzed the data. I wrote the first draft and NMF and I are currently editing the manuscript.

Chapter 5 is a version of a manuscript in preparation. Ardila-Garcia, A.M. and Fast, N.M. (in preparation). Phylogenetic position and genomic survey of the microsporidian *Sporanauta perivermis*. NMF and I designed this project. I collected the sand and nematode samples, screened the infection in the nematodes using microscopy and molecular techniques, conducted the DNA extractions, prepared the Illumina sequencing library, assembled the contigs, performed BLAST to filter the microsporidian contigs, annotated the open reading frames, predicted the identity of the sequences by BLAST, and conducted the phylogenetic analyses. NMF and I analyzed the data. I wrote the first draft and NMF and I are currently editing the manuscript.

Table of Contents

List of Tables

List of Figures

Acknowledgements

I am forever thankful to Dr. Naomi Fast, my supervisor, for giving me the opportunity to conduct research in her lab, for her time, guidance and support through my PhD research, for always maintaining a positive attitude, and for showing me that successful researchers in academia can also have a balanced and healthy life style. I would like to thank my committee members, Dr. Brian Leander, Dr. Patrick Keeling, and Dr. Keith Adams for their time, guidance, and feedback during my PhD. I would like to extend my gratitude to Dr. Martin Adamson for introducing me to the world of nematology.

I am grateful to all members of the Fast lab for creating a perfect atmosphere to conduct research, help each other, and have interesting research-related and off-topic related conversations: Renny Lee, Dr. Cameron Grisdale, Dr. Erin Gill, Donald Wong, and Thomas Whelan. Also, I would like to thank the members of the Adams Lab, Graham lab, Keeling Lab, Leander lab, Moerman lab, and Suttle lab for their help in various aspects of my research projects. I thank Dr. Naoji Yubuki, Dr. Kevin Wakeman, and the UBC Bioimaging faciltity for their help with microscopy. I would like to thank Dr. Jean-François Pombert for introducing me bioinformatics.

I am most thankful to all members of my family, my parents and my siblings, for their love, encouragement, and support to pursue this endeavor. I would like to extend my gratitude to my aunt Rosita, my uncle Jens, my cousin David, and all my friends, especially Alejandra Herrera.

Dedicado a mis hermanos Felipe, Andrea, Maria Lucia, e Isabella

Chapter 1: Introduction

1.1 The Microsporidia

Microsporidia are a group of spore-forming unicellular fungi that are obligate endoparasites of animals and a small number of protists. The first formal description of a microsporidian parasite was in 1857 with the characterization of *Nosema bombycis* as the pathogen responsible for the 19th century's pébrine disease epidemic in the silkworm industry (Nägeli 1857; Corradi and Keeling 2009). Since then, 1,300-1,500 microsporidian species have been named (Vávra and Lukeš 2013), but this number represents a small fraction of their overall diversity (Stentiford *et al.* 2013).

1.1.1 Microsporidian morphology

Morphologically, microsporidian spores are small (2-40 μm), oval in shape (usually), and highly refractive when observed under the light microscope. They possess a thick chitinous wall composed of two layers (exospore and endospore) that cover the external portion of the plasma membrane (Vávra and Larsson 1999). The sporoplasm contains one or two nuclei, a vacuole at the posterior end, and highly reduced mitochondria (mitosomes) (Williams *et al*. 2008). Their diagnostic morphocharacter is a structure known as the polar filament, which is the infection apparatus (Vávra and Larsson 1999). The polar filament is a long hollow tube that is coiled at the posterior end of the spore (Xu and Weiss 2005; Delbac and Polonais 2008). The number of coils is highly variable between species and may also vary within species. The polar filament extends to the spore's anterior where it attaches to the plasma membrane. The attachment site is characterized as forming a bell-shaped structure (the anchoring disk) that is surrounded by the

lamellar polaroplast (Xu and Weiss 2005; Delbac and Polonais 2008). Microsporidian parasites are diagnosed based on the morphology of their spores since their intracellular stages (meronts) are nondescript (Wittner and Weiss 1999). Meronts are usually round, granular cells surrounded by a plasma membrane and lacking most morphocharacters found in the spore, such as the polar filament (Wittner and Weiss 1999).

1.1.2 Microsporidian life cycle

The microsporidian life cycle may be divided into two life stages: an extracellular infective stage (sporal) and an obligate intracellular proliferative stage (merogonial) (Wittner and Weiss 1999). In their extracellular stage, microsporidian spores have a resilient wall (see above) that allows them to survive in the environment for extended periods of time (months or even years). They remain "dormant" in the environment awaiting a suitable host to infect with their versatile infection apparatus, the polar filament (Keohane and Weiss 1998).

The polar filament is used as a harpoon that contacts the host, to attach and penetrate its tissues (Xu and Weiss 2005; Delbac and Polonais 2008). During this process, the polar filament evaginates as it rapidly exits the spore through the anchoring disk, which serves to anchor the proximal end of the polar filament to the spore (Xu and Weiss 2005; Delbac and Polonais 2008). If the distal end of the polar filament is successful in attaching to and penetrating the host's tissues, the polar filament becomes a "tube" through which the spore's contents (sporoplasm) travel to be subsequently deposited into the host's tissues (Witter and Weiss 1999; Keeling and Fast 2002; Franzen 2004). Once inside the host, the sporoplasm differentiates into meronts (merogony) that proliferate and differentiate into spores (sporogony). Spores may then infect

adjacent tissues to repeat the cycle inside the host, or they may be released in the environment to start the cycle once more.

It is important to note that merogony and sporogony can vary considerably between species. One key distinction is that these processes may occur in direct or indirect contact with the host. In direct contact, microsporidian parasites are not isolated from the host cytoplasm and they frequently gather the host's mitochondria around them and "steal" ATP (Scanlon et al. 2004; Rönnebäumer et al. 2008). Conversely, in indirect contact, microsporidian parasites are enclosed within a membrane-bound envelope that isolates them from the host cell contents. The envelope may be formed by the microsporidian, by the host (parasitophorous vacuole), or from contributions from both (Cali and Takvorian 1999). Remarkably, the presence of a "barrier" does not necessarily stop microsporidia from parasitizing the host's energy resources. A small number of microsporidian species (i.e. *E. cuniculi*) complete their entire life cycle inside a parasitophorous vacuole (Larsson et al. 1997; Schottelius et al. 2000; Bohne, et al. 2011), whereas multiple microsporidian species have both direct and indirect interactions during their life cycle (Cali and Takvorian 1999).

1.1.3 Microsporidian transmission: horizontal vs vertical

Microsporidian parasites may be transmitted horizontally or vertically, depending on the species (Didier and Bessinger 1999; Dunn and Smith 2001). Horizontal transmission is thought to be the most common, while vertical transmission is considered rare, and has only been reported in a small number of lineages (e. g. *Amblyospora* spp. and *Nosema plodiae*).

Horizontal transmission usually begins by accidental contact, ingestion, or inhalation of microsporidian spores by the host. Oral ingestion is the most common route of entry and it is generally followed by infection of the host's digestive system (Didier and Bessinger 1999; Dunn and Smith 2001). Infection is often constrained within the digestive tissues, but secondary infection of other tissue types can occur depending on the pathogenicity of the microsporidian involved and the host's immune response. Infections may be acute or chronic, and the effects on the host can vary considerably from mild to severe, and even lethal (Didier and Bessinger 1999). Acute infections often cause extreme enlargement of infected tissues (hypertrophism) due to large accumulation of microsporidian spores, while chronic infections tend to lack this feature since they usually cause minor damage to the host. An extreme example of an acute intestinal microsporidian infection was reported for *Nematocida parisii* ("nematode killer") infecting *Caenorhabditis elegans* lab strains (Troemel et al. 2008). *N. parisii* infects intestinal cells, after accidental ingestion of spores by the nematodes, which become filled with *N. parisii* spores (Troemel et al. 2008). Then, *N. parisii* spores exit the nematodes through the digestive tract until the nematodes perish (100% lethal) due to the severity of the infection (Troemel et al. 2008).

Vertical transmission differs from horizontal transmission in that the microsporidians are directly transmitted from one generation to the next (from mother to offspring) (Dunn and Smith 2001). Since microsporidian parasites are usually host-specific, vertical transmission could facilitate, in theory, the uninterrupted continuation of the microsporidian life cycle in perpetuity. In this process, female hosts (usually animals) play a vital role while male contributions are nearly nil. Vertically transmitted microsporidia may reduce the number of males in the host population by being more virulent to males than females (Dunn and Smith 2001). This results in a larger

proportion of females in the population, hence increasing the probability for successful transmission of the microsporidian between generations (Dunn and Smith 2001). A number of microsporidians, however, have evolved mechanisms to exploit males by converting them into females. “Feminizing” microsporidia, such as *Nosema granulosis*, reverse genetic males into reproductively viable females by altering the endocrine system of juveniles before they become adults (Rodgers-Gray et al. 2004; Jahnke et al. 2013).

Transmission from the mother to the offspring can be transovarial or transovum (Becnel and Andreadis 1999). Transovarial transmission is the most common, especially in invertebrates (Dunn and Smith 2001), and it consists of infection of the ovaries and associated reproductive tissues before infection of the eggs. Infection of the eggs usually takes place before fertilization and formation of the zygote (Dunn and Smith 2001). Transovum transmission occurs when microsporidian spores contaminate the surface of the egg, and the offspring become infected during eclosion (Becnel and Andreadis 1999). In vertebrates, vertical transmission has been reported to occur transplacentally in a wide range of mammals (Dunn and Smith 2001).

Horizontal and vertical transmission are not mutually exclusive. In fact, the majority of microsporidian parasites that have been shown to be transmitted vertically are also transmitted horizontally (Andreadis 2007). Exclusive vertical transmission appears to be rare, while exclusive horizontal transmission is thought to be common (Dunn and Smith 2001). However, this notion may change as increased sampling documents a wider range of microsporidian species and their hosts.

1.1.4 Microsporidian systematics

The placement of the Microsporidia in the tree of life has long been a subject of contention (Corradi and Keeling 2009), but the monophyly of the group has almost never been in doubt (Vossbrinck and Debrunner-Vossbrinck 2005; Vávra and Lukeš 2013). Morphologically, the Microsporidia are unified by a single apomorphy that is unique for this group: the polar filament (Vossbrinck and Debrunner-Vossbrinck 2005). This was strongly supported by molecular data (Vávra and Lukeš 2013). However, the placement of Microsporidia in the eukaryotic tree has been challenging due to the lack of suitable morphocharacters and due to the fast rates of evolution of microsporidian sequences, which led researchers to relocate Microsporidia across the eukaryotic tree multiple times throughout history (Corradi and Keeling 2009; Vávra and Lukeš 2013). For instance, in the 1980s the Microsporidia were proposed to be a group of amitochondriate organisms that, based on the molecular data available at the time, appeared to be an early-diverging archezoan lineage (Archezoa hypothesis) (Cavalier-Smith 1983). It took nearly two decades to show that Microsporidia have mitochondria, albeit highly reduced (mitosomes) (Burri et al. 2006; Williams et al. 2008), and that their phylogenetic placement at the base of the tree of eukaryotes was a phylogenetic analysis artifact (long-branch attraction) (Hirt et al. 1999; Vávra and Lukeš 2013; James et al. 2013). Today, there is wide consensus that the Microsporidia are a group that is closely related to fungi, but their exact placement is still a source of contention. It is unclear whether Microsporidia are a basal lineage within fungi, or a sister group to fungi (Fischer and Palmer 2005; Capella-Gutierrez et al. 2012; Cuomo et al. 2012; Vávra and Lukeš 2013; Keeling 2014). Only time, more data, and further analysis will tell whether this conundrum will be resolved.

The phylogenetic relationships within Microsporidia have also not been entirely resolved. Currently, there are 1,300 to 1,500 microsporidian named species divided into 187 genera (Vávra and Lukeš 2013). Higher-level classifications are far from clear. The topology of the microsporidian tree is subject to constant modifications since most of the diversity of the group remains undescribed (Keeling 2009). Early attempts tried to classify microsporidian species based on morphological characters such as spore shape, nuclei number, or number of polar filament coils (Weiss and Vossbrinck 1999). However, this proved to be a difficult and slow process that did not provide sufficient resolution, especially at higher taxonomic levels (e.g. family) (Vávra and Lukeš 2013). Other features, such as life cycle and host ecology (Vossbrinck and Debrunner-Vossbrinck 2005), were used for microsporidian classification but faced similar difficulties due to their high variability.

1.1.5 Microsporidian genomes

Microsporidian genome sizes (GS) range from the smallest eukaryotic genome known to date, 2.3 Mbp of *Encephalitozoon intestinalis* (Corradi and Pombert et al. 2010), to 23 Mbp of *Anncaliia algerae* (Peyretaillade et al. 2012). The 10-fold range does not correlate with variation in gene number given that *E. intestinalis* (1,848 genes) and *A. algerae* (2,075 genes) have a similar number of genes (Corradi and Pombert et al. 2010; Peyretaillade et al. 2012). In fact, the highest number of open reading frames (ORFs) has been annotated in *Trachipleistophora hominis* (3,266 ORFs), a microsporidian with a medium sized genome (8.5-11.6 Mbp) by microsporidian standards (Heinz et al. 2012). Variation in genome size within the group is not the result of significant differences in gene number or length, but instead is largely attributed to differences in the length of intergenic regions and to the number of repeat sequences and

transposable elements (Cuomo et al. 2012; Heinz et al. 2012; Peyretaillade et al. 2012). Thus, genome size variation within Microsporidia is similar to that observed in other eukaryotic groups (e.g. animals and green plants) in that expansion or reduction of non-coding regions is the primary driver of this variability.

One of the most fascinating features of microsporidian genomes is their highly reduced nature. In this regard, microsporidian parasites appear to have excelled in discarding genomic sequences that are no longer necessary for their parasitic life style. Microsporidian genomes have few or no introns, short intergenic regions, and a reduced splicing machinery. Furthermore, their last common ancestor (LCMA) was predicted to have lost 1,590 protein families (Nakjang et al. 2013). In fact, microsporidian parasites have significantly fewer genes when compared to other eukaryotes. In comparison to fungal genomes (Kullman et al. 2005), a given microsporidian genome contains 2,000-3,200 genes, while unicellular yeast and filamentous fungi contain 5,000-7,000 and 9,000-17,000 respectively (Soanes et al. 2008). In addition, gene lengths and intergenic regions are significantly shorter in microsporidian genomes than in fungal genomes. Overall, based on the currently available fungal genome size estimates on the Fungal Genome Size Database (Kullman et al. 2005), the average microsporidian genome (~10 Mbp) is one-fifth the size of the average fungal genome (~50 Mbp) and the range of microsporidian genome sizes falls at the lower range of estimated fungal genome sizes (6.5-790 Mbp) (Kullman et al. 2005). Microsporidian genomes are also remarkable in that they have maintained high levels of gene synteny despite the drastic rearrangement of their genomes (Cuomo et al. 2012; Heinz et al. 2012; Peyretaillade et al. 2012; Pombert et al. 2012; Nakjang et al. 2013). For instance, comparison of the genomes of four different *Encephalitozoon* spp. (*E. cuniculi*, *E. romelae*, *E.*

intestinalis, and *E. hellem*) showed that over 90% of the genes (1,854) were syntenic across the 11 linear chromosomes present in this genus (Pombert et al. 2012). Most recently, whole-genome sequencing of the microsporidian *Ordospora colligata* (Pombert et al. 2015), the closest known relative of *Encephalitozoon* spp., revealed that *O. colligata* shared most of its 1,801 genes with *Encephalitozoon* spp.. Furthermore, the majority of the syntenic gene clusters found in *Encephalitozoon* spp. were maintained in the same order in *O. colligata* (Pombert et al. 2015), indicating that high levels of synteny can also be found between closely related microsporidian genera.

1.2 The Nematoda

Nematodes, also known as roundworms, are small and abundant aquatic animals. There are over 25,000 described species (Zhang 2013), but their estimated diversity is over 1 million species (Lambshead 2003). They are one of the most abundant animal groups and it is estimated that 80% of all individual living animals on earth are nematodes (Bongers and Bongers 1998). Their distribution is ubiquitous worldwide and they are abundant in most ecosystems. The nematode *C. elegans* is perhaps the best-studied laboratory animal, and has served as an important model to study metazoan morphology, development, and genetics (WormAtlas 2002-2015). On the other hand, the vast majority of nematodes, especially marine nematodes, have never been studied.

1.2.1 Nematode morphology

Nematodes are small and elongated cylindrical animals that usually measure between 0.1 and 2.5 mm in length. Morphologically, they are often described as a “tube inside a tube”. The outer tube is formed by the cuticle (a multilayered exoskeleton), the hypodermis, the muscles, and the

motor and sensory nerves (Bird 1971; WormAtlas 2002-2015) (Figure 1.1). The inner tube is formed by the digestive tract and its associated nervous system, and is separated from the outer tube by a fluid-filled body cavity (pseudocoelom) containing the reproductive tissues (Figure 1.1) (Bird 1971; WormAtlas 2002-2015).

In the outer tube, the hypodermis is the most external cellular layer and is arranged into thick cords connected by thin intercordal sections (Nicholas 1984). Cords and intercords run longitudinally from the head to the tail. The number and thickness of the hypodermal cords can vary depending on the species. Usually, there are four cords as in *C. elegans*: two wide lateral cords, a narrow ventral cord, and a narrow dorsal cord (Nicholas 1984). Muscles are involved primarily in the generation of the undulatory movement that propels nematodes (Bird 1971; Nicholas 1984; Chen et al. 2004). In adult *C. elegans*, there are four longitudinal bundles of somatic cells separated by four hypodermal cords (WormAtlas 2002-2015). Muscle cells have extensions to reach the nerve cells, as opposed to other animals where nerve cells extend to reach the muscles (Nicholas 1984; WormAtlas 2002-2015). In *C. elegans*, the nerve cells and the hypodermis are separated from the muscle by a thin layer called the the basal lamina that separate them from somatic muscle (WormAtlas 2002-2015).

The digestive system is the nematode's "internal tube" and it is composed of the mouth, the buccal cavity, the stoma, the pharynx (esophagus), the intestine, and the rectum (Bird 1971; Nicholas 1984; Chen et al. 2004; WormAtlas 2002-2015). All of these sections are connected by an internal tubular space called the lumen. The mouth and buccal cavity often contain teeth, mandibles, and other structures lined by the cuticle. The pharynx is an elaborate structure having

specialized muscles, nervous system, and structural cells. Its shape can be a uniform or irregular cylinder having one or more expansions (bulbs) (Bird 1971; Nicholas 1984; Chen et al. 2004; WormAtlas 2002-2015). The pharynx acts a pump that expands to draw food into the mouth and that contracts to transfer the food into the intestine's lumen (Bird 1971; Nicholas 1984; Chen et al. 2004; WormAtlas 2002-2015). The intestine is a large cylindrical organ that extends from the head to back and almost reaches the tail (Bird 1971; Nicholas 1984; Chen et al. 2004; WormAtlas 2002-2015). It is made of large granular cells that are not only involved in the digestion and absorption of food, but are also used for storage of nutrients (Bird 1971; Nicholas 1984; Chen et al. 2004; WormAtlas 2002-2015). The intestine is connected to the rectum: usually a short duct lined by the cuticle through which waste is disposed. In males, however, the rectum is called the cloaca, and this duct is shared by the digestive and reproductive systems (Bird 1971; Nicholas 1984; Chen et al. 2004; WormAtlas 2002-2015).

The reproductive system is located in the pseudocoelum and consists of one or two epithelial tubes that are located in the pseudoceolum between the outer tube (hypodermis and muscle tissues) and the internal tube (digestive system) (Bird 1971; Nicholas 1984; Chen et al. 2004). The majority of nematodes are usually dioecious (male and female) (Bird 1971; Nicholas 1984; Chen et al. 2004). However, it is common to find nematode species such as *C. elegans* that have self-fertilizing hermaphrodites instead of females (WormAtlas 2002-2015). Some nematode species are parthenogenic, where females predominate and males are absent or rare, and reproduction is asexual (Nicholas 1984; Lahl et al. 2006). The reproductive system of males usually consists of a single testis (sometimes two), a seminal vesicle, and a vas deferens (Bird 1971; Nicholas 1984; Chen et al. 2004). Spermatogenesis takes place in the testis but the

spermatozoa are stored in the seminal vesicle (Bird 1971; Nicholas 1984; Chen et al. 2004). The vas deferens functions as an ejaculatory duct that connects to the cloaca. In the cloaca, mature males have a specialized copulatory structure, the spicule, which is lined by the cuticle and serves to attach and widen the female's vulva and facilitate the transfer of sperm (Bird 1971; Nicholas 1984).

The reproductive system of females is characterized by having two genital ducts that may be divided into three sections: the ovary, the oviduct, and the uterus (Chen et al. 2004). The ovary contains the germ cells that can be arranged in singular or multiple rows. Oogenesis takes place in the germinal zone of the ovaries, usually located at the tip of the gonoduct. The germinal zone is followed by a maturation zone or growth zone that is connected to the uterus by the oviduct, that may also contain a spermatheca: an area used for sperm storage and fertilization. The uterus in nematodes is specialized for the release of eggs through the vulva, a cuticular opening connecting the gonoducts with the exterior.

1.2.2 Nematode life cycle and development

The nematode life cycle starts with an embryonic stage (fertilized egg), followed by four juvenile (larval) stages, and the adult stage. In embryogenesis, the general body plan of the nematode is formed, and once this process is complete the egg hatches and the nematode enters the first juvenile stage (L1). Nematodes grow by molting, which increases their body size at each stage, but maintains almost the same body plan acquired at the end of embryogenesis. There are three molts between the remaining juvenile stages (L2, L3, and L4), and a final molt from L4 to the adult stage. Maturation of the reproductive tissues occurs late in nematode development, where

distinct gender-specific structures (spicule in males and vulva in females) are present only in the adult stage (Bird 1971; Nicholas 1984; Chen et al. 2004; WormAtlas 2002-2015).

The life cycle of nematodes can vary depending on the species and life strategy adopted (Lee 2002). Parasitic nematodes often develop outside their host until they reach L3, the infectious stage. Their development is arrested here until a suitable host is infected, where they complete their development. Some nematodes, such as *C. elegans*, have a dauer stage that may form in late L1 if environmental conditions (i.e. lack of food) are unfavorable (Hu 2007). The dauer stage is an arrested stage that does not feed and that molts into an L4 stage once environmental conditions improve. The nematodes then completely molt into adults (Hu 2007).

1.3 Microsporidiosis in nematodes

The study of microsporidian infections in nematodes has been restricted to a few accidental discoveries during the past century. Despite this, these reports are sufficient to illustrate the complex and intriguing interactions that take place between nematodes and microsporidian parasites. The first formal report of nematode microsporidiosis dates back to 1922 when parasitic nematodes (*Protospirura muris*) were observed to contain microsporidian parasites in their intestines (epithelial cells) (Kudo and Hetherington 1922). The microsporidian hyperparasite was named *Thelohania reniformis* and, according to the authors, its infection pattern was unlike that of any other intestinal microsporidian infection observed before. *T. reniformis* was unusual in that its proliferation appeared to be restricted by "inhibiting factors" that prevented the microsporidian from multiplying in large numbers. Infected *P. muris* nematodes were reported to

have morphologically normal intestines, containing slowly dividing *T. reniformis* microsporidians, and showed no signs of pathological stress (Kudo and Hetherington 1922). It was almost 50 years before the next reports of nematode microsporidiosis. In 1970, transmissions of microsporidian parasites (*Nosema meslini* and *Pleistophora shubergui*) were reported to occur from caterpillars to parasitic nematodes (*Neoplactana agriotos*) (Veremtchuk and Issi 1970). *N. agriotos* nematodes became infected with *N. meslini* and *P. shubergui* after inoculation into caterpillars infected with these microsporidian parasites. A second study published the same year reported a microsporidian infection in the free-living marine nematode *Metoncholaimus scissus* (Hopper et. al. 1970). The infection was observed to be highly pathogenic with high concentrations of spores causing hypertrophy of the intestinal, hypodermal, muscle, and reproductive tissues. In addition, the microsporidian infection was reported to cause hypertrophism of the eggs of gravid females and was more prevalent in females than in males. The authors speculated on the possibility of transovarial vertical transmission, but favored the view that transmission was horizontal and that the initial infection occurred in the intestinal tissues after oral ingestion of the parasite. Unfortunately, the parasite's description was incomplete by the lack of both morphological (drawings or ultrastructural images) and molecular (lack of DNA sequence) data, raising questions about whether the parasite studied was, in fact, a microsporidian.

The next available description of a microsporidian parasite was that of *Microsporidium rhabdophilum* that was isolated from *Oscheius myriophila* nematodes (Poinar 1986). This was the first nematode-infecting microsporidian to be characterized by transmission electron microscopy (TEM). *M. rhabdophilum* infection was unique in that it was restricted within the

pharyngeal tissues in the dauer stage of *O. myriophila,* whereas in other life stages the infection affected the pharyngeal, hypodermal, reproductive, and intestinal tissues. In hermaphrodites, *M. rhabdophilum* infected mainly the hypodermal and reproductive tissues, and caused sterility when the reproductive tissues were heavily infected. This study provided the first evidence to suggest that the pathology of microsporidian infections in nematodes may vary depending on the developmental stage of the host. Poinar et al. provided a less detailed (no TEM) description of a microsporidian infection in a parasitic nematode (*Neoplactena glaseri*) (Poinar et al. 1988). The microsporidian infection was reported to have a wide range in pathogenicity varying from mild to a highly virulent. High virulence was characterized by infection of most tissues (hypodermal, intestinal, and reproductive), affected all nematode stages (including eggs), and altered normal development of the juvenile stages.

Almost two decades later, the next report of a nematode-infecting microsporidian was reported in *C. elegans* (Troemel et al. 2008). The infection was originally detected in undescribed wild *C. elegans*, but was successfully transferred to a *C. elegans* lab strain (N2) to facilitate its study. The microsporidian, named *Nematocida parisii*, caused an acute and 100% lethal intestinal infection after ingestion of *N. parisii* spores. The infection did not usually involve other tissue types and was only transmitted horizontally (Troemel et al. 2008). A remarkable feature of this parasite is that *N. parisii* spores were shown to exit the nematode's intestine without causing cell lysis by modifying the actin filaments of the intestinal cells to create gaps (Estes et al. 2011). This allowed *N. parisii* spores to enter the lumen and leave the nematode through the posterior end of the digestive tract (Estes et al. 2011). These findings along with the recent release of *N.*

parisii's genome (Cuomo et al. 2012) have established *N. parisii* as a model for the study of microsporidian intestinal infections.

Overall, the past century of sporadic discoveries of nematode microsporidian infections represent a glimpse of the variation of the host-parasite relationships that take place between nematodes and microsporidian parasites. Given the abundance and diversity of both groups, one can only expect that a more intriguing and elaborate co-evolutionary story awaits discovery.

1.4 Objectives

The main objective of this thesis is to advance our understanding of host-parasite interactions in the wild. I focused on those interactions involving Microsporidia, a group of obligate endoparasites of animals and some protists. In addition to examining the broad diversity of microsporidia in the environment, I also characterized the specific interaction between a microsporidian and its marine nematode host. Using morphological, molecular, and phylogenetic approaches, I aimed to provide an in-depth examination of the biology and evolution of microsporidian host-parasite interactions that can more broadly be applied to other systems.

In Chapter 2, I assess the diversity and distribution of microsporidian parasites in the environment in the Vancouver metropolitan area. Microsporidian environmental studies usually sample only water, and screen for a small number of microsporidian species (usually human-infecting). My primary objective in this chapter was to explore the diversity of the Microsporidia from other environmental sources (soil, sand, and compost) that remain largely unexplored and that could harbor a significant portion of microsporidian diversity.

In Chapter 3, my first objective was to identify the host of at least one novel microsporidian parasite detected in Chapter 2. I aimed to find a novel microsporidian parasite that infected an animal group (e.g. nematodes) in which few or no microsporidian infections had been documented. In this chapter, I provided the first detailed report of a microsporidian infection in a marine nematode. I named this novel microsporidian *Sporanauta perivermis* (for "marine spore of roundworms") and I characterized its morphology (spore) and host-parasite interaction in adult hosts.

In Chapter 4, my primary objective was to examine the infection pattern of *S. perivermis* in immature hosts and assess whether or not it differed from the infection pattern observed in adults. In addition, my goal was to elucidate whether *S. perivermis* was vertically transmitted, since I had observed (Chapter 3) that it infected the reproductive tissues of adult females. This is significant because vertical transmission is considered rare for microsporidia, and *S. perivermis* could be the first known microsporidian to be transmitted vertically in nematodes.

In Chapter 5, I sought to better understand the relationship between *S. perivermis* and its nearest relatives. Based on my previous single-gene phylogenetic analyses (Chapters 2 and 3), I predicted that *S. perivermis* is closely related to the *Encephalitozoon* group. The genomic survey presented here allowed for more robust multi-gene phylogenetic analyses that confirmed a close relationship between *S. perivermis* and the *Encephalitozoon*, while also predicting a phylogenetic affiliation with *O. colligata*. Indeed, analyses of gene content and synteny further supported

these phylogenetic inferences, while highlighting chomosomal rearrangements that could be linked to genome reduction.

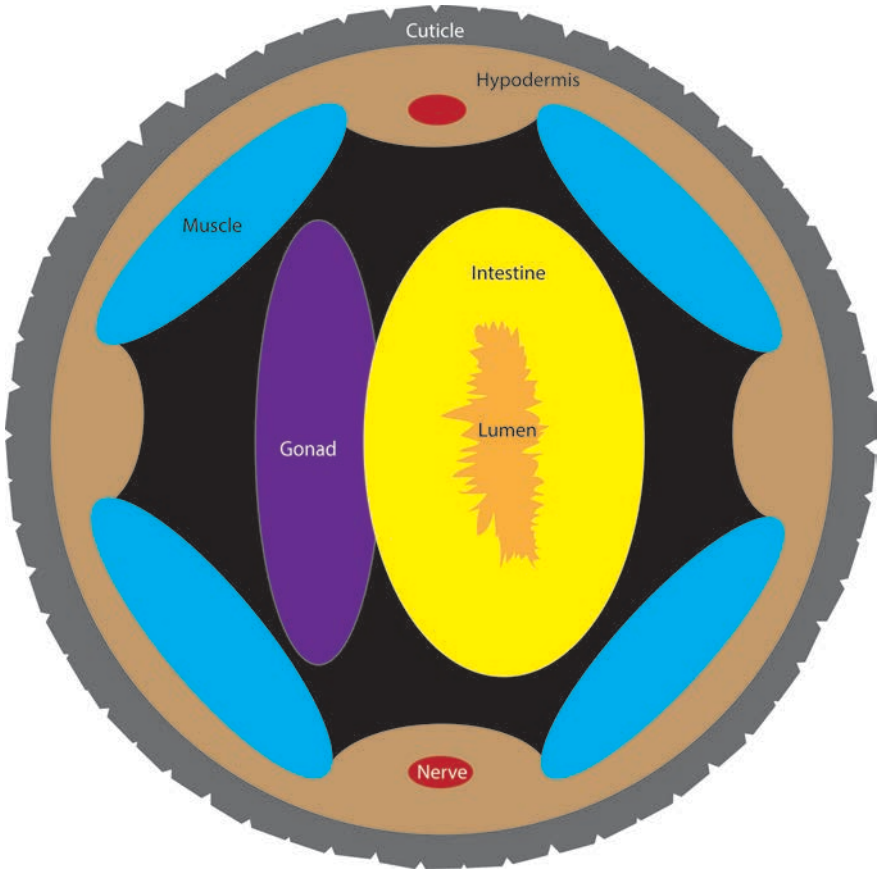

Figure 1.1 Diagram showing a cross-section of the nematode's body.

The nematode's body can be described as a "tube inside a tube". The outer tube contains the cuticle (exoskeleton), the hypodermis, the muscles, and the nerve cords. The inner tube (the intestines) and the outer tube are separated by the pseudoceolum, a fluid-filled cavity that also contains the reproductive tissues.

Chapter 2: Microsporidian diversity in soil, sand and compost of the Pacific Northwest

2.1 Introduction

Microsporidian parasites are often described as being "ubiquitous" in nature (Didier et al. 2004; Kotler and Orenstein 1998; Sharma et al. 2011; Troemel et al. 2008; Weiss and Vossbrinck 1999). This is an assumption based largely on the widespread incidence of microsporidiosis in humans (Brian and Schwartz 1999) and on our inability to identify the microsporidian source(s) in most infection cases (Didier and Weiss 2011). Microsporidian environmental ubiquity implies that humans are exposed constantly to a wide diversity of Microsporidia. Despite this and their importance as emerging pathogens, microsporidian diversity has often been overlooked by focusing mainly on the water and zoonotic diversity of four human-infecting species (*Encephalitozoon* and *Enterocytozoon* genera) (Dado et al. 2012; Didier et al. 2004; Graczyk et al. 2008; Izquierdo et al. 2011; Jamshidi et al. 2012; Lee et al. 2011; Lucy et al. 2008; Magalhaes et al. 2006; Mathis et al. 2005; Mota et al. 2000; Sak et al. 2010; Stine et al. 2005). Other sources of Microsporidia such as soil and compost have previously been excluded in some studies (as in Dado et al. 2012) despite the building evidence to suggest that soil and compost may harbor a wide diversity of microsporidian parasites (Le Goff et al. 2010; Loh et al. 2009; Sharma et al. 2011; Troemel et al. 2008).

The purpose of this study was to explore microsporidian diversity in soil, sand, and compost collected from popular urban sites. Our survey detected 22 novel microsporidian species, a novel

microsporidian species (*Sporanauta perivermis*) that was named and characterized in this thesis (Chapters 3, 4, and 5), and three previously described microsporidian parasites. There were representatives from almost all major microsporidian groups (clades I, II, IV, and V). Overall, our study suggests that microsporidian diversity in soil, sand, and compost is high, and that the prevalence of these parasites is usually restricted to a particular site or habitat.

2.2 Materials and methods

2.2.1 Sampling

Wet sand samples were collected during low tide in July and August 2010 in the Vancouver metropolitan area (BC, Canada) from: 1. Port Moody beach (47.282°N, 122.850°W), 2. Jericho Beach (49.273°N, 123.193°W), 3. Wreck beach (49.263°N, 123.266°W) and 6. Boundary Bay beach (49.013°N, 123.036°W) (BC, Canada). Damp soil samples were also collected from a swamp at Wreck beach, 4. the Reiffel Bird Sanctuary (49.101°N, 123.189°W), and from 5. Barnston Island (49.208°N, 122.726°W). Soil samples were also collected from the Union Bay Natural Area (47.654°N, -122.293°W) in July and August 2011 in Seattle USA (Site 7). At each site, five to 10 samples were collected from the surface (< 10 cm deep) in sterile tubes. Samples were stored at 4 °C in the dark until processing for DNA extraction.

Compost samples (labeled A–O) were obtained in July and August 2010 in Vancouver from 14 home composters across the city, and from the In-Vessel composting facility at the University of British Columbia (sample L). One or two scoops of compost (ca. 500 g) were sealed and stored in the same conditions as described above for the soil and sand samples.

2.2.2 DNA extraction and sequencing

Each sample collected was passed through a paper coffee filter overnight after a small amount of sterile water (ca. 20 ml) was added to remove excess soil and increase the microsporidian concentration in the filtered samples. The filtrate was then pelleted at 16,200 g for 3 min. One to two DNA extractions were performed per sample with the pellet as the maximum load for the DNA extraction kit is 1.0 g. A blank DNA extraction was performed along as a negative control.

DNA extractions were performed using a beadbeater (Mini-Beadbeater-1; BioSpec Products Inc., Bartlesville, OK, USA) and the UltraClean Soil DNA Isolation kit (Mo Bio Laboratories, Inc., Carlsbad, CA, USA). The lysis step was modified to break microsporidian spores by incubating the samples for 5 min at 70 °C followed by beadbeating (2,500 rpm) for 20 s. This 5-min incubation was repeated three times. All other steps followed the manufacturer's protocol.

Microsporidian SSU rDNA amplifications were initially attempted using microsporidian-specific primers from the literature (Weiss and Vossbrinck 1998): ss18f (5′-CACCAGGTTGATTCTGCC-3′), ss350f (5′-CCAAGGAYGGCAGCAGGCGCGAAA-3′) and (ss350r), ss530f (5′-GTGCCAGCMGCCGCGG-3′) and (ss530r), ss1047r (5′-AACGGCCATGCACCAC-3′), and ss1492r (5′-GGTTACCTTGTTACGACTT-3′). However, the use of these forward and reverse primers in different combination pairs resulted in the amplification of sequences from nematodes, apicomplexans, annelids, and other eukaryotes. Therefore, we designed an additional reverse primer: Micro33R (5′-TAGAGACCGTTGTAGTTCCG-3′) (Chapter 3) that, in combination with the forward primer 18ssf (Weiss and Vossbrinck 1998), more consistently amplified microsporidian sequences from

our soil samples. The 18ssf-Micro33R primer set amplifies half (600–700 bp) of the microsporidian SSU rDNA gene. PCR was performed using Illustra puReTaq ready-to-go PCR beads (GE Healthcare, Buckinghamshire, UK) and products were gel purified using the UltraClean 15 DNA purification kit (Mo Bio Laboratories, Inc.). Fragments were cloned into pCR 2.1 (TOPO TA Cloning kit, Invitrogen Inc., Carlsbad, CA, USA) and plasmids were purified using QIAprep Spin Miniprep kit (Qiagen, Gaithersburg, MD, USA). At least three clones were sequenced (Macrogen Inc., Rockville, MD, USA) for each excised band. In total, there were 105 sequenced clones that contained a microsporidian SSU rDNA sequence.

2.2.3 Phylogenetic analysis

Microsporidian SSU rDNA amplifications were initially attempted using microsporidian-specific primers from the literature (Weiss and Vossbrinck 1998): ss18f (5′-CACCAGGTTGATTCTGCC-3′), ss350f (5′-CCAAGGAYGGCAGCAGGCGCGAAA-3′) and (ss350r), ss530f (5′-GTGCCAGCMGCCGCGG-3′) and (ss530r), ss1047r (5′-AACGGCCATGCACCAC-3′), and ss1492r (5′-GGTTACCTTGTTACGACTT-3′). However, the use of these forward and reverse primers in different combination pairs resulted in the amplification of sequences from nematodes, apicomplexans, annelids, and other eukaryotes. Therefore, we designed an additional reverse primer: Micro33R (5′-TAGAGACCGTTGTAGTTCCG-3′) (Chapter 3) that, in combination with the forward primer 18ssf (Weiss and Vossbrinck 1998), more consistently amplified microsporidian sequences from our soil samples. The 18ssf-Micro33R primer set amplifies half (600–700 bp) of the microsporidian SSU rDNA gene. PCR was performed using Illustra puReTaq ready-to-go PCR beads (GE Healthcare, Buckinghamshire, UK) and products were gel purified using the

UltraClean 15 DNA purification kit (Mo Bio Laboratories, Inc.). Fragments were cloned into pCR 2.1 (TOPO TA Cloning kit, Invitrogen Inc., Carlsbad, CA, USA) and plasmids were purified using QIAprep Spin Miniprep kit (Qiagen, Gaithersburg, MD, USA). At least three clones were sequenced (Macrogen Inc., Rockville, MD, USA) for each excised band. In total, there were 105 sequenced clones that contained a microsporidian SSU rDNA sequence.

2.3 Results

2.3.1 Distribution and diversity

There were a total of 26 microsporidian SSU rDNA sequences detected in this study (Table 2.1). Ten SSU rDNA sequences were amplified from 12 of 15 house-compost samples examined in Vancouver (Canada). Four other SSU rDNA sequences were obtained from soil and sand samples collected in Vancouver (Canada) while the remaining SSU rDNA sequences were obtained from soil samples collected at a single site in Seattle (USA) (Figure 2.1). Only four of the SSU rDNA sequences were detected in more than one compost sample. Of these, three SSU rDNA were also detected in soil samples: Comp_CD_Van2, Comp_F_Van5, Comp_DFGHI_Van7. The latter was the only microsporidian sequence to show high prevalence and a wide distribution that extended over 200 km. Comp_DFGHI_Van7 was detected in seven Vancouver-compost samples and eight soil samples collected in Vancouver (site 4) and Seattle (site 7). The distribution of all other SSU rDNA sequences was generally restricted to a single site except for Comp_CD_Van2 and Comp_F_Van5 that were detected in compost and at sites four and one, respectively.

Most of the microsporidian SSU rDNA sequences detected in this study appeared to be novel when compared with GenBank (NCBI) (Geer et al. 2010) (Table 2.1). Ten of the 26 SSU rDNA sequences had an undescribed microsporidium as their top hit while only three sequences (UBN_Seattle1 and UBN_Seattle2) were nearly identical (≥ 98%) to a named microsporidian: *O. muscadomesticae* (host: fly) (Vossbrinck et al. 2010) and *O. operopterae* (host: moth) (Canning et al. 1985, 2001), respectively. An arbitrary cut-off of 98% was employed, and we cannot exclude the possibility, albeit unlikely, that these sequences represent new species that are closely related to the top BLAST hits (Table 2.1). UBN_Seattle3 showed high similarity (96% identity) to a named microsporidium, the hyperparasitic *N. aurantiae* (hosts: Myxozoa and Oligacheata) (Morris and Freeman 2010). The remaining SSU rDNA sequences showed variable similarity (76–93%) to described microsporidian species including the following: the grasshopper-infecting *Liebermannia covasacrae* (Sokolova et al. 2009), the nematode-infecting *Nematocida parisii* (Troemel et al. 2008), the mosquito-infecting *Hazardia milleri* (Hazard et al. 1985), the beetle-infecting *O. popilliae* (Andreadis and Hanula 1987), and the moth-infecting *Endoreticulatus* sp. Zhenjiang isolate (Xu et al. 2012)(Table 2.1). The SSU rDNA sequence of *Sporanauta perivermis* was also amplified from site 6 during this survey. We previously identified *S. perivermis*, characterizing its morphology, phylogenetic placement, and infection pattern of its host, the marine nematode *Odontophora rectangula* (Chapter 3).

2.3.2 Phylogenetic context

Our phylogenetic analyses indicated that the 26 microsporidian sequences detected in this study are highly diverse and include representatives from most major microsporidian clades (Figure 2.2). More than half belonged to clades I and IV. In clade I, there were seven novel

microsporidian species that, in most cases, did not show a specific association. The only exception to this was UBN_Seattle1, which as expected based on its sequence, grouped with *O. muscadomesticae* (99% identity). All clade I novel microsporidian sequences were detected from soil samples collected in either Vancouver (site 4) or Seattle (site 7). In clade IV, there were 10 novel microsporidian sequences (Figure 2.2). In most cases, their closest relative was their respective top blast hit as observed for UBN_Seattle2 and *O. operophterae* (98% identity)(Figure 2.2). The widely distributed Comp_DFGHI_Van7 was recovered within this clade (clade IV) as a basal lineage to the *Endoreticulatus* group, but was not associated with a particular species.

There were only three new SSU rDNA microsporidian sequences recovered in clade V (Figure 2.2). Two of them (UBN_Seattle 9 and UBN_Seattle10) showed moderate support as sister lineages to the long-branch clade formed by *Anncaliia algerae* and *Thelohania solenopsae*. The third novel SSU rDNA sequence (WBS_Van14) in clade V showed strong support as a basal lineage for the *Antonospora–Paranosema* group (Figure 2.2). The placement of the *Antonospora–Paranosema* group within clade V does not correspond to that of recent reports where it was recovered as a sister lineage to the *Nematocida–Ovavesicula* group (clade II) (Troemel et al. 2008) (Chapter 3). It is important to note that clade II was originally proposed to be composed by the *Antonospora–Paranosema* group and a sister cosmopolitan group containing *Caudospora simulli*, *Flabelliforma Montana*, *Polydipyrenia simuli*, and *Weiseria palustris* (here referred to as "CFPW" group) (Vossbrinck and Debrunner-Vossbrinck 2005). This is the first study to include the three "clade II" groups in the same analyses; however, their grouping within a single clade could not be recovered (Figure 2.2). Despite this, the *Nematocida–Ovavesicula*

group and the CFPW group were each strongly supported as independent lineages and were not found to be part of any one of the four major microsporidian clades (Figure 2.2).

The *Nematocida–Ovavesicula* group contained four novel microsporidian SSU rDNA sequences amplified in this study and *Ovavesicula popillae* was recovered as the most basal lineage within the *Nematocida–Ovavesicula* group. It is worth noting that the monophyly for the *Nematocida–Ovavesicula* group is robust (1/1/100) (Figure 2.2), as are the relationships within this group. Interestingly, three of the novel species within the *Nematocida–Ovavesicula* group were detected from compost samples while the fourth was obtained from soil samples and was found to be the second most basal lineage within the group.

2.4 Discussion

Microsporidian parasites are considered to be diverse because they have been found in nearly all animal groups and some protists and they are assumed to be ubiquitous in the environment. Yet, our understanding of human exposure to these parasites is based mainly on the zoonosis (dogs, cats, and birds) and water prevalence of a small number of described human-infecting species (usually *Encephalitozoon* and *Enterocytozoon* genera) (Dado et al. 2012; Didier et al. 2004; Graczyk et al. 2008; Izquierdo et al. 2011; Jamshidi et al. 2012; Lee et al. 2011; Lucy et al. 2008; Magalhaes et al. 2006; Mathis et al. 2005; Mota et al. 2000; Sak et al. 2010; Stine et al. 2005). Our purpose was to explore microsporidian diversity in soil and sand samples from sites in Vancouver (Canada) and Seattle (USA). In addition, we screened for the presence of Microsporidia in house-compost as Microsporidia have recently been detected and isolated from this source (Le Goff et al. 2010; Troemel et al. 2008).

2.4.1 Microsporidian diversity and distribution

Our study revealed 22 novel microsporidian species and only four described species: *O. operophterae* (host: beetle) (Canning et al. 1985, 2001), *S. perivermis* (host: marine nematode) (Chapter 3), *O. muscadomesticae* (host: fly) (Vossbrinck et al. 2010), and *N. aurantiae* (host: Myxosporidia and Oligochaeta) (Morris and Freeman 2010). The majority of the microsporidian species retrieved in this study were obtained from soil (17 species), followed by compost (10 species), and sand (2 species) (Table 2.1). There was almost no overlap between sample types and the geographic distribution for each microsporidian species was usually restricted to one site and sample type (Table 2.1). A remarkable exception to this was *Microsporidium* sp. Comp_DFGHI_Van7. This novel parasite was detected in five different compost samples in Vancouver and in soil samples collected in Vancouver and Seattle (over 200 km apart). The distribution observed suggest that the majority of microsporidian species appear to be confined to specific habitats and that only a few species may be referred to as ubiquitous.

Our results are in agreement with the notion that microspordian diversity is orders of magnitude higher than known to date (1,300 named species) (Corradi and Keeling 2009; Keeling 2009). Moreover, our data highlight previously understudied sources of microsporidian parasites. It is worth noting here that none of the microsporidian species detected in this study are known to infect humans (85% are undescribed). Human-infecting microsporidia are opportunistic (Didier and Weiss 2011) and diverse (15 species classified in 10 genera) (Choudhary et al. 2011; Didier et al. 2005; Meissner et al. 2012), and this group continues to expand as our ability to detect and identify Microsporidia improves. For instance, *Tubulinosema acridophagus* was recently

recognized in humans as it caused lethal infections in immunosuppressed individuals (Choudhary et al. 2011; Meissner et al. 2012). A similar case is that of *A. algerae*, first discovered in mosquitos (Vávra and Undeen 1970), which has been reported in humans to infect the cornea (Visvesvara et al. 1999) cause lethal myositis (skeletal muscle inflammation) (Coyle et al. 2004), and even infect the vocal cords (Cali et al. 2010).

The way immunocompromised humans acquire microsporidiosis is generally unknown, but any of these opportunistic microsporidian parasites may be acquired by direct contact (e.g. skin wound), ingestion, or inhalation. This highlights the importance of increasing our understanding of the diversity of Microsporidia found in common urban environments such as those examined here.

2.4.2 Microsporidian phylogenetic classification

Our phylogenetic analysis showed that the 22 novel SSU rDNA sequences and the four SSU rDNA sequences from described microsporidian species that were detected in this study belong to all major microsporidian groups except for clade III (Figure 2.2). Clade I (six novel sequences and *O. muscadomesticae*) and clade V (three novel sequences) contained microsporidian sequences that were only detected in soil samples from Vancouver or Seattle. On the other hand, clade IV microsporidian sequences (eight novel sequences, *O. operophterae*, and *S. perivermis*) were obtained from soil, sand, and compost from Vancouver and Seattle. The presence of microsporidian sequences from clade IV in all sample types may suggest that there are shared features (e.g. decomposing organic matter) between the source samples examined and the hosts that inhabit them.

Our phylogenetic examination also revealed that previously described microsporidian clade II may be a long-branch attraction artifact between the three groups proposed to be part of this clade: *Antonospora–Paranosema*, *Nematocida–Ovavesicula*, and the "CFPW" group. Clade II was weakly supported in all previous studies. Indeed, clade II was not recovered in our analyses. Instead, the *Antonospora–Paranosema* group was recovered in clade V, which is in agreement with a previous study (Slamovits et al. 2004). The *Nematocida–Ovavesicula* group is a recent lineage composed of only two named species and five other undescribed microsporidian species (four in this study) that, in our trees formed a strongly supported group that did not associate with any other clade, although the backbone of the tree is not completely resolved (Figure 2.2). The same scenario was observed for the "CFPW" microsporidian group. Our analyses show the importance of increasing our knowledge of microsporidian diversity to better understand the phylogenetic relationships and evolutionary history of these parasites.

Overall, our results suggest that there is a wide diversity of microsporidian species in soil, sand, and compost. We retrieved 22 novel microsporidian sequences and only four from named species belonging to almost all major microsporidian lineages. This reaffirms the fact that a major portion of microsporidian diversity remains unexplored in soil, sand, and compost despite their potential as common sources for microsporidian parasites. Our findings suggest that the distribution for each species was usually restricted to a particular site, and that only a small number of species appear to be more widespread. This work highlights the diversity of Microsporidia in common, urban habitats and emphasizes the importance of understanding diversity in elucidating phylogenetic relationships.

Table 2.1 Microsporidian diversity in soil, sand, and compost

Microsporidium sp. (accession no.)[a]	Top BLAST hit (accession no.)	Max identity (%)	Phylogenetic placement	Sampling source (site no.)
Comp_C_Van1 (KC111783)	*Orthosomella operophterae* (AJ302316.1)	93	Clade IV	Compost (C)
Comp_CD_Van2 (KC111784)	*Microsporidium* sp. *BBRE2* (FJ755987.1)	93	Clade IV	Compost (C, D); Soil (4)
Comp_L_Van3 (KC111787)	*Microsporidium* sp. *GPM2* (HM991452.1)	85	Clade IV	Compost (L)
Comp_A_Van4 (KC111780)	*Nematocida parisii* (FJ005051.1)	81	N.O.G	Compost (A)
Comp_BK_Van5 (KC111781)	*Nematocida* sp. (FJ005052.1)	81	N.O.G	Compost (B, K)
Comp_C_Van6 (KC111782)	*Nematocida* sp. (FJ005052.1)	81	N.O.G	Compost (C)
Comp_DFHHI_Van7 (KC111785)	*Endoreticulatus* sp. *Zhenjiang* (FJ772431.1)	92	Clade IV	Compost (D, F, G, H, I); Soil (4, 7); Sand (6)
Comp_L_Van8 (KC111786)	*Liebermannia covasacrae* (EU709818.1)	81	Clade IV	Compost (L)
Comp_E_Van9 (KC111788)	*Microsporidium* sp. *HEM-2006WLa* (AM411635.1)	88	Clade IV	Compost (E)

Microsporidium sp. (accession no.)[a]	**Top BLAST hit (accession no.)**	**Max identity (%)**	**Phylogenetic placement**	**Sampling source (site no.)**
Comp_F_Van10 (KC111789)	*Microsporidium* sp. *BPAR2 TUB2* (FJ56099.1)	97	Clade IV	Compost (F); Sand (1)
RBS_Van11 (KC111792)	*Microsporidium* sp. *BTUB8* (FJ756168.1)	87	Clade IV	Soil (4)
RBS_Van12 (KC111790)	*Hazardia milleri* (AY090067.1)	94	Clade I	Soil (7)
RBS_Van13 (KC111791)	*Hazardia milleri* (AY090067.1)	89	Clade I	Soil (7)
WBS_Van14 (KC111793)	*Microsporidium* sp. *BBRE3* (FJ755988.1)	86	Clade V	Soil (3)
UBN_Seattle1[b] (KC111797)	*Octosporea muscadomesticae* (FN794114.1)	99	Clade I	Soil (7)
UBN_Seattle2[b] (KC111803)	*Orthosomella operophterae* (AJ302316.1)	98	Clade IV	Soil (7)
UBN_Seattle3[b] (KC111802)	*Neoflabelliforma aurantiae* (GQ206147.1)	96	N.A.	Soil (7)
UBN_Seattle4 (KC111795)	*Hazardia milleri* (AY090067.1)	88	Clade I	Soil (7)
UBN_Seattle5 (KC111804)	*Hazardia milleri* (AY090067.1)	92	Clade I	Soil (7)
UBN_Seattle6 (KC111798)	*Hazardia* sp. *isolate 1* (AY090066.1)	92	Clade I	Soil (7)
UBN_Seattle7 (KC111800)	*Ovavesicula popilliae* (EF564602.1)	76	N.O.G.	Soil (7)

Microsporidium sp. (accession no.)[a]	**Top BLAST hit (accession no.)**	**Max identity (%)**	**Phylogenetic placement**	**Sampling source (site no.)**
UBN_Seattle8 (KC111801)	*Microsporidium* sp. *BLAT1 CAN* (FJ756034.1)	97	Clade IV	Soil (7)
UBN_Seattle9 (KC111794)	*Microsporidium* sp. *BKES2*(FJ756021.1)	94	Clade V	Soil (7)
UBN_Seattle10 (KC111796)	*Microsporidium* sp. *BKES2*(FJ756021.1)	90	Clade V	Soil (7)
UBN_Seattle11 (KC111799)	*Microsporidium* sp. *MIC1 BRN01*(FJ94863.1)	83	Clade I	Soil (7)

[a] Novel microsporidian sequences detected in the cities of Vancouver (Canada) and Seattle (USA) showing the top blast hit and their identity values, phylogenetic placement, and sampling source. House-compost samples were collected in Vancouver (Canada) and labeled (A–N). Soil and sand samples were collected in seven sites in Vancouver (Canada) and Seattle (USA) (refer to Figure 2.1). GenBank accession numbers are provided for each sequence. N.O.G., *Nematocida–Ovavesicula* group; N.A., not assigned.

[b] BLAST hit nearly identical to a named species.

Table 2.1 Microsporidian diversity in soil, sand, and compost

Microsporidium sp. (accession no.)[a]	Top BLAST hit (accession no.)	Max identity (%)	Phylogenetic placement	Sampling source (site no.)
Comp_C_Van1 (KC111783)	*Orthosomella operophterae* (AJ302316.1)	93	Clade IV	Compost (C)
Comp_CD_Van2 (KC111784)	*Microsporidium* sp. *BBRE2* (FJ755987.1)	93	Clade IV	Compost (C, D); Soil (4)
Comp_L_Van3 (KC111787)	*Microsporidium* sp. *GPM2* (HM991452.1)	85	Clade IV	Compost (L)
Comp_A_Van4 (KC111780)	*Nematocida parisii* (FJ005051.1)	81	N.O.G	Compost (A)
Comp_BK_Van5 (KC111781)	*Nematocida* sp. (FJ005052.1)	81	N.O.G	Compost (B, K)
Comp_C_Van6 (KC111782)	*Nematocida* sp. (FJ005052.1)	81	N.O.G	Compost (C)
Comp_DFHHI_Van7 (KC111785)	*Endoreticulatus* sp. *Zhenjiang* (FJ772431.1)	92	Clade IV	Compost (D, F, G, H, I); Soil (4, 7); Sand (6)
Comp_L_Van8 (KC111786)	*Liebermannia covasacrae* (EU709818.1)	81	Clade IV	Compost (L)
Comp_E_Van9 (KC111788)	*Microsporidium* sp. *HEM-2006WLa* (AM411635.1)	88	Clade IV	Compost (E)

Microsporidium sp. (accession no.)[a]	**Top BLAST hit (accession no.)**	**Max identity (%)**	**Phylogenetic placement**	**Sampling source (site no.)**
Comp_F_Van10 (KC111789)	*Microsporidium* sp. *BPAR2 TUB2* (FJ56099.1)	97	Clade IV	Compost (F); Sand (1)
RBS_Van11 (KC111792)	*Microsporidium* sp. *BTUB8* (FJ756168.1)	87	Clade IV	Soil (4)
RBS_Van12 (KC111790)	*Hazardia milleri* (AY090067.1)	94	Clade I	Soil (7)
RBS_Van13 (KC111791)	*Hazardia milleri* (AY090067.1)	89	Clade I	Soil (7)
WBS_Van14 (KC111793)	*Microsporidium* sp. *BBRE3* (FJ755988.1)	86	Clade V	Soil (3)
UBN_Seattle1[b] (KC111797)	*Octosporea muscadomesticae* (FN794114.1)	99	Clade I	Soil (7)
UBN_Seattle2[b] (KC111803)	*Orthosomella operophterae* (AJ302316.1)	98	Clade IV	Soil (7)
UBN_Seattle3[b] (KC111802)	*Neoflabelliforma aurantiae* (GQ206147.1)	96	N.A.	Soil (7)
UBN_Seattle4 (KC111795)	*Hazardia milleri* (AY090067.1)	88	Clade I	Soil (7)
UBN_Seattle5 (KC111804)	*Hazardia milleri* (AY090067.1)	92	Clade I	Soil (7)
UBN_Seattle6 (KC111798)	*Hazardia* sp. *isolate 1* (AY090066.1)	92	Clade I	Soil (7)
UBN_Seattle7 (KC111800)	*Ovavesicula popilliae* (EF564602.1)	76	N.O.G.	Soil (7)

Microsporidium sp. (accession no.)[a]	**Top BLAST hit (accession no.)**	**Max identity (%)**	**Phylogenetic placement**	**Sampling source (site no.)**
UBN_Seattle8 (KC111801)	*Microsporidium* sp. *BLAT1 CAN* (FJ756034.1)	97	Clade IV	Soil (7)
UBN_Seattle9 (KC111794)	*Microsporidium* sp. *BKES2*(FJ756021.1)	94	Clade V	Soil (7)
UBN_Seattle10 (KC111796)	*Microsporidium* sp. *BKES2*(FJ756021.1)	90	Clade V	Soil (7)
UBN_Seattle11 (KC111799)	*Microsporidium* sp. *MIC1 BRN01*(FJ94863.1)	83	Clade I	Soil (7)

[a] Novel microsporidian sequences detected in the cities of Vancouver (Canada) and Seattle (USA) showing the top blast hit and their identity values, phylogenetic placement, and sampling source. House-compost samples were collected in Vancouver (Canada) and labeled (A–N). Soil and sand samples were collected in seven sites in Vancouver (Canada) and Seattle (USA) (refer to Figure 2.1). GenBank accession numbers are provided for each sequence. N.O.G., *Nematocida–Ovavesicula* group; N.A., not assigned.

[b] BLAST hit nearly identical to a named species.

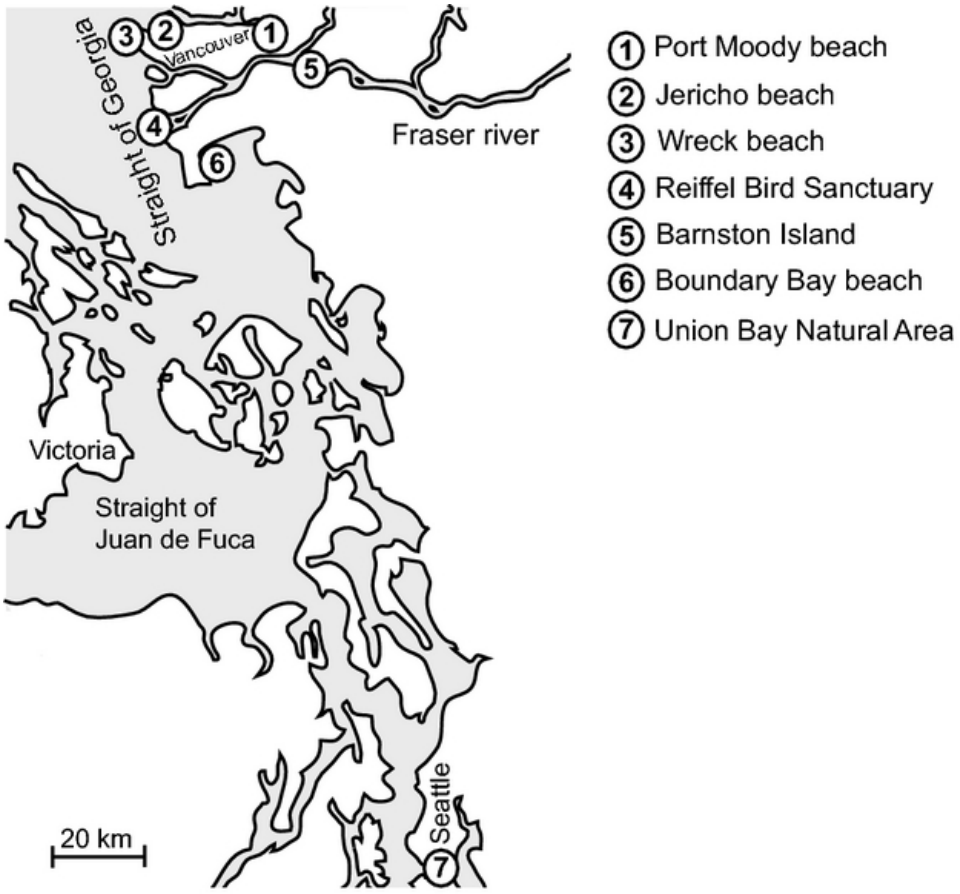

Figure 2.1 Soil and sand collection sites in Vancouver (Canada) and Seattle (USA)

There were six sites: 1. Port Moody beach (sand), 2. Jericho beach (sand), 3. Wreck beach (soil) and beach (sand), 4.Reiffel Bird Sanctuary (soil), 5. Barnston Island (soil), 6. Boundary bay beach (sand), and 7. Union Bay Natural Area (soil).

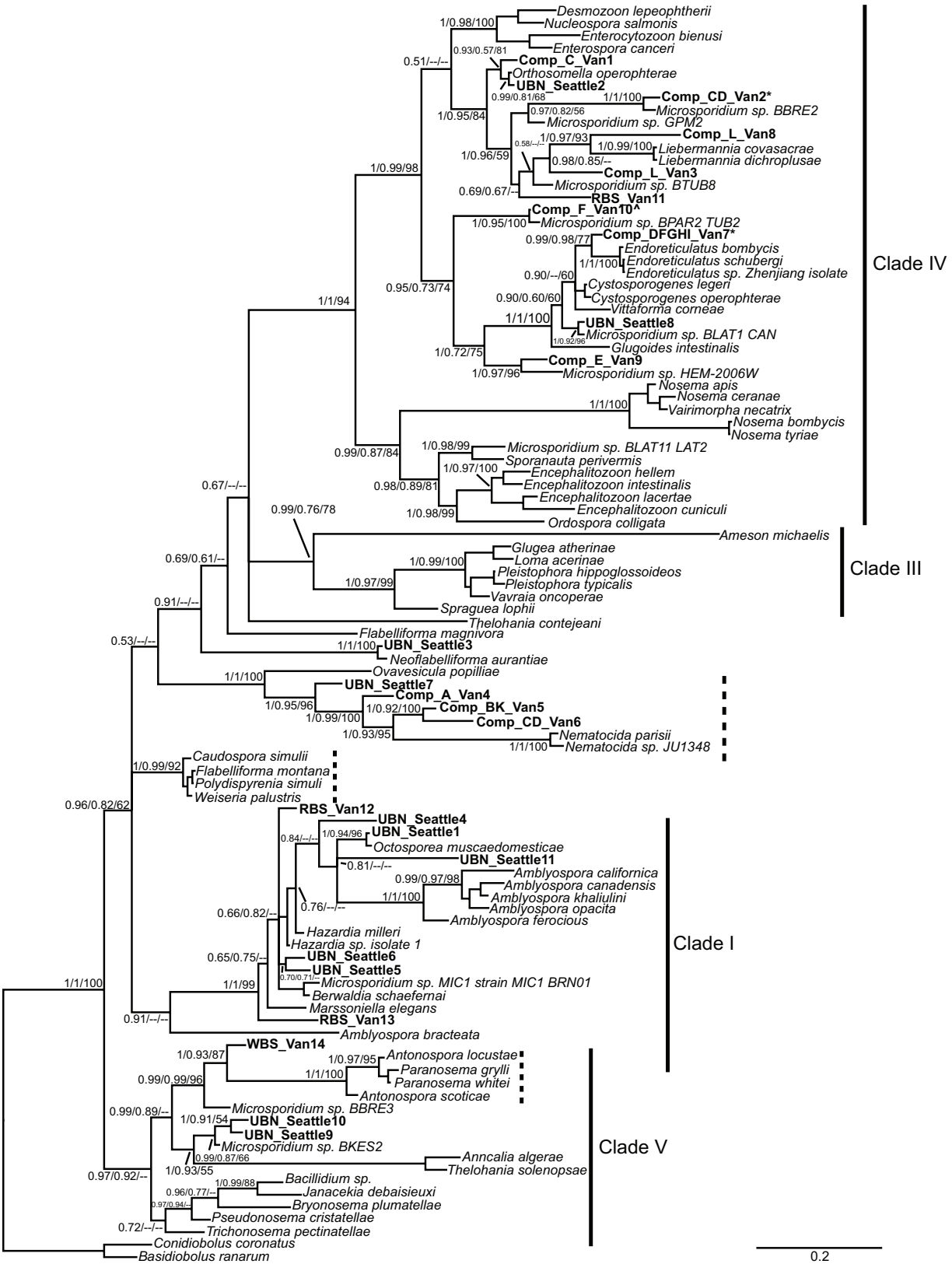
Desmozoon lepeophtherii
Nucleospora salmonis
Enterocytozoon bienusi
Enterospora canceri
Comp_C_Van1
Orthosomella operophterae
UBN_Seattle2
Comp_CD_Van2*
Microsporidium sp. BBRE2
Microsporidium sp. GPM2
Comp_L_Van8
Liebermannia covasacrae
Liebermannia dichroplusae
Comp_L_Van3
Microsporidium sp. BTUB8
RBS_Van11
Comp_F_Van10^
Microsporidium sp. BPAR2 TUB2
Comp_DFGHI_Van7*
Endoreticulatus bombycis
Endoreticulatus schubergi
Endoreticulatus sp. Zhenjiang isolate
Cystosporogenes legeri
Cystosporogenes operophterae
Vittaforma corneae
UBN_Seattle8
Microsporidium sp. BLAT1 CAN
Glugoides intestinalis
Comp_E_Van9
Microsporidium sp. HEM-2006W
Nosema apis
Nosema ceranae
Vairimorpha necatrix
Nosema bombycis
Nosema tyriae
Clade IV
Microsporidium sp. BLAT11 LAT2
Sporanauta perivermis
Encephalitozoon hellem
Encephalitozoon intestinalis
Encephalitozoon lacertae
Encephalitozoon cuniculi
Ordospora colligata
Ameson michaelis
Glugea atherinae
Loma acerinae
Pleistophora hippoglossoideos
Pleistophora typicalis
Vavraia oncoperae
Spraguea lophii
Thelohania contejeani
Clade III
Flabelliforma magnivora
UBN_Seattle3
Neoflabelliforma aurantiae
Ovavesicula popilliae
UBN_Seattle7
Comp_A_Van4
Comp_BK_Van5
Comp_CD_Van6
Nematocida parisii
Nematocida sp. JU1348
Caudospora simulii
Flabelliforma montana
Polydispyrenia simuli
Weiseria palustris
RBS_Van12
UBN_Seattle4
UBN_Seattle1
Octosporea muscaedomesticae
UBN_Seattle11
Amblyospora californica
Amblyospora canadensis
Amblyospora khaliulini
Amblyospora opacita
Amblyospora ferocious
Hazardia milleri
Hazardia sp. isolate 1
UBN_Seattle6
UBN_Seattle5
Microsporidium sp. MIC1 strain MIC1 BRN01
Berwaldia schaefernai
Marssoniella elegans
RBS_Van13
Amblyospora bracteata
Clade I
WBS_Van14
Antonospora locustae
Paranosema grylli
Paranosema whitei
Antonospora scoticae
Microsporidium sp. BBRE3
UBN_Seattle10
UBN_Seattle9
Microsporidium sp. BKES2
Anncalia algerae
Thelohania solenopsae
Bacillidium sp.
Janacekia debaisieuxi
Bryonosema plumatellae
Pseudonosema cristatellae
Trichonosema pectinatellae
Clade V
Conidiobolus coronatus
Basidiobolus ranarum
0.2

Figure 2.2 Microsporidian phylogeny showing the diversity of the 22 novel microsporidian sequences detected in this study

The major microsporidian clades are labeled. Dotted line shows "clade 2" groups. The Bayesian tree shown contains the node support in the following order: posterior probabilities/maximum likelihood/bootstrap. Support values below 0.5 are shown as "- -". * denotes species retrieved from more compost and soil samples.

Chapter 3: Microsporidian infection in a free-living marine nematode

3.1 Introduction

Microsporidian infections (microsporidiosis) are highly variable and cause a wide range of symptoms depending on the host and the microsporidium involved. Infections are usually acquired by ingestion of spores (horizontal transmission), but vertical transmission (from mother to offspring) has been observed (mainly in insects) (Becnel and Andreadis 1999). Microsporidian infections may be acute or chronic, affect one or multiple tissue types, cause mild or lethal symptoms, and even change the host's sex (Hurst 1991; Murray and Weiss 1999).

Nematodes, commonly known as roundworms, are ubiquitous in the environment. In marine sediments, nematodes account for more than 90% of individual animals and over 50% of the total biomass (Giere 2009), yet reports of microsporidian infections in this animal group are limited and unclear. Indeed, most reports of microsporidian infections in nematodes, including marine nematodes, failed to clearly demonstrate morphologically (presence of polar filament) and genetically that the infecting agent was a microsporidian (Kudo, and Hetherington 1922; Hopper et al.1970; Poinar and Hess 1986; Poinar 1988). The only exception is the microsporidian infection described 4 years ago in a lab strain (N2) of the soil nematode *Caenorhabditis elegans* (Troemel et al. 2008). In this strain, ingestion of microsporidian spores (*Nematocida parisii*) causes an acute and extremely virulent (100% lethal) infection that affects only the intestinal tissues. *N. parisii* was originally isolated from a wild *Caenorhabditis sp.* and transferred to the lab strain; effects of the parasite on the native host are unclear. Given that nematodes are arguably the most abundant and diverse animal phylum (Fonseca et al. 2010), the

dearth of knowledge regarding their microsporidian parasites is surprising. Here we present the first morphological and molecular description of a microsporidian infection in a marine nematode. We describe *Sporanauta perivermis*, a novel microsporidian species infecting the free-living marine nematode, *Odontophora rectangula* (family Axonolaimida). This is, to our knowledge, the first confirmed case of an interaction between a fungal group and nematodes in marine environments (Bhadury et al. 2009; Bhadury et al. 2011). Moreover, the characteristics of *S. perivermis* infection challenge our current understanding of how microsporidia and nematodes interact in the wild by providing a completely different infection pattern from that observed in the lab with *N. parisii*. Unlike infection with *N. parisii*, infection with *S. perivermis* is mild and not severe, chronic and not acute, and it affects the hypodermal and muscles tissues and not the intestines. *S. perivermis* even differs in its mode of transmission, which appears to be vertical (infection of the eggs) and not exclusively horizontal (ingestion of spores) as it is in *N. parisii*. Indeed, by comparison, *S. perivermis* infection represents the opposing end of the spectrum of microsporidian infection variability, suggesting that host-parasite relationships between nematodes and microsporidia are considerably more complex and diverse than previously considered.

3.2 Materials and methods

3.2.1 Marine nematode sampling

Marine nematodes were collected in July and August 2010 and 2011 from Boundary Bay beach (49.013N, 123.036W), Tsawwassen (British Columbia, Canada). Surface sand and sediment samples (1 to 10 cm deep) were collected at low tide using sterile 50-ml falcon tubes (filled 3/4 with sand and 1/4 with seawater). All samples were kept on ice until they were stored

permanently at 4°C in the dark and with loosened caps. For each tube, 1 to 2 g of sand was transferred to a sterile petri dish and flooded with cold (4°C) sterile seawater. Live nematodes were observed using a dissecting microscope and transferred individually to a sterile petri dish containing cold sterile seawater. Marine nematodes were then used for DNA extraction, fluorescent in situ hybridization (FISH), and transmission electron microscopy (TEM).

3.2.2 Microsporidian and nematode rDNA extraction and sequencing

Microsporidian and marine nematode rDNA were initially extracted from 0.5 to 1 g of sand using the Mobio UltraClean soil DNA isolation kit (Bio/Can Scientific). Beads (included in this kit) and a beadbeater (Mini-Beadbeater-1; BioSpec Products Inc.) were used to disrupt the tissues during the lysis step. This step was modified from the manufacturer's protocol by adding a 15-min incubation period at 70°C with a 20-s beadbeating (2,500 rpm) treatment every 5 min. Microsporidian small-subunit (SSU) ribosomal DNA (rDNA) sequences were amplified using the microsporidian-specific forward primer 18ss (35) and a novel microsporidian-specific primer Micro33R (5′-TAGAGACCGTTGTAGTTCCG-3′) (this study). This microsporidian primer set amplifies fragments of 550 to 650 bp long from the 5′ end of the microsporidian SSU rDNA. PCR amplicons were separated on agarose gels (2%), purified with the UltraClean 15 Mobio DNA purification kit (Bio/Can Scientific), and cloned using the TOPO TA cloning kit with pCR 2.1 vector (Invitrogen). At least three independent clones were sequenced for each DNA extraction. The same procedures were performed on individual live nematodes to determine the host and prevalence of microsporidian infections. Marine nematodes were barcoded using 18S rDNA marine nematode-specific primers (M18F 5′-AGRGGTGAAATYCGTGGAC-3′ and M18R 5′-TCTCGCTCGTTATCGGAAT-3′) (2) and an *S. perivermis*-specific primer set (5′-

CGAGATGTGCAGTATGTCTGGG-3′) designed from previously amplified sequences. These primers were also used in combination with 530 and 1492 microsporidian primers (35) to generate a large 5'end fragment (1,385 bp) of *S. perivermis* SSU rDNA sequence (GenBank accession no. JN195782).

Given that the initial isolations were done with a pooled, mixed marine nematode sample, we performed DNA extractions on individual marine nematodes to determine the host. Using a primer set specific for a fragment of the SSU sequence described above, individual nematodes were screened for both their infection status with the novel microsporidian and with a set of nematode barcoding primers. In all cases, microsporidian infections were observed only in a single nematode species, predicted to be *Odontophora rectangula* (Axonolaimida). Overall, the majority of *O. rectangula* nematodes (84%; n = 27) were infected, and the proportion of infected individuals in each sex was almost the same (83% males and 84% females). Morphologically, these nematodes match the predicted barcoding identification; *O. rectangula* nematodes are distinguished by their body size and tail shape and for having a distinctive set of large teeth (Lorenzen 1971; Platt and Warwick 1988).

3.2.3 Phylogenetic analysis

The small-subunit rDNA sequence of *S. perivermis* was examined phylogenetically by comparing it with that of 43 other microsporidian species that were selected to include representatives from the five major microsporidian groups (Vossbrinck and Debrunner-Vossbrinck 2005). We also included an environmental microsporidian sequence (accession no. FJ756061.1) identified from the nucleotide BLAST analysis. The fungal species *Basidiobolus*

ranarum and *Conidiobolus coronatus* were included as outgroups (Vossbrinck and Debrunner-Vossbrinck 2005). All sequences were obtained from GenBank.

All sequences were viewed and aligned using the molecular sequence analysis multiplatform SeaView version 4. The alignment was adjusted automatically (trmAL;Phylemon) and by eye. The final alignment was used in three phylogenetic analyses: Bayesian inference, maximum likelihood (ML), and approximate likelihood ratio test based on Shimodaira-Hasegawa-like procedure (aLRT-SH).

To perform Bayesian inference, we used the program MrBayes version 3.2. One million generations were run using the general time reversible (GTR) model with two separate runs of four chains each. Sampling was performed every 1,000 trees of which the initial 25% (approximately 25 thousand trees) were discarded before the generation of the best supported consensus tree. To test the position of *S. perivermis* we performed ML and aLRT-SH tests, we used Phyml version 3.0 using default settings and 100 bootstraps.

3.2.4 Transmission electron microscopy

Live *O. rectangula* nematodes were transferred into a sterile polyethylene embedding capsule (size 3; BEEM Inc.) containing 30 µl of cold (4°C) sterile seawater. Nematodes were centrifuged at 3,000 × g for 30 s, and cuticles were nicked with a razor blade. Fixation proceeded immediately by capping the capsules with a piece of Whatman filter paper soaked in a fixative solution containing 1% (wt/vol) osmium tetraoxide in 0.2 M sodium cacodylate buffer (pH 7.2) and left on ice for 30 min. Fixative solution was then added directly to each sample and kept on

ice for 2 h. This was followed by three 5-min washes with 0.2 M sodium cacodylate buffer (pH 7.2). The samples were dehydrated through an ethanol series (25%, 50%, 75%, 90%, 95%, and 100%) of 20 min at each step. Ethanol was substituted with an ethanol and acetone mixture (1:1) twice (20 min each) and then repeated twice with pure acetone. Acetone was removed, and a mixture (1:1) of acetone and Spurr's resin was added and left at room temperature for 24 h. Spurr's resin was changed twice (24 h each) before polymerizing overnight (12 h) at 70°C. Sectioning of each resin was performed using a Leica EM UC6 ultramicrotome (Leica Microsystems) and then stained twice with 2% (wt/vol) uranyl acetate and lead citrate (Reynolds 1963). Each ultrathin section was examined on a Hitachi H7600 TEM.

3.2.5 Fluorescent *in situ* hybridization

Staining of *S. perivermis* was modified from methods described previously (Troemel et al. 2008). A specific *S. perivermis* probe (5' GTCCAGTCAGGGTCCTCAC 3') targeting *S. perivermis*'s SSU rDNA gene was purified by high-performance liquid chromatography (HPLC) and synthesized with Quasar 570 (Cy3) at the 5′ end (Biosearch Technologies, Inc.). Live *O. rectangula* nematodes were placed in a 1.5-ml Eppendorf tube containing 30 µl of sterile seawater and aggregated into a pellet by centrifugation (3,000 × g for 30 s). Excess seawater was removed, and cuticles were nicked with a razor blade before a 2-h fixation with 4% paraformaldehyde. The samples were then washed twice with 250 µl of phosphate-buffered saline (PBS) plus 0.1% Tween 20 and hybridized at 46°C for 12 h with 60 µl of hybridization buffer (900 mM NaCl, 20 mM Tris [pH 7.5], 0.01% SDS, and 5 ng/µl probe). Following this, samples were washed with 500 µl of wash buffer (900 mM NaCl, 20 mM Tris [pH 7.5], 0.01% SDS, 5 mM EDTA) and placed at 48°C for 1 h. Samples were then stained and mounted with

4′,6′-diamidino-2-phenylindole (DAPI) Vectashield mounting medium (Vector Laboratories) and examined using an Olympus FV10i confocal microscope (Olympus Inc.). Marine nematodes collected from the same sand samples as *O. rectangula* were collected and stained alongside as negative controls.

3.3 Results

3.3.1 The free-living marine nematode *Odontophora rectangula* is infected with a microsporidian parasite

Live marine nematodes were collected at low tide from Boundary Bay beach (Tsawwassen, British Columbia, Canada). DNA was extracted from the nematodes, and microsporidian infection was assessed by PCR amplifying the microsporidian small-subunit (SSU) rRNA gene. An identical 668-bp fragment was amplified, and this sequence was most similar (88% similarity by BLAST) to an undescribed microsporidian sp. (accession no. FJ756061.1), suggesting the presence of a novel and single microsporidian infection in local nematodes.

3.3.2 Phylogenetic position of the novel microsporidian, *Sporanauta perivermis*

To establish the phylogenetic placement of the novel microsporidian SSU rDNA sequence, we compared it with 43 microsporidian species that span the known diversity of the group. Overall, recovered trees reflected our current understanding of microsporidian relationships, with the five major microsporidian clades strongly supported by all methods (Figure 3.1) (Vossbrinck and Debrunner-Vossbrinck 2005). Surprisingly, the new species did not show an affiliation with the only other known nematode-infecting microsporidian (*N. parisii*). Instead, all trees strongly

support placing the microsporidian infecting *O. rectangula* within clade IV (Figure 3.1). We have named this species *Sporanauta perivermis* (for marine spores of roundworms).

The subclade containing *S. perivermis* includes four other microsporidian lineages: (i) the bark louse-infecting microsporidian *Mockfordia xanthocaecila* (Sokolova et al. 2010), (ii) the daphnia-infecting microsporidia *Ordospora colligata* (Refardt et al. 2002), (iii) an undescribed microsporidian species (top BLAST hit), and (iv) the genus *Encephalitozoon* (five species) that infect a variety of animal hosts (Figure 3.1). The position of *S. perivermis* relative to the rest of its subclade could not be fully resolved, even when restricting the analysis to members of this group and outgroup representatives within clade IV (data not shown).

3.3.3 Microscopic characterization of *S. perivermis*

O. rectangula nematodes were examined using standard light microscopy techniques for any behavioral changes (i.e., less active) or any morphological abnormalities such as enlargement of specific tissues that could be signs of microsporidian infection. However, no external signs of infection were evident. Therefore, to examine the parasite's effect on the nematode and confirm morphologically that *S. perivermis* is a microsporidian parasite, we examined *O. rectangula* nematodes by transmission electron microscopy (TEM). All nematode digestive tissues (pharynx, intestine, and lumen) appeared normal. However, dense oval structures were located within the hypodermal and muscle tissues (Figures 3.2.A and B). These structures were morphologically consistent with microsporidian spores by their size (2.0 to 2.5 μm by 1.1 to 1.5 μm) and ovoid shape. Conclusive evidence that these structures are indeed microsporidian spores includes the presence of a polar filament (3 or 4 coils), an anchoring disk surrounded by

polaroplast membranes, and a thin electron-dense exospore over a thick electron-transparent endospore surrounding the cell membrane (Figures 3.2.C and D).

Spores were not observed to be in direct contact with the host cytoplasm. Instead, each microsporidian spore appeared to be enclosed within a vesicle that was often observed to be connected to adjacent vesicles (Figure 3.2). This resulted in a large "cluster" of interconnected vesicles containing *S. perivermis* spores. Proliferative microsporidian life cycle stages (i.e., meronts) were not observed in the tissues examined.

3.3.4 Fluorescent *in situ* hybridization reveals *S. perivermis* infection of *O. rectangula* eggs

To further assess the extent of *S. perivermis* infection in *O. rectangula*, we performed fluorescent in situ hybridization (FISH) using a fluorescent probe targeting the *S. perivermis* SSU rDNA sequence. Surprisingly, FISH indicated infection differences in male and female nematodes. In males, FISH confirmed our previous TEM observations in which *S. perivermis* infection was localized to the hypodermal and muscular tissues, surrounding the intestine but never within it (Figure 3.3). Within these tissues, spores were observed in clusters (few to hundreds of spores) which appeared to be distributed along the length of the body but were never observed in the head. In addition, spore "clusters" appeared enclosed within large vesicles. We interpret these as vesicles of microsporidian origin due to the hybridization of the microsporidian tag. *S. perivermis* spores were oval and consistent in size (~2 μm by 1 μm) with those observed by TEM.

In females, spores were also observed in clusters within the hypodermal and muscle tissues; however, the spores appeared to be markedly less abundant. Surprisingly, FISH revealed that in female nematodes the microsporidian infection was localized to *O. rectangula* eggs (Figure 3.4). In all infected females examined, the eggs showed a very strong signal for *S. perivermis*, but the parasite did not appear to be in the spore stage, as spores were not observed within the eggs (Figure 3.4). Aside from the eggs, there appeared to be no other infection of female reproductive tissues.

A small number of juveniles were observed to be infected. Generally, the infection pattern was the same as in adults, but in some cases, the reproductive tissues were labeled with the FISH probe. The sex of most nematodes, including *O. rectangula*, cannot be resolved in juveniles, so it is unclear how this labeling pattern correlates with the gender differences observed in adults.

3.4 Taxonomy

3.4.1 *Sporanauta* n. gen. Ardila-Garcia & Fast 2012.

This is a novel microsporidian lineage that belongs to microsporidian clade IV (Vossbrinck and Debrunner-Vossbrinck 2005) based on SSU rDNA phylogenetic analyses. The closest relatives to *Sporanauta* are the microsporidian genera *Mockfordia*, *Encephalitozoon*, and *Ordospora*. The type species is *Sporanauta perivermis* Ardila-Garcia & Fast 2012. The Latin "sporo" (spore) and the Latin "nauta" (mariner) refer to microsporidian spores to the habitat (marine). Vouchers were deposited at the Herbarium Collection of the University of British Columbia (Accession no. F22194).

3.4.2 *Sporanauta* n. sp. Ardila-Garcia & Fast 2012.

The spores are ovoid and measured 2.0 to 2.5 μm by 1.1 to 1.5 μm. The polar filament has 3 or 4 coils. Spores are found in vesicles that prevent them from being in direct contact with the host cells. Vesicles may contain a few spores to hundreds of spores. Infection is localized to the hypodermal and muscle tissues in adults, mature eggs in adult females, and the reproductive tissues of juveniles. Infection does not affect the intestinal tissues. Infection is chronic and appears to cause minor symptoms (if any) on the host. Transmission appears to be vertical (transovary). The type host is the free-living marine nematode *Odontophora rectangula* (family Axonolaimidae). The Latin "peri" (round) and the Latin "vermis" refer to roundworms, the common name for nematodes.

3.5 Discussion

Fungi and nematodes are highly abundant and diverse in marine ecosystems (Hyde et al 1998; Lambshead and Boucher 2003), but the nature of their interactions remains largely unknown (Bhadury et al. 2009l; Bhadury et al. 2011). The present study is, to our knowledge, the first to provide morphological and genetic evidence to show that fungi (Microsporidia) can parasitize marine nematodes. We describe the infection of a novel microsporidian species, *S. perivermis*, in its wild host, the free-living marine nematode *O. rectangula*. The characteristics of *S. perivermis* infection challenge the current view of the nature of microsporidian infections in nematodes. The only other described microsporidian infection in nematodes involves inoculation of *N. parisii* from wild nematodes to a *C. elegans* lab strain (Troemel et al. 2008; Estes et al. 2011; Cuomo et al. 2012). Here the exposure to a microsporidian parasite was lethal, but it raises questions as to whether this particular parasite or any other nematode-infecting microsporidian is as damaging

and virulent in its natural host. Our observations on *S. perivermis* infection in its wild host indicate that microsporidian infections in the wild can vary considerably in almost every aspect compared to that observed with *N. parisii*.

S. perivermis represents a novel microsporidian lineage that grouped with eight other species in a subclade of microsporidian clade IV. Its closest relatives were isolated from a diversity of hosts, including mammals (Didier et al. 1991; Didier et al. 1994; Didier and Bessinger 1999; Weber et al. 1994), lizards (Canning 1981), crustaceans (Refardt 2002), and insects (Lange et al. 2009; Sokolova et al. 2010). Despite their differences in hosts, all members of this subclade are morphologically similar in that they are considerably small (spore size, 2 to 4 μm) by microsporidian standards (spore size range, 2 to 40 μm). In addition, their spores are always found within vesicles that prevent them from being in direct contact with the host cytoplasm. Other members of the *S. perivermis* subclade, *O. colligata* and the *Encephalitozoon* group, also develop in isolation from their hosts' tissues. However, their separation is achieved by means of a membrane-bound parasitophorous vacuole (host origin) instead of a vesicle (Larsson et al. 1997; Schottelius et al. 2000). The host-parasite interface varies considerably for other members of clade IV, as some (i.e., *Endoreticulatus* species) develop in parasitophorous vacuoles, while others (i.e., *Nosema*) develop in direct contact with the host tissues (Cali and Takvorian 1999). Even though *N. parisii* spores were also observed inside vesicles (Troemel et al. 2008), *N. parisii* and the undescribed *Nematocida* sp. strain 1247 did not group in clade IV with *S. perivermis*. Instead, *Nematocida* falls within microsporidian clade II with their closest relative being the beetle-infecting microsporidian *Ovavesicula popillae* (a position consistent with Troemel et al. 2008).

S. perivermis and *N. parisii* also have stark differences in how they interact with their respective hosts. *S. perivermis* causes minor lesions (if any) in the hypodermal and muscle tissues and does not infect the intestinal tissues of *O. rectangula* nematodes. The parasites do not appear to affect *O. rectangula*'s motility, behavior, or life expectancy. In fact, the infection was highly prevalent (84%), and it was not possible to distinguish uninfected from infected nematodes with standard light microscopy. Conversely, *N. parisii* infection of the *C. elegans* N2 lab strain was reported to invade the intestine and be highly destructive, sickening N2 nematodes severely, reducing their motility considerably, and causing rapid death (Troemel etal. 2008; Eses et al. 2011). Each case represents opposing ends on the full spectrum of the host-parasite relationships between animals and microsporidia (Didier and Bessinger 1999). The features of *S. perivermis* are typical of chronic microsporidian infections, which are usually asymptomatic and cause minor effects on the host. On the other hand, *N. parissii* infection is typical of unbalanced, opportunistic, acute infections which are usually characterized by uncontrolled microsporidian propagation, severe symptoms, and high host lethality (Didier and Bessinger 1999). The striking differences between the two may be explained by the fact that our observations were performed in the natural host of *S. perivermis*. Our observations on *S. perivermis* suggest that nematodes are capable of dealing with microsporidian infections and that *N. parisii* is perhaps a "nematode killer" of *Caenorhabditis* (particularly N2) but that its lethality should not be generalized as a feature of all nematode-infecting microsporidia. Indeed, one would expect microsporidian-nematode relationships to encompass the full spectrum of infection (Didier and Bessinger 1999) once additional species are described and their interactions with their hosts are understood.

Transmission of microsporidian parasites in their host is generally horizontal (ingestion of spores) as was reported for *N. parisii*, while microsporidian vertical transmission in this animal group remains unknown. Vertical transmission of microsporidia is common in insects, in which it is usually transovarial and involves the transfer of the parasite within the female's eggs (Becnel and Andreadis 1999). In the present study, we provided evidence that microsporidian parasites may be transmitted in this manner in nematodes. *S. perivermis* infects the eggs of adult *O. rectangula* females and the reproductive tissues of *S. perivermis* juveniles, suggesting that *S. perivermis* is transmitted from mother to offspring via the eggs.

Our observations of the infection of *S. perivermis* in the free-living marine nematode *O. rectangula* provide the first description of a fungal parasite of nematodes in marine environments. They provide the first indications that the interactions between microsporidia and nematodes in the wild can be highly intricate and involve versatile adaptations such as microsporidian vertical transmission. Our understanding of microsporidia in nematodes is no longer limited to “nematode killers” but has broadened to include interactions more indicative of coexistence.

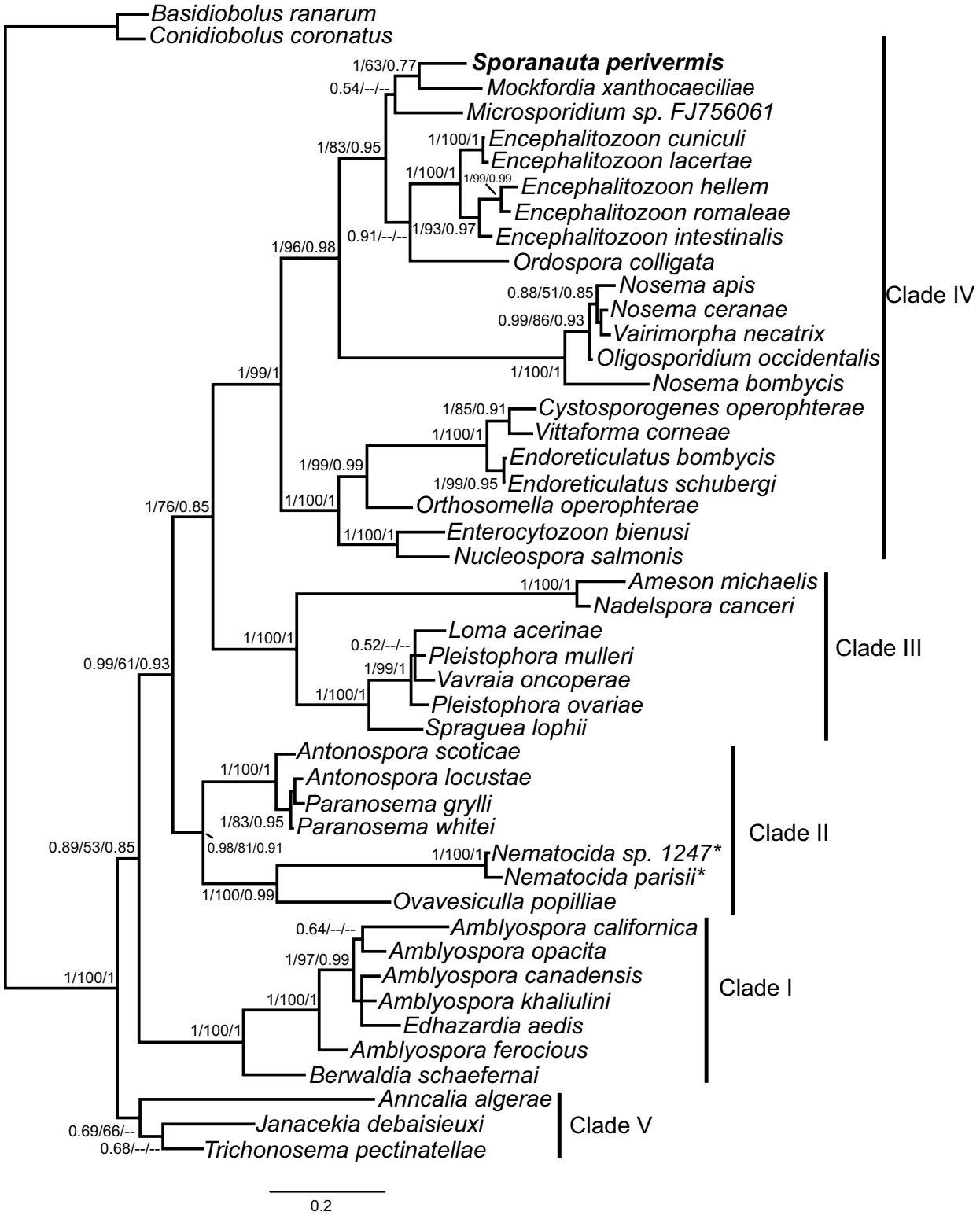
Basidiobolus ranarum
Conidiobolus coronatus
Sporanauta perivermis
Mockfordia xanthocaeciliae
Microsporidium sp. FJ756061
Encephalitozoon cuniculi
Encephalitozoon lacertae
Encephalitozoon hellem
Encephalitozoon romaleae
Encephalitozoon intestinalis
Ordospora colligata
Nosema apis
Nosema ceranae
Vairimorpha necatrix
Oligosporidium occidentalis
Nosema bombycis
Cystosporogenes operophterae
Vittaforma corneae
Endoreticulatus bombycis
Endoreticulatus schubergi
Orthosomella operophterae
Enterocytozoon bienusi
Nucleospora salmonis
Ameson michaelis
Nadelspora canceri
Loma acerinae
Pleistophora mulleri
Vavraia oncoperae
Pleistophora ovariae
Spraguea lophii
Antonospora scoticae
Antonospora locustae
Paranosema grylli
Paranosema whitei
Nematocida sp. 1247*
Nematocida parisii*
Ovavesiculla popilliae
Amblyospora californica
Amblyospora opacita
Amblyospora canadensis
Amblyospora khaliulini
Edhazardia aedis
Amblyospora ferocious
Berwaldia schaefernai
Anncalia algerae
Janacekia debaisieuxi
Trichonosema pectinatellae
Clade IV
Clade III
Clade II
Clade I
Clade V
1/63/0.77
0.54/--/--
1/83/0.95
1/100/1
1/100/1
1/99/0.99
0.91/--/--
1/93/0.97
1/96/0.98
0.88/51/0.85
0.99/86/0.93
1/100/1
1/99/1
1/85/0.91
1/100/1
1/99/0.99
1/99/0.95
1/100/1
1/76/0.85
1/100/1
1/100/1
0.99/61/0.93
1/100/1
0.52/--/--
1/99/1
1/100/1
1/100/1
1/83/0.95
0.98/81/0.91
0.89/53/0.85
1/100/1
1/100/0.99
0.64/--/--
1/97/0.99
1/100/1
1/100/1
1/100/1
0.69/66/--
0.68/--/--
0.2

Figure 3.1 Phylogenetic placement of the novel microsporidium *S. perivermis*

The tree shown was obtained by Bayesian inference using microsporidian SSU rDNA sequences. The same tree topology was obtained by maximum likelihood. Support values from Bayesian inference, maximum likelihood bootstrapping, and the approximate likelihood ratio test Shimodaira-Hasegawa-like procedure (BI/MLB/aLRT-SH) are indicated in the figure. Support values below 50% are not shown. Other nematode-infecting microsporidia are denoted by an asterisk. Bar at the bottom indicates estimated number of changes per site.

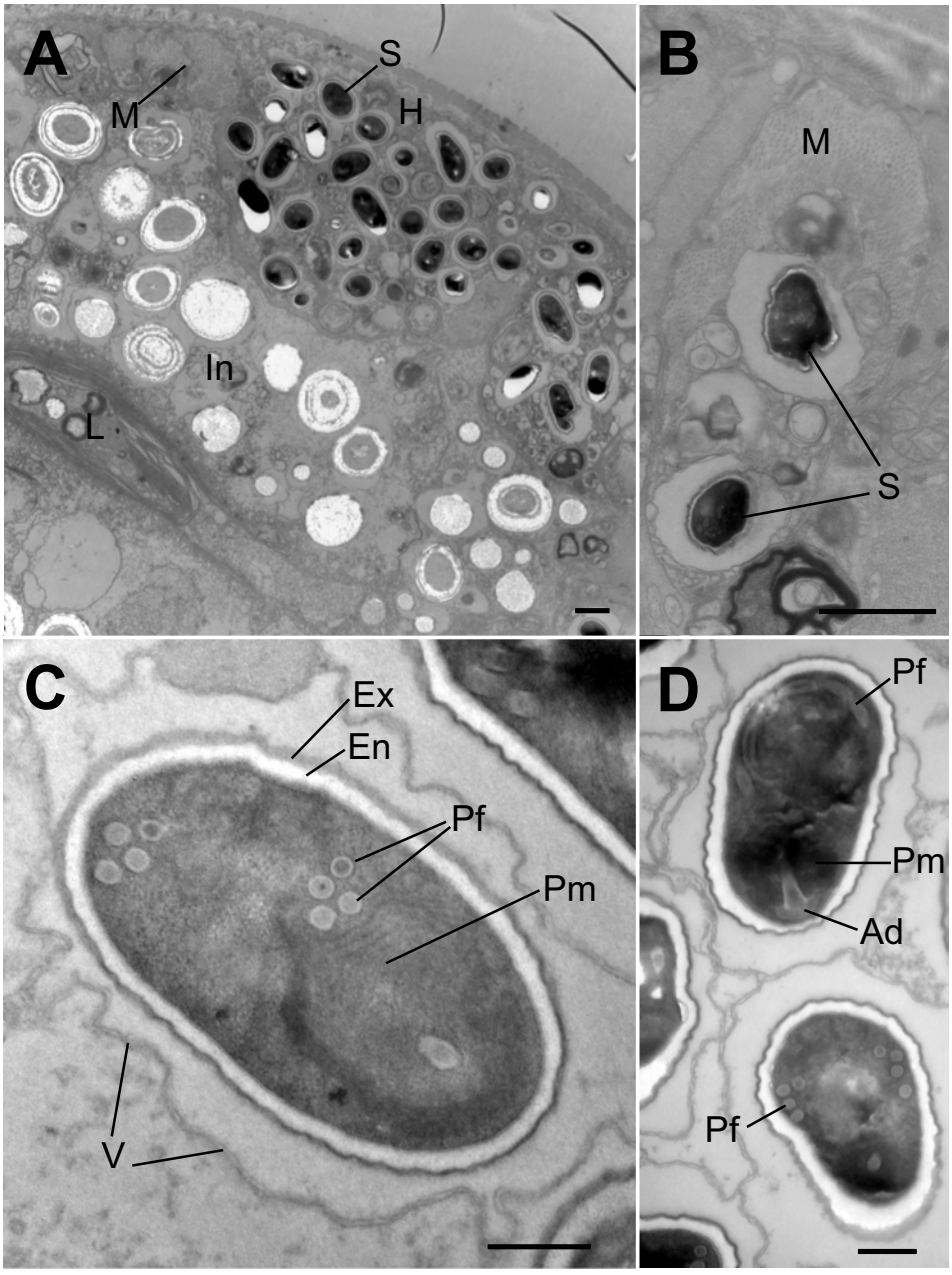

Figure 3.2 Ultrastructure of *S. perivermis* spores by TEM

(A) Cross section of an infected *O. rectangula* nematode showing the localization of *S. perivermis* spores (S) in the hypodermal tissues (H). Note the absence of spores in the lumen (L) and intestinal (In) tissues. Localization of the spores in the muscle tissues (M) is also shown. Bar = 0.5 µm. (B) *S. perivermis* spores surrounded by muscle fibers (M). Bar = 2 µm. (C) *S. perivermis* spore showing the four coils of its polar filament (Pf), the exospore (Ex), the endospore (En), the polaroplast membranes (Pm), and a vesicle (V) enclosing the spore. Bar = 0.5 µm. (D) *S. perivermis* spores showing four coils of the polar filament (Pf), the anchoring disk (Ad), and the polaroplast membranes (Pm). Bar = 0.5 µm

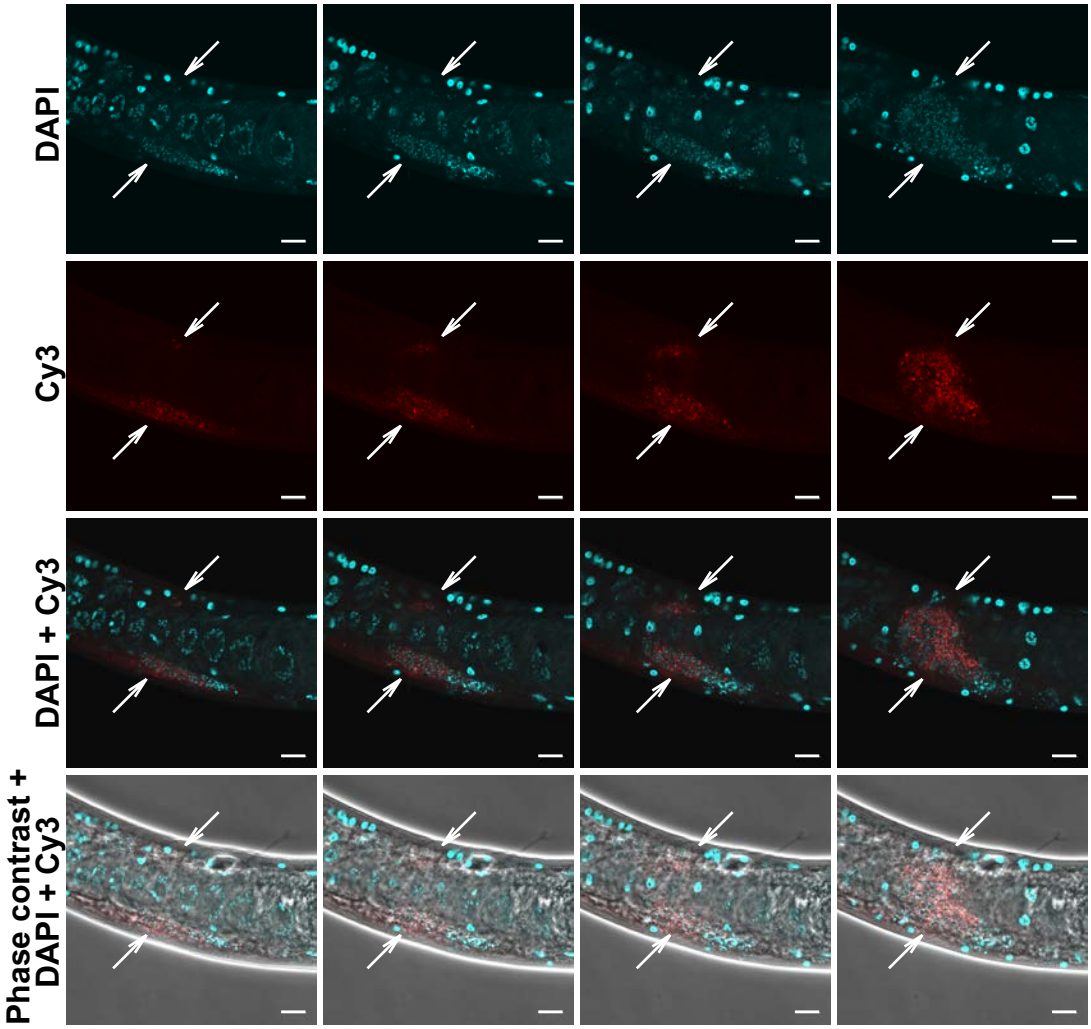

Figure 3.3 Localization of *S. perivermis* infecting the free-living marine nematode *O. rectangula* by fluorescent *in situ* hybridization (FISH)

The columns show cross sections of nematode tissues at sequential depths, moving from interior to exterior (left to right) to show *S. perivermis* surrounding the intestine and localized to hypodermal and muscle tissues (long white arrows). Note the absence of *S. perivermis* in the intestine, whose position is clearly marked by the concentric rings of DAPI-stained nematode nuclei in the leftmost column. Each row shows a different light filter showing the nuclear stain DAPI (shown in blue), the *S. perivermis* fluorescent probe (Cy3 [shown in red]), a combination of the two dyes, and the view of the image under phase contrast. Bars = 10 μm.

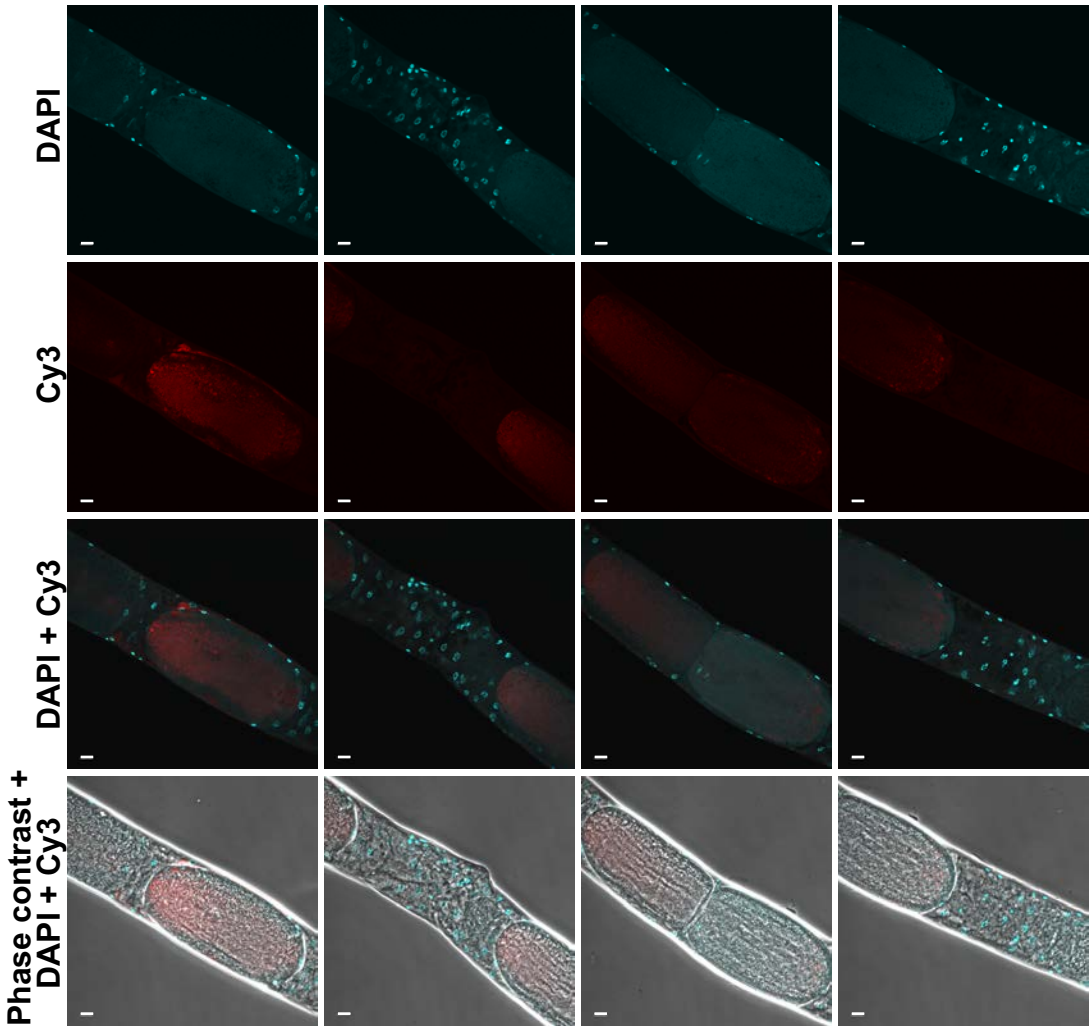

Figure 3.4 *S. perivermis* infection in *O. rectangula* eggs by FISH

Each column shows a sequence of images taken on the same plane to show the localization of *S. perivermis* inside eggs (arrow). Each row shows a different light filter: the nuclear stain DAPI (shown in blue), the *S. perivermis* fluorescent probe (Cy3 [shown in red]), a combination of the two dyes, and the view of the image under phase contrast. Bars = 10 μm.

Chapter 4: *Sporanauta perivermis* infection in juvenile *Odontophora rectangula*

4.1 Introduction

In Chapter 3, I characterized the microsporidian parasite *S. perivermis* infecting the free-living marine nematode *O. rectangula*. I revealed that in adult *O. rectangula* nematodes, *S. perivermis* infects the hypodermal and muscle tissues of both males and females. Infection of these tissues was characterized by the presence of *S. perivermis* spores, which were usually more abundant in males than in females. Adult males and females also differed in the infection pattern of their reproductive tissues. No infections were observed in male reproductive tissues, but in females, *S. perivermis* was localized inside the eggs and surrounding reproductive tissues. In these tissues, *S. perivermis* was observed to be in an intracellular life-stage (possibly meront) and spores were not observed. The presence of *S. perivermis* inside eggs of infected gravid females suggested that *S. perivermis* was transmitted vertically (from mother to offspring).

Since I described *S. perivermis*, a novel microsporidian parasite (*Nematocenator marisprofundi*) was found infecting another free-living marine nematode (*Desmodora marci*) (Sapir et al. 2014). Similar to *S. perivermis*, *N. marisprofundi* was reported to cause a chronic infection that affected the muscle and reproductive tissues of adult *D. marci* nematodes (Sapir et al. 2014). But *N. marisprofundi*'s infection pattern differed from *S. perivermis* in that *N. marisprofundi* infected the reproductive tissues of both genders (Sapir et al. 2014). In adult *D. marci* males, *N. marisprofundi* was reported infecting the cloaca and vas deferens only. In adult *D. marci*

females, *N. marisprofundi* was found solely in the uterus and, in contrast to *S. perivermis*, it was not found inside the eggs of infected *D. marci* gravid females (Sapir et al. 2014). Based on *N. marisprofundi*'s infection pattern, the authors proposed that *N. marisprofundi* was transmitted sexually but they did not completely rule out the possibility that *N. marisprofundi*'s transmission also occurred vertically in a manner similar to that of *S. perivermis* (Sapir et al. 2014). The absence of infected eggs in gravid females could support a different mode of sexual transmission for *N. marisprofundi* that is still vertical: transovum transmission (see section 1.1.3). In transovum vertical transmission, microsporidian spores could stick to the surface of the egg and infect the larvae at eclosion (Becnel and Andreadis 1999). This mode of transmission was documented for the moth-infecting microsporidian *Endoreticulatus shubergi* (Goertz and Hoch 2008) and it is possible that *N. marisprofundi* is transmitted in a similar manner.

S. perivermis and *N. marisprofundi* differ considerably from the only other microsporidian known to infect nematodes, *Nematocida parisii* (Troemel et al. 2008). *N. parisii* was isolated from wild *Caenorhabditis* nematodes (soil-dwelling) and was successfully transferred to a lab culture of *C. elegans* (N2 strain) (Troemel et al. 2008). In contrast with *S. perivermis* and *N. marisprofundi*, *N. parisii*'s infection in adult *C. elegans* was acute and highly virulent (100% lethal) (Troemel et al. 2008). In addition, *N. parisii* differed in that it only infected the intestines and it did not infect the reproductive tissues (including eggs) of adults (Troemel et al. 2008). The characterization of *N. parisii*'s infection in *C. elegans* lab cultures permitted the description of *N. parisii*'s transmission and infection pattern through the entire *C. elegans*'s life cycle: the transmission of *N. parisii* was exclusively horizontal (oral ingestion of spores) and not vertical (Troemel et al. 2008). Eggs and the dauer stage (does not feed) were never infected, while all

other juvenile stages (L1, L2, L3, and L4) acquired an intestinal infection as observed in adults (Troemel et al. 2008). This is the only description available for a microsporidian infection in juvenile nematodes since few or no observations in juvenile hosts were reported for *S. perivermis* (Chapter 2) and *N. marisprofundi* (Sapir et al. 2014). In spite of this, it is reasonable to hypothesize that *S. perivermis* and *N. marisprofundi* differ considerably from *N. parisii* in how they interact with juvenile nematodes. This hypothesis is based in part on the distinct infection patterns observed for these microsporidians in adult hosts, and on the strong possibility that *S. perivermis* (Chapter 3) and *N. marisprofundi* are transmitted vertically, and not only horizontally like *N. parisii*.

Vertically transmitted microsporidians can evolve complex host-parasite interactions that are not observed in microsporidians that are only transmitted horizontally (Becnel and Andreadis 1999). For instance, "male-killing" and feminization of the host are solely observed in microsporidians that are transmitted vertically (Dunn and Smith 2001; Ironside et al. 2003). "Male-killing" microsporidians are lethal to males but benign to females and this is often associated with a higher load of parasite in males when compared to females (Dunn and Smith 2001; Andreadis 2007). In mosquitoes, "male-killing" microsporidians (genus Amblyospora) kill males in their last larval stage (fourth instar) but infected female larvae develop into normal adults (Hurst 1991; Andreadis 2007). In contrast, feminizing microsporidians do not kill male hosts but convert them into females (Rodgers-Gray et al. 2004; Terry et al. 2004; Jahnke et al. 2013). In amphipods, such microsporidians (e.g. *Nosema granulosis*) modify the androgenic gland of male larvae to transform them into phenotypic females that develop as normal and fertile adults (Rodgers-Gray et al. 2004; Terry et al. 2004; Jahnke et al. 2013). "Male-killing" and feminization only take

place during juvenile development and, for this reason, they are only detected in immature hosts making these events difficult, or even impossible, to detect in adult hosts (Becnel and Andreadis 1999; Dunn and Smith 2001; Andreadis 2007; Jahnke et al. 2013). Indeed, examination of host larval stages has often proved essential to improving our understanding of microsporidian host-parasite interactions and life cycles during vertical transmission. For instance, intracellular stages of the vertically transmitted microsporidian *Thelohania solenopsae* were only observed in the egg and larval stages of ants (*Solenopsis invicta*), while spores were only observed in adult ants (Knell et al. 1977; Briano et al. 1996). In mosquitos, microsporidian infections that are vertically transmited and are more easily detected in larvae and not in adults because they are most virulent (high parasite load) and often lethal in the last larval stage (Andreadis 2007).

Given the importance of characterizing microsporidian infections in immature hosts, I examined *O. rectangula* juveniles infected with *S. perivermis* by fluorescent in situ hybridization (FISH). My objective was to assess similarities and differences in infection between juveniles and adults, including parasite life stage, infected tissue location, and degree of infection. Gender comparisons were expected to be limited, as sex cannot be determined in juvenile free-living marine nematodes. Juveniles lack gender-defining morphocharacters: the spicule in males and the vulva in females, as these are only attained in the adult stage. I characterized the infection in *O. rectangula* juveniles by performing fluorescent in situ hybridization (FISH) following the same protocol I used to examine the infection in adult *O. rectangula* (Chapter 3). FISH showed two distinct infection patterns in juveniles that resembled the infection patterns observed in adults: 1. Pronounced infection of the hypodermal and muscle tissues (similar to adult males) 2. Infection of the reproductive tissues (similar to adult females). Based on this, I hypothesize that

the infection patterns may serve to predict the sex of juveniles prior to spicule/vulva development. Juveniles destined to be males are those in which the infection affects the hypodermal and muscle tissues only, while juveniles destined to be females are those in which the infection involves the reproductive tissues. During the examination of juvenile nematodes, I encountered an infected adult non-gravid female in which the infection was localized in the uterus. Overall, my results suggest that host-parasitic interactions between *S. perivermis* and *O. rectangula* vary depending on the sex and life stage of the host, and that *S. perivermis* infects *O. rectangula* eggs in the uterus of gravid females suggesting that *S. perivermis* vertical transmission is transovum and not transovarial.

4.2 Methods

4.2.1 Nematode sampling

O. rectangula nematodes were collected and examined from sand samples collected at Boundary Bay beach (49.013N, 123.036W) (British Columbia, Canada) in the summers of 2010, 2011, and 2012. Surface sand samples (1 to 10 cm deep) were collected at low tide using sterile 50-ml falcon tubes and were stored permanently at 4°C in the dark with loosened caps. Small sand samples (1 to 2 g) were placed in sterile petri dishes and flooded with cold (4°C) sterile seawater. Since there are no morphological identification keys available for identifying *O. rectangula* juveniles, I included juvenile nematodes that appeared similar to adult *O. rectangula* nematodes in terms of overall body shape, head shape, mouth shape (odontia), and tail shape. Juveniles were only collected from sand samples in which at least one adult *O. rectangula* nematode was observed. Nematodes that were suspected to be *O. rectangula* juveniles were picked manually using a dissecting microscope (40x) and were transferred individually to sterile petri dishes

containing sterile seawater. Then, each nematode was examined in more detail using an inverted microscope (400x) and was included in this study based on its morphological similarity with adult *O. rectangula* nematodes. The abundance of nematodes suspected to be *O. rectangula* nematodes was usually high (hundreds) when examined at 40x, but only a small proportion met the morphological criteria when examined at 400x. Overall, 36 juvenile nematodes were selected for this study. Seven adult *O. rectangula* nematodes were included as positive controls for FISH.

To track *S. perivermis* infection throughout the development of the host, I attempted to establish an *O. rectangula* culture in the lab. I manually removed other nematode species from the sand samples, or manually transferred *O. rectangula* nematodes to seawater and sand grains collected from the same site. The food source of *O. rectangula* is unknown but I added algal debris, protists, and other nematode species from the original sand samples, and even bacteria (*E. coli*) from the lab. However, my attempts to establish an *O. rectangula* culture were unsuccessful. The nematodes would perish for unknown reasons a few days after disturbance.

4.2.2 FISH

FISH was performed as described in chapter 3. Nematodes were fixed for 2 hours in 4% paraformaldehyde. The fixative was then removed and the samples were washed with 250 µl of phosphate-buffered saline (PBS) containing 0.1% Tween 20. Washing was repeated before addition of 60 µl of hybridization buffer (900 mM NaCl, 20 mM Tris [pH 7.5], 0.01% SDS, and 5 ng/µl probe). The probe (5’ GTCCAGTCAGGGTCCTCAC 3’) was specific to *S. perivermis* SSU rDNA and was purified and synthesized with Quasar 570 (Cy3) at the 5′ end (Biosearch Technologies, Inc.) (Chapter 3). The hybridization step was performed at 46°C overnight (12

hours). The hybridization buffer was removed, washed with 500 µl of wash buffer (900 mM NaCl, 20 mM Tris [pH 7.5], 0.01% SDS, 5 mM EDTA), and placed at 48°C for 1 h. The nematodes were prepared for confocal imaging by mounting two to three nematodes on a glass slide with 4′,6′-diamidino-2-phenylindole (DAPI) Vectashield mounting medium (Vector Laboratories).

4.2.3 Imaging

Nematodes were imaged using an Olympus FV10i confocal microscope (Olympus Inc.) and the FV10-ASW imaging software (Version 02.01.03.10 Olympus Inc.). Nematode body sizes were measured using the rule tool of the FV10-ASW imaging software (Figure 4.1) (Version 02.01.03.10 Olympus Inc.). Stacked images were obtained from infected tissues and were used to generate 3D images using Volocity 3D image analysis software (Version 6.3 Perkin Elmer Inc.).

4.3 Results

4.3.1 Juvenile *O. rectangula* nematodes

To improve our understanding of the host-parasite relationship between *O. rectangula* and *S. perivermis*, I characterized *S. perivermis* infection in *O. rectangula* juveniles. The estimated prevalence rate was 25% (n = 36) and was considerably lower than the prevalence observed in adults (84%) (Chapter 3). It was not possible to specifically determine the life stage of the *O. rectangula* juveniles examined in this study since these nematodes cannot be reared in the lab and there are no morphological keys available for these life stages. Therefore, we used an arbitrary designation for juveniles, based on size and lack of mature reproductive structures. (See Methods).

4.3.2 *S. perivermis* infection in *O. rectangula* juveniles

S. perivermis infection was localized by FISH in nine *O. rectangula* juveniles. Infections were not uniform and were observed to display three distinct infection patterns: Two patterns closely resembled the infection patterns observed in adults (Chapter 3) while a third was distinct to juveniles. Each of these juvenile infection patterns is described below.

4.3.3 *S. perivermis* infection in *O. rectangula* juveniles resembles infection in adult *O. rectangula* males

There were three *O. rectangula* juveniles infected with *S. perivermis* spores localized below the cuticle in a region that corresponds with the expected location of the hypodermis (Figure 4.2). It was not possible with FISH to determine whether the longitudinal muscles located below the hypodermis were also infected as observed in adults by TEM (Figure 3.2), but this may also occur in juveniles. In these juveniles, *S. perivermis* spores were packed in "pockets" that contained a few to hundreds of spores (Figure 4.2). This pattern was the same as that generally observed in adult *O. rectangula* males (Figure 3.3). In addition, the spores observed by FISH in these juveniles were highly similar in shape (oval) and size (~ 2 μm long by ~ 1 μm width) (Figure 4.2) to the spores observed by FISH in adults (Figure 3.3). High numbers (thousands) of spores (Figure 4.2) were observed in only one juvenile, while small spore numbers (dozens) were observed in two other juveniles suggesting that *S. perivermis* virulence varies in juvenile *O. rectangula*. Variation in *S. perivermis* spore numbers was also observed in adults (n = 7) where high numbers of spores (thousands) were generally only observed in males while small numbers of spores (dozens) were common in females (Chapter 3). However, it was not possible to

correlate spore load and gender in juveniles because juvenile nematodes lack mature reproductive tissues.

4.3.4 *S. perivermis* intracellular stage infect the hypodermis of *O. rectangula* juveniles

FISH showed that *S. perivermis* infection in four *O. rectangula* juveniles was unique in that *S. perivermis* was observed at an intracellular stage (likely meronts) (Figure 4.3). The intracellular stage was circular in shape and not oval (as spores), measured 1-1.5 μm in diameter (smaller than spores), and did not appear to have an external spore wall (Figures 4.3). *S. perivermis* spores were not observed in these juveniles (Figure 4.3). This is in sharp contrast with *S. perivermis* infection of the hypodermal tissues in other juveniles (Figure 4.2) and adults (Figure 3.3) in which *S. perivermis* spores were only observed and the intracellular stage appeared absent. This could suggest *S. perivermis* sporogony may be synchronized with the host's development (e.g. molting) or hypodermal configuration.

The hypodermis of the *O. rectangula* juveniles infected with *S. perivermis* intracellular stage was unique in that it was partially cellular. A partially cellular hypodermis is characterized by being divided into sections that contain cells (cords) and sections that lack cells (intercords) (Bird 2012). The infection pattern of *S. perivermis* when observed by FISH showed that the hypodermis of the *O. rectangula* juveniles was divided into eight longitudinal cords and eight intercords (Figure 4.4). There were two large lateral cords (~18 μm wide), three slim dorsal and ventral cords (~3 μm wide), and eight intercords with intermediate width (~ 7 μm wide) (Figure 4.3 and 4.4). The intercords were intercalated between the cords (Figure 4.3 and 4.4). The

presence of eight cords is considered rare since nematodes usually have four cords (or sometimes six) as seen in *C. elegans* (Bird 1971; Nicholas 1984; Maggenti 1981; Bird and Bird 1991). Some Chromadorians, including those in the same family as *O. rectangula* (Axonolaimida) have also been reported to have eight cords (Maggenti 1981), lending support to our identification of these juveniles as *O. rectangula*. However, it was not possible to directly compare our results with Maggenti's (1981), as their report did not provide species names, life stage, or images of the nematodes examined. In the infected juveniles examined in the present study, the lateral cords were nucleated and subdivided with membrane-bound structures that were usually filled with parasites (Figure 4.3 and 4.4). The dorsal and ventral cords were also heavily infected but were anucleated and appeared to lack the cellular divisions observed in the lateral cords (Figure 4.3 and 4.4). The intercords were not infected, were anucleated, and internal divisions were apparent (Figure 4.3 and 4.4). In addition, the intercords appeared to have longitudinal fibers which possibly were longitudinal muscle fibers from the somatic muscles located underneath the hypodermis (Figure 4.3). This feature has been observed in other nematodes with "partially cellular" hypodermis (Bird 1971; Nicholas 1984; Bird and Bird 1991) and suggests that the intercords in these *O. rectangula* juveniles were significantly thinner than the cords.

4.3.5 *S. perivermis* infects the reproductive tissues of an *O. rectangula* juvenile

FISH showed that *S. perivermis* infection in one *O. rectangula* juvenile was localized in a tubular structure in the middle portion of the juvenile's body (Figures 4.5 and 4.6). The placement, shape, and size of this structure suggested that this tube-like structure was the juvenile's reproductive system and not the digestive system. In nematodes, the reproductive system is a tubular organ that is composed of at least one gonadal tube that is localized in the

pseudoceoulom: a fluid-filled cavity that separates the inner tube (digestive tract) from the outer tube (cuticle, hypodermis, and longitudinal muscles). Gonadal tubes are usually small with respect to the nematode's body in early juvenile stages and they elongate and widen as the nematode matures. This may explain why the infection is only observed in the middle portion of the body (Figure 4.6). On the other hand, the digestive tract is a large granular tube that stretches from the nematode's head to the tail throughout the nematode's development. The possibility that the infected tubular structure was a section of the digestive tract can be excluded since the anterior and posterior sections of the digestive tract appeared free of infection. In addition, *S. perivermis* has never been observed infecting *O. rectangula*'s digestive system, but it has been observed infecting the reproductive system of *O. rectangula* females (Chapter 3).

4.4 Discussion

4.4.1 Determining the gender of *O. rectangula* juveniles based on *S. perivermis* infection pattern

Gender cannot be determined morphologically in juvenile *O. rectangula*, yet my data suggest that their *S. perivermis* infection pattern could allow to predicting their gender. I predict that *O. rectangula* juveniles that were infected in the hypodermis only, and not in their reproductive tissues, were destined to molt into adult males. This prediction is supported by the fact that the hypodermis of these juveniles usually contained high loads of *S. perivermis*, a feature that was usually only observed in adult males.

In contrast, I predict that juveniles that have infected reproductive tissues are destined to molt into adult females. This pattern was observed in one juvenile and resembled the infection pattern

observed in adult gravid females (Chapter 3) and in one infected adult non-gravid female (without eggs) that was included in this study as a positive control (Figures 4.5 and 4.7). The reproductive system of adult *O. rectangula* females contains two genital tubes (didelphic) that are arranged opposite to each other from their uteri's end (amphidelphic). The vulva is localized where the uteri meet, half way between the head and tail. In both the non-gravid female and the juvenile, the infection was heavily concentrated in the middle section of the body. In the infected non-gravid female, *S. perivermis* infected the reproductive tissues in the uteri only where spores were observed (Figure 4.7). The ovaries and other sections of the gonadal tubes were not infected, as observed by FISH. In the juvenile with infected reproductive tissues, there were no *S. perivermis* spores observed, but the infection appeared to extend through the entire reproductive system (Figure 4.6). However, I note that the intra-structure (e.g. ovaries) of the reproductive tissues in this juvenile could not be differentiated. In summary, I believe that the juvenile with infected reproductive tissues is destined to be a female because its infection pattern is similar to the infection pattern observed in adult females.

It should be noted that my gender predictions based on *S. perivermis* infection patterns should be tested empirically since there is the possibility that secondary infection of the reproductive tissues may occur in *O. rectangula* juveniles with heavily infected hypodermal tissues. The reproductive tissues of most nematodes (including *O. rectangula*) are located in close proximity to the hypodermis, separated mainly by the longitudinal muscles, which were observed to contain *S. perivermis* spores in adult *O. rectangula* (Chaper 3). In addition, it is also important to note that due to the difficulty in finding and identifying *O. rectangula* juveniles in the sand samples, I cannot rule out the possibility that many juveniles included in this study were

misidentified. The low prevalence levels of *S. perivermis* in *O. rectangula* juveniles may be due in part to high virulence levels in larval stages or the egg stage that may reduce the estimated prevalence rates in this group. Attempts to test my predictions by establishing an *O. rectangula* culture in the laboratory were unsuccessful since it was not possible to culture *O. rectangula* nematodes in the lab (See methods).

4.4.2 Hypodermal configuration in infected *O. rectangula* juveniles

In addition to the two infection patterns discussed above, *S. perivermis* infection of the hypodermis of *O. rectangula* juveniles was observed to be partially cellular. A partially cellular hypodermis was unique to juveniles infected with *S. perivermis* intracellular stages (likely meronts) and appeared to lack spores (Figure 4.3 and 4.4). Based on this, I predict that the life cycle of *S. perivermis*, specifically progression to sporogony, may be triggered by rearrangements in the configuration of *O. rectangula*'s hypodermis.

Changes in hypodermal configuration in nematodes can vary within species as hypodermal cells multiply or fuse depending on the life stage of the nematode (Nicholas 1984). In some nematodes, the hypodermis may be cellular in the larval stage but become partially cellular or syncytial in the adult stage (Nicholas 1984). This process is poorly understood for most nematodes since immature life stages are difficult to obtain and identify, and because delimiting hypodermal cellular boundaries is challenging (Nicholas 1984). In *C. elegans*, the majority of the hypodermal cells fuse in the embryonic stage, but others multiply or fuse at different immature stages (WormAtlas 2002-2015). The hypodermis of adult *C. elegans* is a large syncytium (139

nuclei) that encloses most of the body except for parts of the head and tail where other uninucleated or multinucleated cells form (WormAtlas 2002-2015).

The association of *S. perivermis* intracellular stages with a partially cellular hypodermis (Figures 4.3, 4.4, and 4.5) and the association of *S. perivermis* spores with a syncytial hypodermis (Figures 3.3 and 4.2) suggest that *S. perivermis* and *O. rectangula* have co-evolved a complex host-parasitic relationship in which the development of the host and the parasite may be synchronized. This could resemble the synchronization observed in other vertically transmitted microsporidians such as members of the genus *Amblyospora* (Becnel and Andreadis 1999). For example, the life cycle of *A. connecticus* was shown to be synchronized with the development of its host (mosquito and copepods) where intracellular proliferative stages are usually observed during host immature stages, while differentiation into spores usually occurs in the host's adult stage (Becnel and Andreadis 1999). A similar interaction may occur between *O. rectangula* and *S. perivermis* in that *S. perivermis* remains in its proliferative intracellular stage until the partially cellular hypodermis becomes syncytial.

It was not possible to determine the life-stage in which the host undergoes hypodermal rearrangement since the life stage of the juveniles examined could not be determined morphologically. This was because body size varied considerably in juveniles with a hypodermis infected with *S. perivermis* spores (1.57-2.04 mm) and with a hypodermis infected with *S. perivermis* intracellular stage (1.64-2.36 mm), but both groups overlapped. Hence, it remains unclear whether these represent juveniles in the same life stage or in different life stages. In nematodes, the most significant growth in body size usually occurs in the last juvenile stage

since adult nematodes do not grow. Given that adult *O. rectangula* nematodes measure 2-2.5 mm and that the two types of hypodermal *S. perviermis* infection were observed in juveniles of adult size, it could suggest that the hypodermal rearrangement from partially cellular to syncytial, and *S. perivermis* progression to sporogony in the hypodermal tissues occurred in the fourth and last juvenile stage. We can not exclude the possibility that *S. perivermis* intracellular stages are also present in the hypodermis of adult nematodes, however, based on our observations it is possible that this parasite stage is exclusive to juveniles. Such is the case in the vertically transmitted microsporidian *Thelohania solenopsae* whose merogonial stages were only observed in the egg and larval stages of ants while spores were only found in adult ants (Knell et al. 1977; Briano et al. 1996). In summary, I predict that *S. perivermis* proliferative stages in juvenile nematodes with a partially cellular hypodermis undergo sporogony as a response to the transition from a partially cellular to a syncytial hypodermis.

4.4.3 Reconsidering transmission of *S. perivermis*

Taking together the infection pattern in juveniles and the non-gravid female described here with the infection patterns observed previously (Chapter 3), we can reconsider the mode of transmission for *S. perivermis*. Restriction of *S. perivermis* infection to only the uteri in adult females suggests that *S. perivermis* may be transmitted transovum (spore to egg) and not transovarially as suggested in Chapter 3. Transovum vertical transmission in the moth-infecting microsporidian *Endoreticulatus shubergi* occurs during eclosion, when the larva accidentally ingests *E. shubergi* spores that were attached to the surface of the egg (Goertz and Hoch 2008). However, *S. perivermis* infects *O. rectangula* eggs before eclosion as shown by the presence of infected eggs in infected gravid females (Figure 3.4). It is unclear whether *S. perivermis* spores

can infect the eggshell of *O. rectangula* eggs with their polar filaments. The nematode eggshell is usually a tough and resilient structure that is composed by one to five layers (usually three) including a thick chitinous wall (Lee 2002). *O. rectangula*'s eggshell structure has not been characterized, so it is possible that it is less resilient. By comparison, *N. parisii* cannot infect *C. elegans* eggs even when the eggs are surrounded by hundreds of spores produced by their deceased mother (Troemel et. al 2008). The *C. elegans* eggshell is composed of three layers (Johnston and Dennis 2012), which probably prevents infection of the egg by *N. parisii*.

Penetration of *O. rectangula*'s eggs by *S. perivermis* is perhaps a simple explanation for the infection of *O. rectangula* eggs, but appears less plausible when considering that the eggshell in nematodes is usually formed in the uterus after fertilization (Johnston and Dennis 2012). This suggests the possibility that *S. perivermis* spores that are present in the uterus infect *O. rectangula* eggs before the eggshell is built. To my knowledge, this would be the first example of transovum transmission before eclosion for a microsporidian parasite, while providing a novel example of the opportunistic nature of these versatile endoparasites.

In addition to *S. perivermis* transovum vertical transmission, there is also the possibility that *S. perivermis* could be transmitted horizontally given the difference between observed prevalence levels in juveniles (25%) and adults (84%) (Chapter 3). Indeed, variation in transmission mode has been linked to differences in prevalence of the microsporidian *T. solenopsae*. The vertically transmitted microsporidian *T. solenopsae* infects fire ants, and was found to have low prevalence rates (20%) in larval stages I, II, and III, medium prevalence rates (44-45%) in larval stage IV and pupae, and high prevalence rates in most adult castes (75-95%), except for queens (29%) and

wingless females (34%) (Briano et al. 1996). The underlying cause of this is unknown, but the authors concluded that the differences observed in *T. solenopsae* prevalence rates suggested that *T. solenopsae* may not only be transmitted vertically but also horizontally (Briano et al. 1996). Whether a similar situation exists for *S. perivermis* remains to be seen.

Variation in transmission efficiency and virulence could also be explained *S. perivermis* variation in prevalence rates between juveniles and adults (Hurst 1991; Andreadis 2007). Transmission efficiency can vary considerably depending on the transmission mode, host and parasite life histories, host fecundity (vertical transmission), parasite dose, and environmental factors such as ambient temperature (Hurst 1991; Agnew and Coella 1999; Kelly et al. 2003; Vizoso et al. 2005; Vizoso and Ebert 2005; Campbell et al. 2007). Virulence can also significantly alter estimated prevalence rates, and virulence in microsporidian parasites can vary depending on the host's life stage or gender (Dunn and Smith 2001). In mosquitoes, the majority of microsporidian genera infecting this group are lethal to the last (4th) larval stage where they often reach the highest parasite load in the host (Andreadis 2007).

Understanding how *S. perivermis* infects *O. rectangula* marine nematodes has expanded our view of microsporidian parasite and nematode interactions. *S. perivermis* infection patterns differed between genders in adults and were similar in juveniles, suggesting that infection patterns could be used to predict juvenile genders prior to morphological distinction in the adult stage. *S. perivermis* is perhaps the first example of a nematode-infecting microsporidian parasite that is transmitted vertically (likely transovum) and illustrates that host-parasite interactions between microsporidian and nemadotes are far from simple.

Figure 4.1 *Odontophora rectangula* juvenile

Notice the absence of a vulva (in females) and a spicule (in males), which means that this nematode was not an adult and had immature reproductive tissues. Imaging was performed using a FV10i confocal microscope (Olympus Inc.) and the imaging software FV10-ASW (Version 02.01.03.10 Olympus Inc.). Body size measurements were obtained using the ruler function of this software. Scale bar = 50 μm.

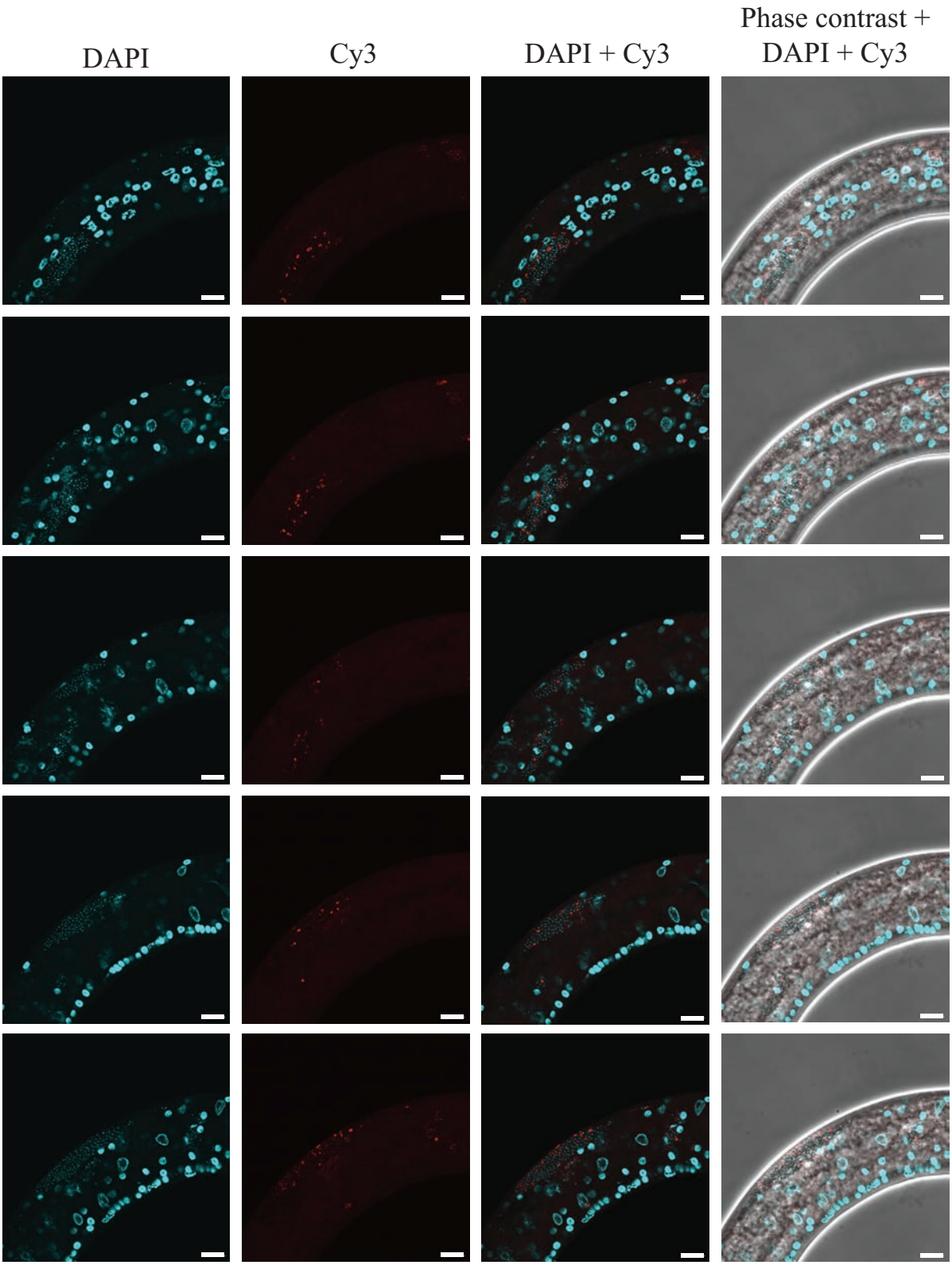
DAPI
Cy3
DAPI + Cy3
Phase contrast +
DAPI + Cy3

Figure 4.2 *S. perivermis* spores infecting the hypodermis measurement of an *O. rectangula* juvenile observed by FISH

Spores appeared clustered in "pockets" in a similar manner to that observed in adult hosts (Figure 3.3). The rows show cross sections of the nematode tissues at sequential depths, moving from exterior to interior (top to bottom). The columns show different light filters (from left to right): the nuclear stain DAPI (shown in blue), the *S. perivermis* fluorescent probe (Cy3 [shown in red]), a combination of the two dyes, and phase contrast with both dyes. Scale bar = 10 μm. Magnification: 600x.

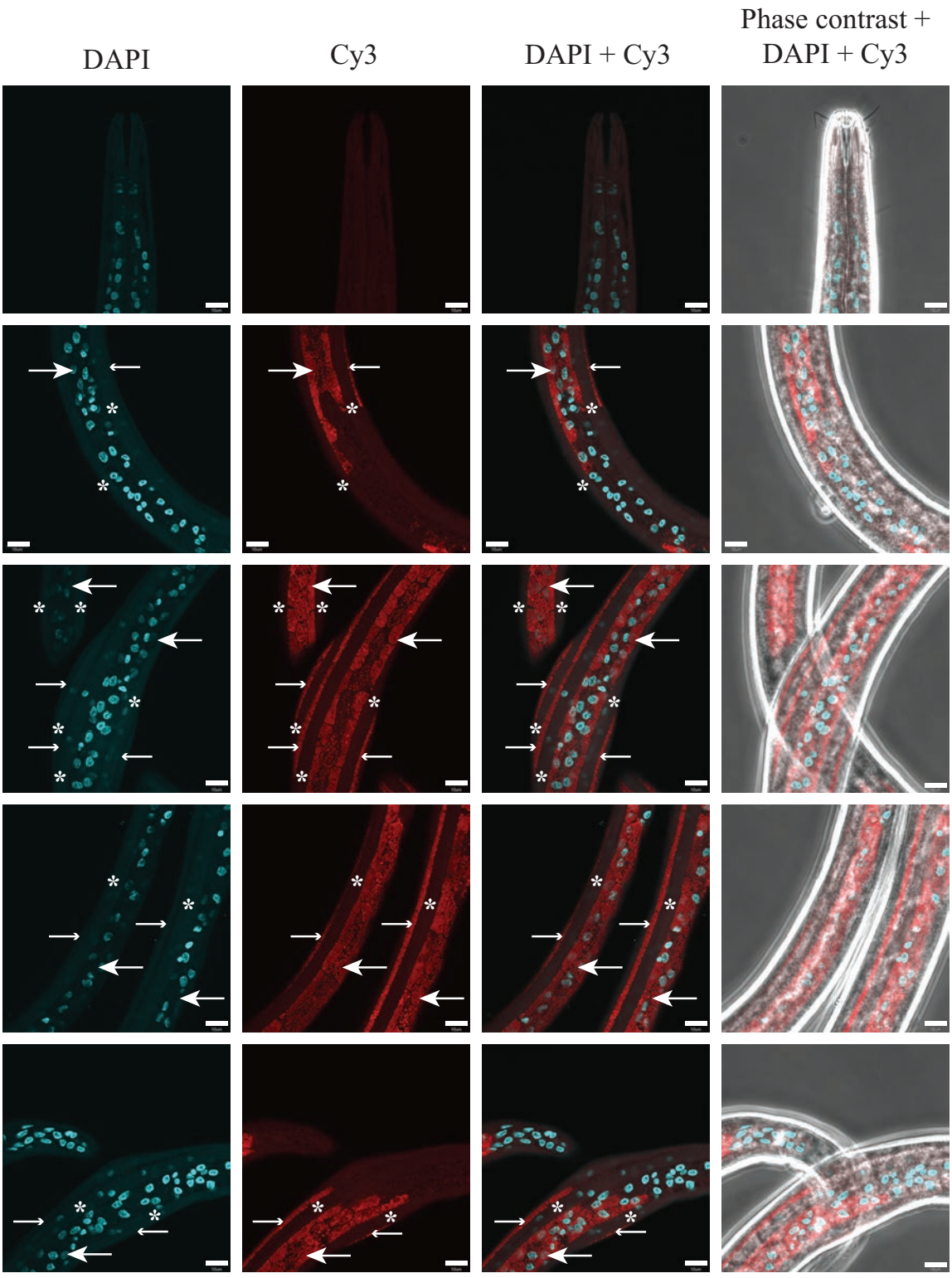
DAPI
Cy3
DAPI + Cy3
Phase contrast +
DAPI + Cy3

Figure 4.3 *S. perivermis* intracellular stage (possibly meronts) observed by FISH in the hypodermis of the *O. rectangula* juvenile shown in figure 4.1.

S. perivermis intracellular stage (possibly meronts) was circular in shape and have an approximate diameter of 1-1.5μm. The intracellular stage was only observed in infected juveniles (four in total) that had a hypodermis that was partially cellular and not syncytial (spores only). This suggests that *S. perivermis* sporogony is associated with developmental rearrangements of the hypodermis in *O. rectangula* nematodes from partially cellular to syncytial. The partially cellular hypodermis in the juveniles examined was divided into cordal (infected) and intercordal (uninfected) regions. The lateral cords (large arrows) were nucleated and cellular while the ventral and dorsal cords (small arrows) and the intercords (*) were anucleated and appeared acellular. Longitudinal muscle fibers located underneath the hypodermis can be seen under the intercoral regions in the first column. The rows show different body sections of the juvenile's body from the head to the tail (top to bottom). The columns show different light filters (from left to right): the nuclear stain DAPI (shown in blue), the *S. perivermis* fluorescent probe (Cy3 [shown in red]), a combination of the two dyes, and phase contrast with both dyes. Scale bar = 10 μm.

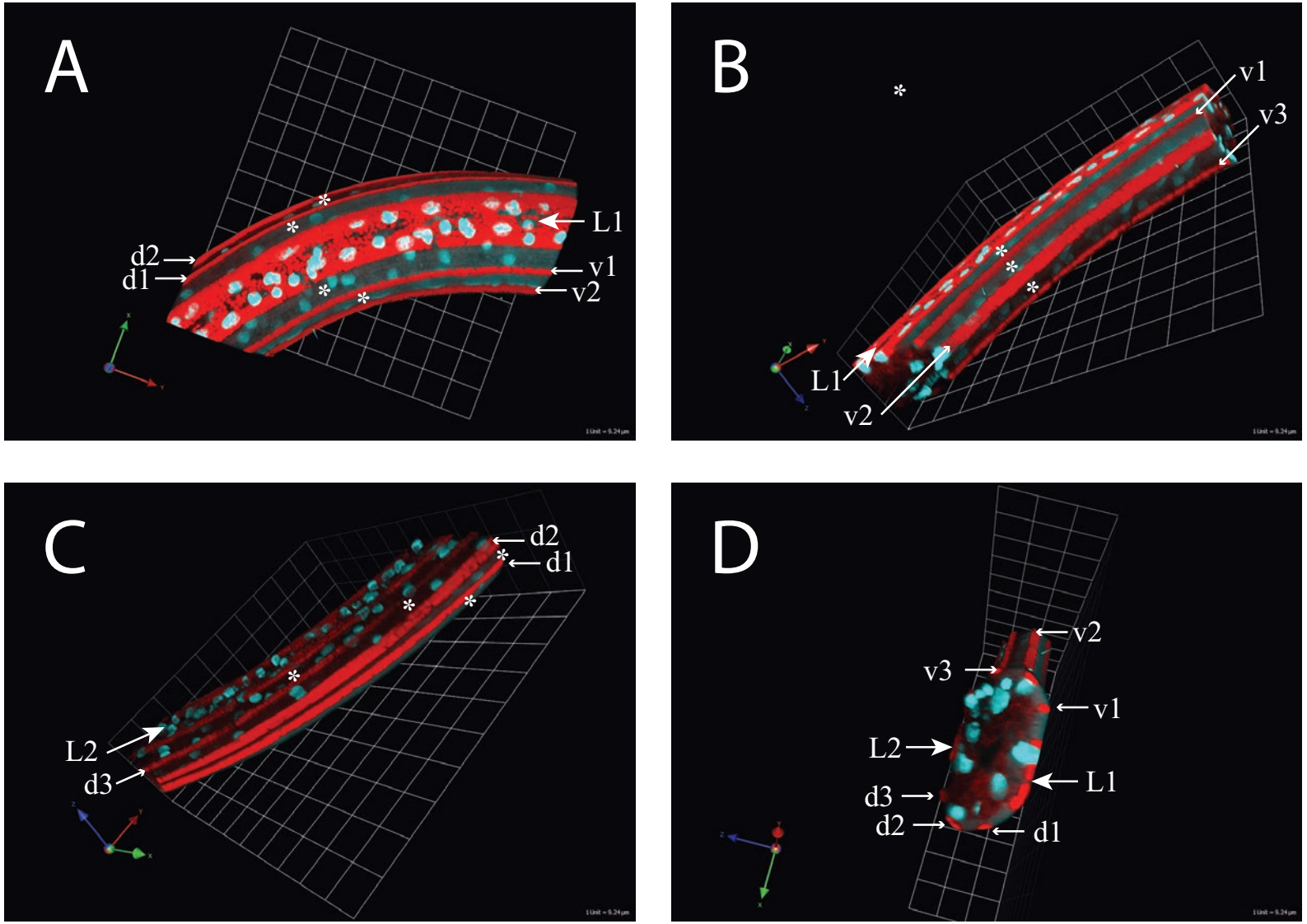
A
d2
d1
L1
v1
v2
B
v1
v3
L1
v2
C
d2
d1
L2
d3
D
v2
v3
v1
L2
L1
d3
d2
d1

Figure 4.4 *S. perivermis* infection in a juvenile *O. rectangula* nematode with a partially cellular hypodermis shown in 3D.

S. perivermis partially cellular hypodermis is divided in eight cords intercalated by eight intercords. There are two wide lateral cords (~18 μm; large arrows), three thin ventral cords (~3 μm; small arrows), and three thin dorsal cords (~3 μm; small arrows). All of the intercords are of intermediate width (~7 μm; asterix) and the muscle fibers of the longitudinal muscles can be seen underneath these regions. A) Lateral cord (L1), two ventral (v1 and v2), two dorsal (d1 and d2) cords, and four intercords (*). B) Three ventral cords (v1,v2, and v3), lateral cord one (L1), and three intercords (*), C) Three dorsal cords (d1,d2,and d3), lateral cord two (L2) and four intercords (*), and D) Cross-section showing the eight cords and intercords. The nuclear stain DAPI is shown in blue and the *S. perivermis* fluorescent probe (Cy3) is shown in red.

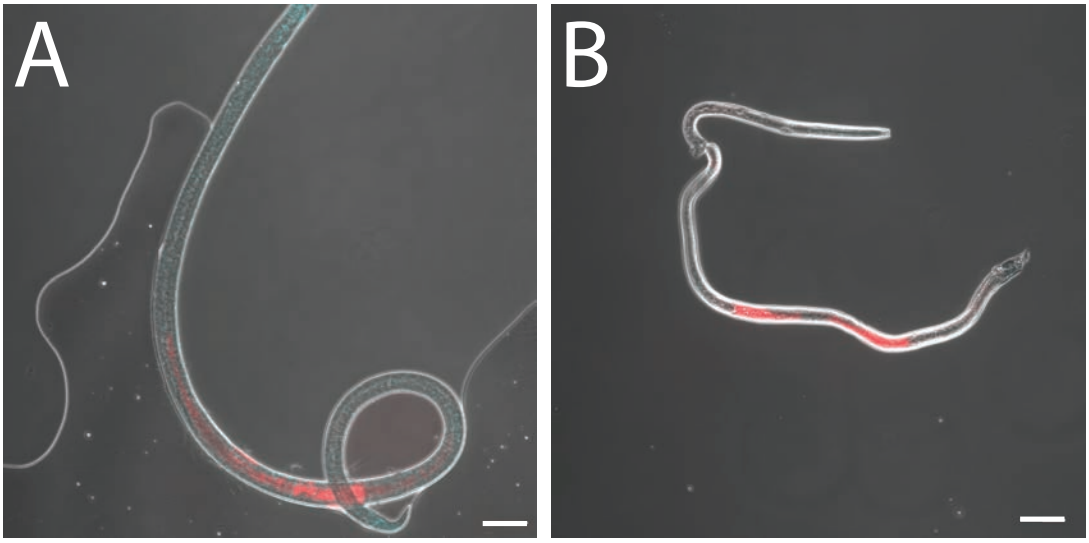

Figure 4.5 *S. perivermis* infection (red) of the reproductive tissues of a juvenile (A) and a non-gravid female (B) viewed under phase contrast.

Close-up images are shown in figures 4.6 (juvenile) and 4.7 (non-gravid female). Scale bar = 50 μm.

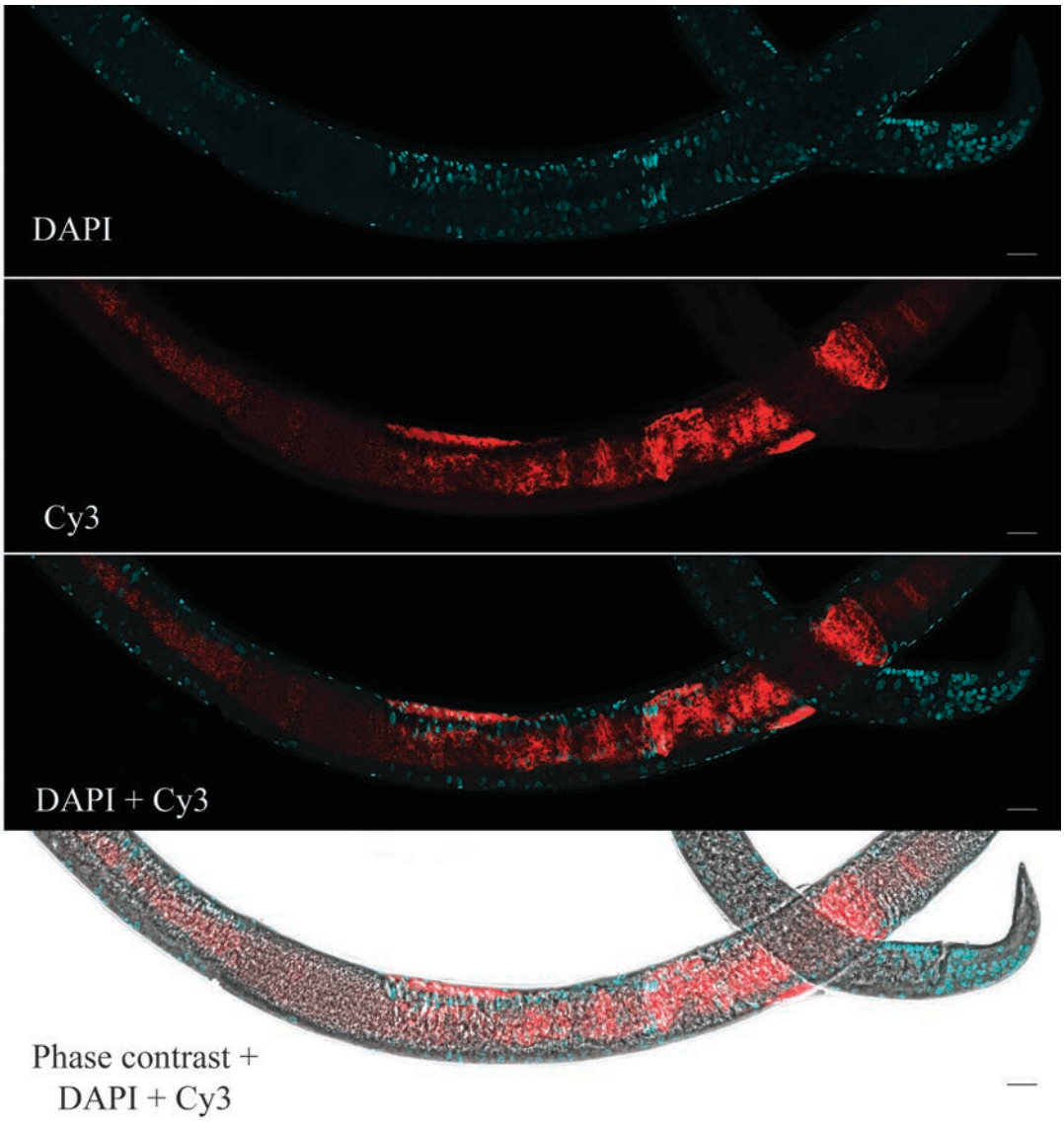

Figure 4.6 *S. perivermis* infection in the reproductive tissues of an *O. rectangula* juvenile

Close-up image of the infected *O. rectangula* juvenile shown in Figure 4.5.A. The infection pattern overlaps with the expected localization of the reproductive tissues. However, the internal structure of the reproductive tissues could not be distinguished with certainty.
Different light filters are shown: the nuclear stain DAPI (blue), the *S. perivermis* specific fluorescent probe Cy3 (red), a combination of the two dyes, and phase contrants with both dyes. Scale bar = 20 μm.

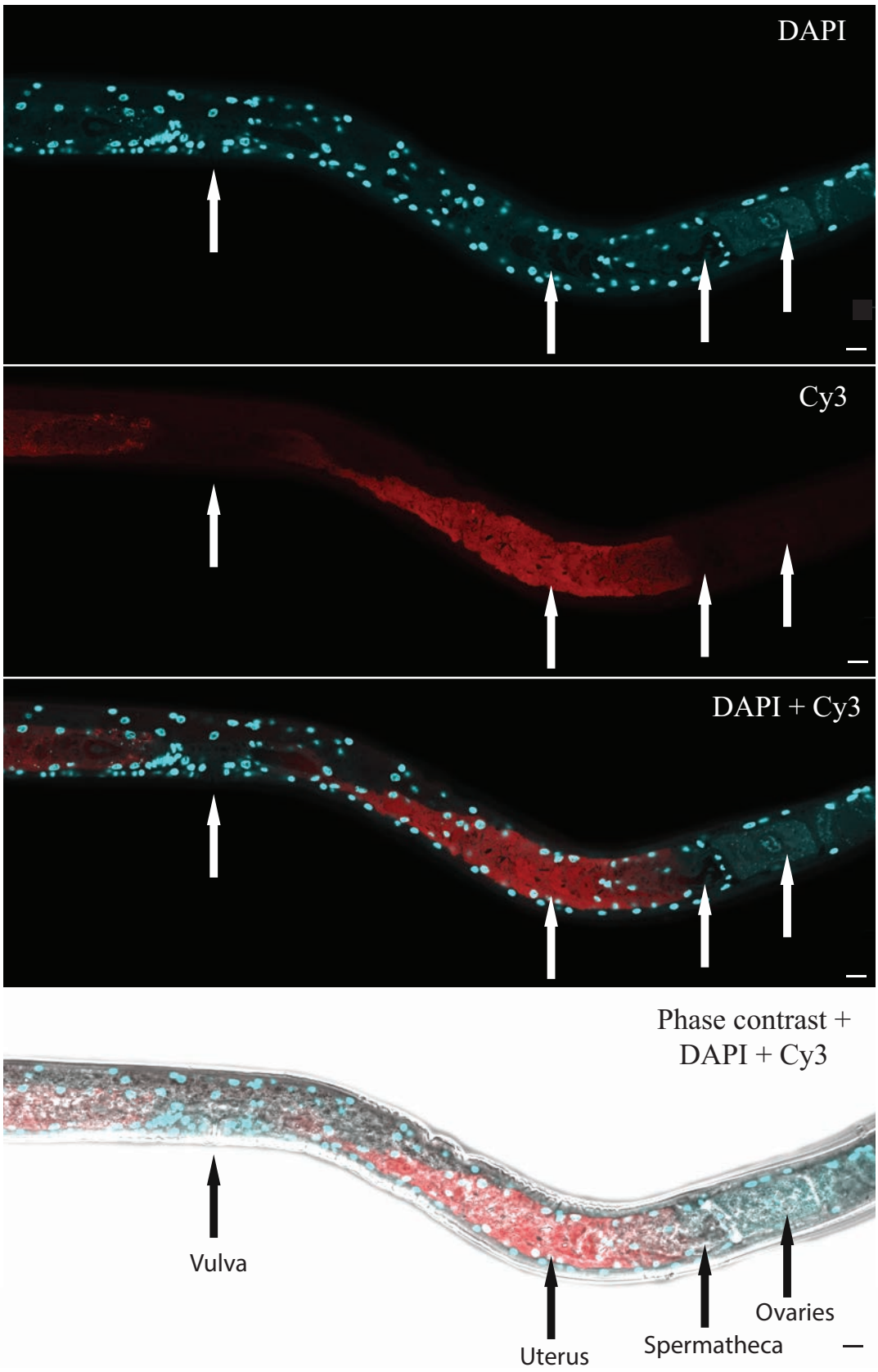
DAPI
Cy3
DAPI + Cy3
Phase contrast +
DAPI + Cy3
Vulva
Uterus
Spermatheca
Ovaries

Figure 4.7 *S. perivermis* infection in the reproductive tissues of a non-gravid *O. rectangula* female examined by FISH.

Close-up image of the infected non-gravid *O. rectangula* female shown in Figure 4.5.B. FISH showed that the infection is localized in the uterus, the only place where *S. perivermis* spores can be observed. The internal structure of the reproductive tissues is labelled: the vulva, the uterus, the spermatheca, and the ovaries. Note that the ovaries are not infected. Different light filters (from top to bottom): the nuclear stain DAPI (blue), the *S. perivermis* fluorescent probe Cy3 (red), a combination of the two dyes, and phase contrants with both dyes. Scale bar = 10 μm.

Chapter 5: Phylogenetic position and genomic survey of the microsporidian *Sporanauta perivermis*

5.1 Introduction

Microsporidian parasites are highly reduced unicellular fungi that have modified mitochondria (mitosomes) and a modified Golgi apparatus. These intracellular parasites have eliminated a large number of metabolic pathways (i.e. tricarboxylic acid cycle) and genomic sequences resulting in highly reduced genomes (Keeling and Corradi 2011; Corradi and Selman 2013). Microsporidian nuclear genomes are among the smallest eukaryotic genomes known, ranging between 2.3 and 51.2 Mbp (average genome size [GS] = 10 Mbp; N = 15) (Microsporidian Comparative Database 2010). In comparison to other fungal groups, the average microsporidian genome is tiny, given that the average fungal GS measures 50 Mbp (Kullman et al. 2005). In fact, over 90% of all available fungal genomes size estimates are larger than 10 Mbp (Kullman et al. 2005).

The smallest microsporidian nuclear genomes are found in the genus *Encephalitozoon* (GS range = 2.3-2.9 Mbp; N= 4). The *Encephalitozoon* lineage is the best-studied microsporidian lineage at the genomic level. Whole-genome sequencing of *Encephalitozoon* species (*E. cuniculi*, *E. hellem*, *E. romaleae*, and *E. intestinalis*) revealed that the genomes in this genus are highly similar to each other (Katinka et al. 2001; Corradi et al. 2010; Pombert et al. 2012). They all have 11 linear chromosomes and they share over 90% (1,824) of their protein-coding genes (Pombert et al. 2012). In addition, *Encephalitozoon* genomes conserve remarkable levels of

synteny across species where nearly all shared protein-coding genes are arranged within 55 perfect syntenic blocks (Pombert et al. 2012). Non-coding sequences are highly reduced in the *Encephalitozoon* species, and consist of short intergenic regions (125 bp) and less than 40 small introns (16-79 bp) (Pombert et al. 2012). Recently, whole-genome sequencing of the closest known relative of the *Encephalitozoon* group, the *Daphnia*-infecting microsporidian *Ordospora colligata*, showed that the *O. colligata* genome is highly similar to *Encephalitozoon* genomes (Pombert et al. 2015). *O. colligata* and *Encephalitozoon* share over 90% of their genes, have intergenic regions of similar lengths, and the majority of the syntenic blocks in the *Encephalitozoon* group are conserved in *O. colligata* (Pombert et al. 2015). The major difference between *O. colligata* and the *Encephalitozoon* group is that *O. colligata* was predicted to have 10 chromosomes instead of 11 (Pombert et al. 2015).

It is possible that the genome of the nematode-infecting microsporidian *Sporanauta perivermis* could share similar features to that of *O. colligata* and *Encephalitozoon* since SSU rDNA phylogenetic analyses (Figures 2.2 and 3.1) suggested that *S. perivermis* is a sister lineage to *O. colligata* and the *Encephalitozoon* clade. Surveying the *S. perivermis* genome will not only serve to assessing reduction in *O. colligata* and *Encephalitozoon* genomes but it will improve our understading of extreme reduction in microsporidian genomes in general.

In this chapter, I performed a genomic survey of *S. perivermis* to understand the genomic architecture of this species, and to facilitate a multi-gene phylogenetic analysis that tested the phylogenetic relationships between *S. perivermis*, *O. colligata*, and *Encephalitozoon*. My analyses indicated that these three lineages form a strongly supported monophyletic group,

where *S. perivermis* is sister to *O. colligata* and *Encephalitozoon*. However, *S. perivermis* and *O. colligata* share a large number of changes when compared to *Encephalitozoon*. One of the most significant rearrangements identified here appears to be a chromosomal breakage between chromosomes five and ten in *Encephalitoozoon* which is absent in *S. perivermis* and *O. colligata*. This supports the estimated number of chromosomes in *O. colligata* (10), one less than that of the *Encephalitozoon* (11) (Pombert et al. 2015). It was not possible to estimate the number of *S. perivermis* chromosomes, since the number of contigs assembled was very large (678), but given the similarity of *S. perivermis* to *O. colligata*, it is predicted that *S. perivermis* also has 10 chromosomes. Overall, the genomic survey of *S. perivermis* showed that *S. perivermis* is sister to the *O. colligata* and *Encephalitozoon* clade, that gene synteny has been maintained through the evolution of the genomes in this clade, and that chromosomal rearrangements (such as chromosomal breakage) may be a mechanism by which extreme genome size reduction was achieved by *Encephalitozoon* genomes: some of the smallest eukaryotic genomes known to date.

5.2 Methods

5.2.1 *S. perivermis* sampling and DNA extraction

Sand samples containing *Odontophora rectangula* nematodes (*S. perivermis*'s host) were collected in 50 ml sterile Falcon tubes from Boundary Bay beach (49.013N, 123.036W) (British Columbia, Canada) in 2011. *O. rectangula* nematodes were manually isolated from the sand samples and were screened for *S. perivermis* infection by PCR using a specific primer set (5′-CGAGATGTGCAGTATGTCTGGG-3′) targeting the *S. perivermis* SSU rDNA gene. Attempts to separate spores from the host by density gradient ultracentrifugation were unsuccessful, so DNA was collected from infected host material.

Genomic DNA was extracted from 20 adult *O. rectangula* nematodes isolated from a collected sample exhibiting an infection rate of over 80% as determined by PCR screening. The extraction method was the same as that employed for *E. intestinalis* (Corradi and Pombert et al. 2010). *O. rectangula* nematodes were put in 1.5 ml tubes containing 300 µl of lysis solution (Epicentre Biotechnologies) and Proteinase K, and mixed by vortexing. This was followed by the addition 200 µl of glass beads (diameter: 150-212 µm) and incubating the samples at 65 °C for 15 mins. During incubation, the samples were bead-beaten (2,500 rpm) every 5 mins for 30 secs to rupture *S. perivermis* spores. The samples were then cooled to 37 °C, 2 µl (5 µg/µl) of RNase A warmed at 37 °C were added, and the samples were incubated for 30 mins at 37 °C. Once the RNase treatment was completed, the samples were put on ice for 5 mins. Then, protein precipitation was performed by vortexing the samples for 10 s after adding 150 µl of MPC Protein Precipitation Reagent (Epicentre Biotechnologies). Proteins were separated by pelleting for 10 mins at 10,000 g and by transferring the supernatant to a sterile microcentrifuge tube. DNA was precipitated with isopropanol, and rinsed three times with 70% ethanol. The DNA was suspended in TE buffer and stored at -20 °C. The final concentration of DNA was 5 ng/µl.

5.2.2 Sequencing, *de novo* assembly, and annotation

The next-generation sequencing library was prepared using The Ovation Ultralow DR Multiplex System (NuGEN Technologies, Inc.) since this protocol is optimized for preparing Illumina libraries with small amounts of starting material (1.0 ng DNA). The standard protocol was followed and the library's quality control and sequencing (IlluminaHiSeq 2000; Pair ends; read size = 100 bp) was performed by the sequencing facility at the Biodiversity Research Centre

(University of British Columbia). A test run (1/4 lane) was performed (before sequencing a full lane) to confirm the presence of microsporidian (*S. perivermis*) sequences. The reads from both the partial lane and a subsequent full lane were combined (341,003,601) and assembled with the CLC Genomics Workbenh 7 (CLC bio; http://www.clcbio.com). A total of 347,940 contigs were obtained and microsporidian contigs were filtered locally (BLASTX) against a microsporidian database built with all microsporidian sequences available on the NCBI website (Geer et al. 2010). The first filtering attempt (e-5) resulted in the selection of 16,119 contigs, but the majority of these contigs were not microsporidian. A more stringent parameter (e-30) selected 711 contigs. These contigs were queried (BLASTX) individually against the entire NCBI database (Geer et al. 2010) to ensure that they were microsporidian. This resulted in a final set of 678 contigs (Average length = 3,256.91; Average coverage = 18.13x) that forms the genome survey presented here. The genes in these contigs were annotated using the gene-prediction engine AUGUSTUS (Stanke et al. 2008). AUGUSTUS has been optimized to predict genes in the *Encephalitozoon cuniculi* genome and is suitable to predict genes in close relatives (Stanke et al. 2008). Microsporidian protein sequences predicted by AUGUSTUS (Stanke et al. 2008) were identified by BLASTP against the NCBI database (Geer et al. 2010).

5.2.3 Phylogenetic analysis

The phylogenetic analyses performed in this study included the same taxa used in the most recent and complete multi-gene phylogenetic analysis performed for Microsporidia (Pombert et al. 2015). This included 21 microsporidian species, 11 strains for four species, and two outgroups. Comparing to Pombert et al. (2015) is useful because Pombert et al. (2015) aimed to resolve the phylogenetic relationship between *O. colligata* and the *Encephalitozoon* lineage,

which were shown to be in the same clade as *S. perivermis* in our single gene (SSU rDNA gene) phylogenetic analyses (Figures 2.2 and 3.1).

In the present study, two multi-gene phylogenetic analyses (Maximum likelihood [ML] and Bayesian) were performed using a sub-set (29 orthologs) of the 104 orthologs included in Pombert et al. (2015). The 29 *S. perivermis* orthologs were selected using the following criteria: complete gene sequence in a single *S. perivermis* contig and presence on a contig surrounded by other *S. perivermis* genes. *S. perivermis* genes that were fragmented in more than one contig or that were located at the ends of a contig were not included, since their sequences were incomplete. J.F. Pombert kindly provided the ortholog sequences for all taxa included in his phylogenetic analysis.

Inferred protein sequences (including *S. perivermis*) were aligned using SEAVIEW v.4.5.3 (MUSCLE)(Gouy et al. 2010), inspected visually, and trimmed with BMGE (default settings) (Criscuolo and Gribaldo 2010). Ortholog sequences for each lineage were concatenated resulting in an alignment containing 9,906 amino acids. ML inferences were performed in RAxML (version 2.31 GUI) (Stamatakis 2014) using the following settings: ML + thorough bootstrap, PROTGAMMABLOSUM62 model, and 200 bootstrap. Bayesian analysis was performed using PhyloBayes 3.3 (Lartillot et al. 2009) by running two parallel chains with the following settings: CAT model and 4 gamma degrees. The consensus tree for the Bayesian analysis was obtained once the maximum discrepancy between the two chains was below 0.1.

5.3 Results

5.3.1 Phylogenetic position of *S. perivermis*

Multi-gene ML and Bayesian phylogenetic analyses indicated that *S. perivermis*, *O. colligata*, and the *Encephalitozoon* lineage (four species) form a clade with maximum support (bootstrap = 100; posterior probability = 1) (Figure 5.1). In this clade, *S. perivermis* is the most basal lineage (Figure 5.1). These phylogenetic relationships, as well as the monophyly of the *Encephalitozoon* group, had maximum support in both analyses (Figure 5.1). In both trees, the genus *Nosema* branches as sister to the *Sporanauta-Ordospora-Encephalitozoon* clade (Figure 5.1). In contrast, the genus *Nematocida* (the only other known nematode-infecting microsporidian genus) is an early-diverging microsporidian lineage (with maximum support) (Figure 5.1).

5.3.2 *S. perivermis* genomic survey

The genomic survey of *S. perivermis* resulted in the annotation of 1,533 distinct open reading frames (ORFs) encoded in 678 *S. perivermis* contigs that were filtered by BLAST from host (*O. rectangula*) contigs. There were 144 contigs that contained a portion of a single gene only, while the remainder contained more than two ORFs (and up to 11). Overall, the average contig length was 3,256.91 bp (Average coverage = 18.13x), totaling 2,208,182 Mbp (G+C = 41.4%) (Table 1). Of the 1533 *S. perivermis* ORFs, 679 ORFs (46%) were complete, and the average ORF length was 930 bp (Table 5.1). The remaining ORFs were incomplete and usually coded on one contig, but 251 fragmented ORFs were found on more than one contig (usually two). The average length of the intergenic regions was 192 bp (Table 5.1).

Querying the *S. perivermis* ORFs against the NCBI database (Geer et al. 2010) indicated that the top hit for the vast majority (1479) of ORFs is either an *Encephalitozoon* or an *O. colligata* ortholog. There are only 16 ORFs whose top BLAST hits is not from these genera, while 12 of the 16 ORFs do not have an *Encephalitozoon* or *O. colligata* ortholog. In most of these ORFs, the top BLAST hit is a *Nosema* ortholog, but they also include top hits from the genera *Vavraia*, *Vittaforma*, *Anncalia*, *Trachipleistophora*, and *Edhazardia*. There are 11 ORFs for which no significant similarity is found on the NCBI database. Lastly, there are 26 ORFs on the 678 microsporidian contigs that had non-microsporidian top hits. The 26 non-microsporidian ORFs are usually incomplete and located at the end of their contigs, and their top BLAST hits include nematodes and other animals, yeast and other fungi, protists, and bacteria.

Over half (278) of the contigs containing multiple *S. perivermis* ORFs are in synteny with their *Encephalitozoon* and *O. colligata* orthologs (see an example in Figure 5.2). In these contigs, not only the orientation of the ORFs is the same, but also the ORF lengths and intergenic distances are highly similar to that reported for their *O. colligata* and *Encephalitozoon* orthologs (Figure 5.2). In contrast, nearly half of the contigs containing more than one *S. perivermis* ORF have nearly complete synteny with *O. colligata* but not with *Encephalitozoon* species. The most striking example of this involved a chromosomal breakage in *Encephalitozoon* genomes, which is not present in *O. colligata* and *S. perivermis* (Figure 5.3). In *E. intestinalis*, the terminal end of chromosome 10 ends with gene Eint_101770 (black arrow)(Figure 5.3.A). *E. hellem* and *E. romaleae* have the same ortholog on the terminal end of chromosome 10 (not shown), but *E. cuniculi* has nine extra genes downstream of this ortholog (ECU10_1800) (Figure 5.3A). In *O. colligata*, the same ortholog (also shown in black; M896_051810) and upstream genes are

located in contig 05 and they are in perfect synteny with their corresponding *Encephalitozoon* orthologs located at the terminal end of chromosome 10 (Figure 5.3.A). However, the ORFs downstream of *O. colligata* M896_051810 are not located downstream of the ortholog ECU10_1800 in *E. cuniculi* (Figure 5.3.A). Instead, *O. colligata* has a similar arrangement as *S. perivermis* in that the genes located upstream (orange) and downstream (yellow, purple, brown, and green) of *O. colligata* M896_051810 (black) are in synteny with *S. perivermis*, except that *S. perivermis* lacks an ortholog to M896_051810 (Figure 5.3.A), which was not present in any of *S. perivermis* contigs. *O. colligata* ORF M896_051820 (yellow), and downstream ORFs (purple, brown, and green) are in perfect synteny with *S. perivermis* (Figure 5.3.A), but their *Encephalitozoon* orthologs are encoded on a different chromosome: chromosome 5 (Figure 5.3.A and B, where ortholog colours are maintained). The genes located upstream of the *Encephalitozoon* Eint_051220 and ECU05_1170; yellow) on chromosome 5 are encoded in nearly perfect synteny with each other, and with their corresponding orthologs in *O. colligata* and *S. perivermis* (Figure 5.3.B). *E. intestinalis* has an additional ORF (Eint_051210; grey) (Figure 5.3.B). In addition, *O. colligata* and *S. perivermis* share an additional ortholog (M896_011350 in *O. colligata*) that is absent in *Encephalitozoon* species (Figure 5.3.B). Lastly, *S. perivermis* contig 4439 has an ORF (light blue) at one end of contig 4439 that is highly similar to the N-terminal half of *Vavraia culicis* hypothetical protein (VCUG_0124) (Figure 5.3.B). This is likely a pseudogene for which no orthologs are found in *O. colligata* and *Encephalitozoon*. It is worth noting that the length of intergenic spaces are highly similar across the three genera in spite of the major chromosomal re-arrangement observed.

5.4 Discussion

5.4.1 Phylogenetic position of *S. perivermis*

The phylogenetic analyses performed here indicate that *S. perivermis*, *O. colligata*, and the *Encephalitozoon* (four species) are monophyletic (Figure 5.1). In this group, *S. perivermis* is the most basal lineage and *O. colligata* is more closely related to the *Encephalitozoon* species (Figure 5.1). This is in line with phylogenetic relationships recovered previously using single-gene (SSU rDNA) phylogenetic analyses (Figures 2.2 and 3.1). However, the single-gene analyses failed to recover the topology with the same level of support (Figures 2.2 and 3.1). This is possibly due to the inclusion of sequences from top BLAST hits for *S. perivermis* from the NCBI database: the beetle-infecting microsporidian *Mockfordia xanthocaeciliae* and the undescribed microsporidian *Microsporidium* sp. BLAT11 LAT2 (Figures 2.2 and 3.1). In SSU phylogenetic analyses, *S. perivermis*, *M. xanthocaeciliae*, and *Microsporidium* sp. BLAT11 LAT2 formed a clade that is sister to *O. colligata.* It is worth noting that in all of the SSU and multi-gene analyses available to date (Pombert et al. 2015; Vossbrinck and Debrunner-Vossbrinsk 2005; Refardt et al. 2001), including this thesis (Figures 2.2, 3.1, and 5.1), *O. colligata* has always been the closest known relative of the genus *Encephalitozoon*. Unfortunately, it was not possible to include *M. xanthocaeciliae* and *Microsporidium* sp. BLAT11 LAT2 in the multi-gene analysis performed in this study because only their SSU rDNA gene sequences are available. Adding these taxa to future multi-gene phylogenetic analyses will probably not change the tight link between *O. colligata* and the *Encephalitozoon* lineage, however their addition could serve to improve our understanding of the phylogenetic relationships of *S. perivermis* with its closest relatives, including *Ordospora* and the *Encephalitozoon* clade.

5.4.2 *S. perivermis* genomic structure and evolution

The genome survey of *S. perivermis* revealed that the genetic composition and genomic structure of the *S. perivermis* genome is highly similar to the *O. colligata* and *Encephalitozoon* genomes. Over 95% of the *S. perivermis* ORFs (1479) annotated in this study had a top BLAST hit that is either an *Encephalitozoon* or *Ordospora* ortholog. Only a minor portion of *S. perivermis* ORFs do not have orthologs from these genera. These results are congruent with single (Figures 2.2 and 3.1) and multi-gene phylogenetic analyses (Figures 5.1) that placed *S. perivermis* within a monophyletic group (max. support) containing *O. colligata* and *Encephalitozoon* species. Furthermore, their proposed relationship is strengthened by the fact that *S. perivermis* ORFs shared high levels of synteny with both *O. colligata* and *Encephalitozoon* spp. However, *S. perivermis* appeared to be more similar in structure to *O. colligata* than to *Encephalitozoon* genomes, since *O. colligata* and *S. perivermis* share a large number of organizational changes in gene syntenic blocks that are not seen in *Encephalitozoon* genomes (Pombert et al. 2015). This suggests that the structural organization of *S. perivermis* and *O. colligata* is an ancestral state that underwent one or multiple changes during the evolution of *Encephalitozoon* genomes.

A key example is a chromosomal breakage/rearrangement that is unique to the *Encephalitozoon* group (Figure 5.3). We predict that this chromosomal breakage between chromosomes 5 and 10 in the *Encephalitozoon* ancestor could be correlated with a change in chromosome number. *O. colligata* has 10 chromosomes, one chromosome less than *Encephalitozoon* species (Pombert et al. 2015). Even though it is not possible to predict with certainty the number of chromosomes in

S. perivermis, we predict that *S. perivermis* has the same number of chromosomes as *O. colligata*.

When considering the genome size of *S. perivermis,* it is at least 2.2 Mbp, based on the number of assembled sequences. Given that *S. perivermis* has slightly longer intergenic regions than *O. colligata*, we predict that the *S. perivermis* genome could be larger than the estimated size of *O. colligata* (3.0 Mbp) (Pombert et al. 2015), which is larger than the estimated genome sizes of the *Encephalitozoon* genomes (2.3-2.5 Mbp) (Pombert et al. 2012; Pombert et al. 2015) (Table 5.1). It is possible that the *S. perivermis* genome contains ORFs that are not found in either *O. colligata* or *Encephalitozoon*. In this study, there were 16 *S. perivermis* ORFs that do not have an *O. colligata* or *Encephalitozoon* ortholog. These *S. perivermis* ORFs have orthologs in other microsporidian lineages, usually *Nosema*, the closest known genus to the *Sporanauta-Ordospora-Encephalitozoon* clade that is relatively well sampled. Establishing the function and role of these additional ORFs could be important to understand the evolution of this group. There are 11 *S. perivermis* ORFs that did not have significant similarities with the NCBI database while 26 other ORFs encoded on the microsporidian contigs had top BLAST hits that are not microsporidian and include nematode, fungal, or bacterial hits. The presence of the 37 non-microsporidian ORFs (< 1% of all ORFs) encoded on contigs containing microsporidian ORFs may be due to retention or gain of ORFs, or even horizontal gene transfer (HGT) from the host, as reported recently in *O. colligata* (Pombert et al. 2015). However, it is also possible that inclusion of these ORFs on the microsporidian contigs was an assembly error, given that the non-microsporidian ORFs are usually incomplete and located at the contig ends; their presence should be confirmed by either PCR or sequencing.

5.5 Conclusion

S. perivermis is a nematode-infecting microsporidian that formed a monophyletic group with the *Daphnia*-infecting microsporidian *O. colligata* and the *Encephalitozoon* lineage, which contains four described species that infect grasshoppers (*E. romaleae*) and mammals (*E. hellem*, *E. intestinalis*, and *E. cuniculi*), including humans. Multi-gene phylogenetic analyses indicated that *S. perivermis* is sister to the *Ordospora-Encephalitozoon* clade and confirmed that *O. colligata* is the closest known relative of the genus *Encephalitozoon*. The structure of the *S. perivermis* genome is most similar to that of *O. colligata*. Gene synteny is maintained across the three genera in this clade, but *S. perivermis* and *O. colligata* share a large number of structural features that are absent in the *Encephalitozoon* group. This includes the absence of a chromosomal breakage between chomosomes 5 and 10 in the *Encephalitozoon* genomes that we propose occurred in the ancestor of the *Encephalitozoon* group. It is possible that such a rearrangement affected chromosomal number, and could be one mechanism involved in the extreme genome reduction seen in *Encephalitozoon* species.

Table 5.1 Genome comparisons between *S. perivermis*, *O. colligata*, *Encephalitozoon*, and *Nematocida*

	***E. hellem* ATCC 50504**	***E. romaleae* SJ-2008**	***E. intestinalis* ATCC50506**	***E. cuniculi* GB-M1**	***O. colligata* OC4**	***S. perivermis***	***N. parisii* ERTm1**	***N.* sp 1 ERTm2**
Chromosome number[†]	11	11	11	11	10[†]	-	8-9[†]	8-9[†]
Contig number[‡]	12	13	11	11	15	**678**	65	202
Estimated genome size (Mbp)	2.5	2.5	2.3	2.9	3.0	-	-	-
Assembled genome size (Mbp)	2.3	2.2	2.2	2.5	2.3	**2.2**	4.1	5
Estimated genome coverage (%)	92	88	96	86	77	-	-	-
GC content (%)	43.4	40.3	41.4	47.3	38.2	**41.4**	34.4	38
Mean gene length[¶]	1018	1061	999	1041	1041	**930**[¶]	1104	1084
Mean intergenic length	106	130	100	166	176	**192**	418	569
Number of predicted ORFs[§]	1928	1835	1944	2010	1820	**1533**[§]	2661	2831
Number of predicted introns	38	38	38	38	32	**1**	0	0

[†]The estimated number of chromosomes for *O. colligata* (Pombert et al. 2015) and *Nematocida* (Cuomo et al. 2012) genomes was suggested by the authors.
[‡]The number of contigs is the number reported on the last NCBI database (Geer et al. 2010) update (as of February 12, 2015) of the respective genome records.
¶The mean gene length for *S. perivermis* was calculated using the length of predicted genes that had a complete sequence and that were not at the edge of the conitgs. In total, there were 679 genes (45% of the total) that met these criteria. In addition, there were 251 *S.pervermis* ORFs that were fragmented into more than one (usually two) contigs.
§The number of predicted ORFs for *S. perivermis* is the number of genes for which the BLAST against the NCBI database (Geer et al. 2010) showed that they were microsporidian ORFs, 99% of these ORFs had an *Encephalitozoon* or *Ordospora* ortholog.

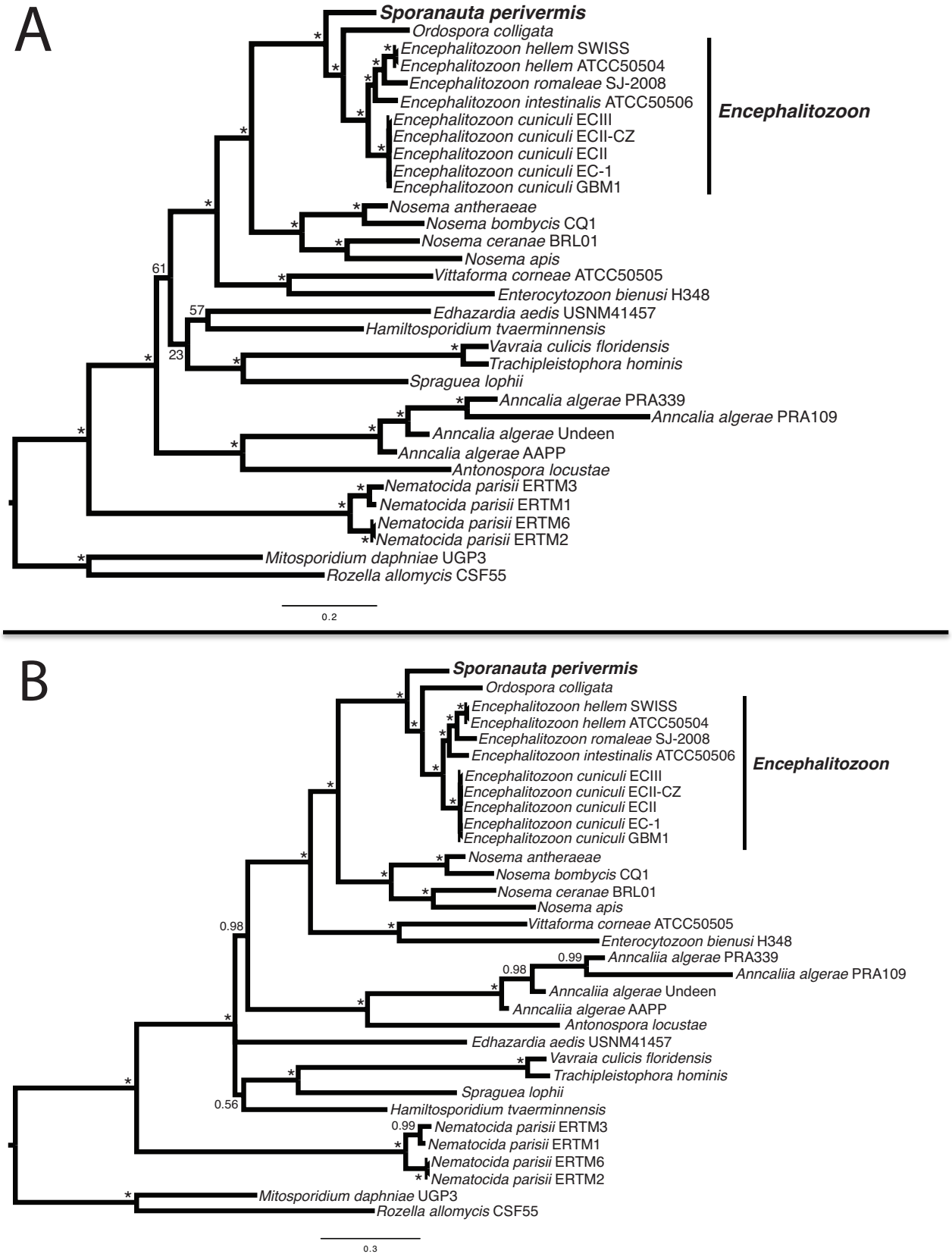
A
Sporanauta perivermis
Ordospora colligata
Encephalitozoon hellem SWISS
Encephalitozoon hellem ATCC50504
Encephalitozoon romaleae SJ-2008
Encephalitozoon intestinalis ATCC50506
Encephalitozoon cuniculi ECIII
Encephalitozoon cuniculi ECII-CZ
Encephalitozoon cuniculi ECII
Encephalitozoon cuniculi EC-1
Encephalitozoon cuniculi GBM1
Encephalitozoon
Nosema antheraeae
Nosema bombycis CQ1
Nosema ceranae BRL01
Nosema apis
Vittaforma corneae ATCC50505
Enterocytozoon bienusi H348
Edhazardia aedis USNM41457
Hamiltosporidium tvaerminnensis
Vavraia culicis floridensis
Trachipleistophora hominis
Spraguea lophii
Anncalia algerae PRA339
Anncalia algerae PRA109
Anncalia algerae Undeen
Anncalia algerae AAPP
Antonospora locustae
Nematocida parisii ERTM3
Nematocida parisii ERTM1
Nematocida parisii ERTM6
Nematocida parisii ERTM2
Mitosporidium daphniae UGP3
Rozella allomycis CSF55
61
57
23
0.2
B
Sporanauta perivermis
Ordospora colligata
Encephalitozoon hellem SWISS
Encephalitozoon hellem ATCC50504
Encephalitozoon romaleae SJ-2008
Encephalitozoon intestinalis ATCC50506
Encephalitozoon cuniculi ECIII
Encephalitozoon cuniculi ECII-CZ
Encephalitozoon cuniculi ECII
Encephalitozoon cuniculi EC-1
Encephalitozoon cuniculi GBM1
Encephalitozoon
Nosema antheraeae
Nosema bombycis CQ1
Nosema ceranae BRL01
Nosema apis
Vittaforma corneae ATCC50505
Enterocytozoon bienusi H348
Anncaliia algerae PRA339
Anncaliia algerae PRA109
Anncaliia algerae Undeen
Anncaliia algerae AAPP
Antonospora locustae
Edhazardia aedis USNM41457
Vavraia culicis floridensis
Trachipleistophora hominis
Spraguea lophii
Hamiltosporidium tvaerminnensis
Nematocida parisii ERTM3
Nematocida parisii ERTM1
Nematocida parisii ERTM6
Nematocida parisii ERTM2
Mitosporidium daphniae UGP3
Rozella allomycis CSF55
0.98
0.99
0.98
0.56
0.99
0.3

Figure 5.1 Phylogenetic position of *S. perivermis* in Microsporidia

Maximum likelihood (A) and Bayesian inference (B) multi-gene (29 genes) phylogenetic analyses showing nodes with maximum support (bootstrap = 100; posterior probability =1) with an asterix (*). Support values are provided for nodes without maximum support.

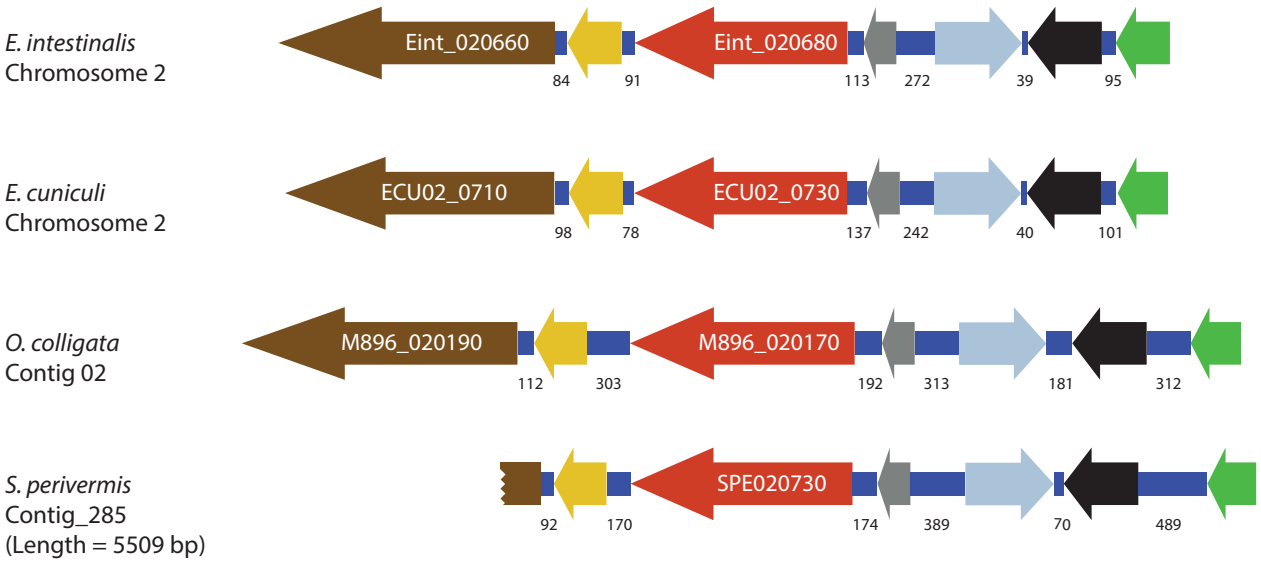

Figure 5.2 Synteny between *S. perivermis* ORFs and their orthologs in *E. intestinalis*, *E. cuniculi*, and *O. colligata*

Arrows of the same colour represent orthologs from different species while intergenic regions are shown in blue. The length (bp) of the intergenic regions is shown under each. The chromosome or contig number and loci names for the longest genes in each species are shown for reference.

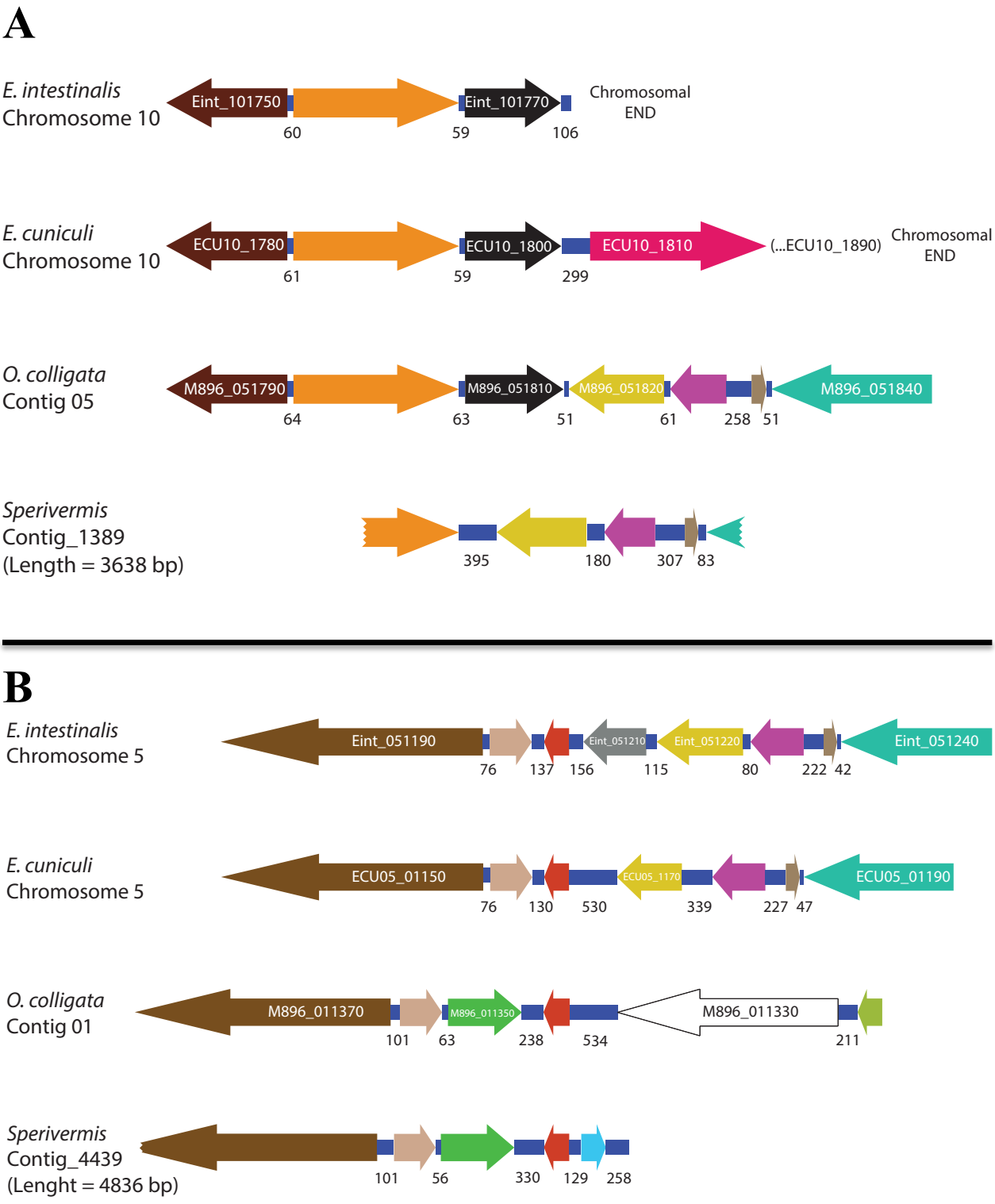
A
E. intestinalis
Chromosome 10
Eint_101750
Eint_101770
Chromosomal
END
60
59
106
E. cuniculi
Chromosome 10
ECU10_1780
ECU10_1800
ECU10_1810
(...ECU10_1890)
Chromosomal
END
61
59
299
O. colligata
Contig 05
M896_051790
M896_051810
M896_051820
M896_051840
64
63
51
61
258
51
Sperivermis
Contig_1389
(Length = 3638 bp)
395
180
307
83
B
E. intestinalis
Chromosome 5
Eint_051190
Eint_051210
Eint_051220
Eint_051240
76
137
156
115
80
222
42
E. cuniculi
Chromosome 5
ECU05_01150
ECU05_1170
ECU05_01190
76
130
530
339
227
47
O. colligata
Contig 01
M896_011370
M896_011350
M896_011330
101
63
238
534
211
Sperivermis
Contig_4439
(Lenght = 4836 bp)
101
56
330
129
258

Figure 5.3 Chromosomal rearrangement in *Encephalitozoon* species, *S. perivermis*, and *O. colligata*

A) Synteny shared between the end of chromosome 10 in *Encephalitozoon* and *O. colligata* contig_05 and *S. perivermis* contig_1389. B) Syntenic regions of *Encephalitozoon* chromosome 5 and *O.colligata* and *S. perivermis* contigs. Please see text for details. Arrows of the same colour represent orthologs from different species while intergenic regions are shown in blue. The length (bp) of the intergenic regions is shown under each. The chromosome or contig number and loci names for the longest genes in each species are shown for reference.

Chapter 6: Conclusion

6.1 Summary

To characterize the diversity of microsporidian parasites in the environment, I collected soil, sand, and house compost samples from various sites in the Vancouver metropolitan area and screened them by PCR using microsporidian SSU rDNA specific primers (Chapter 2). I amplified sequences from 22 undescribed microsporidians, from three previously described microsporidian species (Chapter 2), and from a novel microsporidian parasite (*Sporanauta perivermis*) that was named and characterized in this thesis (Chapters 3, 4, and 5). Phylogenetic analysis revealed that there were representatives from nearly all major microsporidian clades (Chapter 2), and indicated that there is a broad diversity of microsporidian parasites in the environment that remains undescribed (Chapter 2). Screening for the host of the novel parasites revealed that one of them infected a free-living marine nematode (*Odontophora rectangula*) (Chapter 3). I characterized the ultrastructure of this novel microsporidian and named it *Sporanauta perivermis* for "marine spore of roundworms" (Chapter 3). Examination of the infection by fluorescent *in situ* hybridization showed that *S. perivermis* spores infect the hypodermal, muscle, and reproductive tissues of adult and juvenile *O. rectangula* (Chapter 3). However, *S. perivermis* infection differed between genders in that only the reproductive tissues were infected in adult females (uteri and eggs) suggesting that *S. perivermis* is transmitted vertically (Chapter 3). Similar infection patterns were observed in juveniles, suggesting that *S. perivermis* infection patterns could be used to predict the gender of *O. rectangula* juveniles prior to adulthood (Chapter 4). *S. perivermis* infection in some juveniles was unique in that *S. perivermis* was in an intracellular stage (likely meronts), and not in their sporal stage as observed

in adults and other juveniles (Chapter 4). Juveniles infected with *S. perivermis* intracellular stage had a hypodermis that was not syncytial as seen in adults and other juveniles, but was arranged in long segments that were either cellular or acellular (partially cellular hypodermis) (Chapter 4). This suggested that *S. perivermis* sporogony could be associated with a structural reorganization of the host's hypodermis that appeared to occur between different life stages (juvenile to adult) in *O. rectangula* nematodes (Chapter 4).

Single-gene and multigene phylogenetic analyses showed that *S. perivermis* is placed with strong support in a clade containing the microsporidians *Mockfordia xanthocaelliae*, *Ordospora colligata* and the *Encephalitozoon* lineage (five species). I conducted a genome survey of *S. perivermis* to compare its genome structure and content with that of the sequenced genomes available for this clade, which include the smallest eukaryotic genomes known: *O. colligata* (3.0 Mbp) (Pombert et al. 2015) and *Encephalitozoon* species (2.3-2.9 Mbp) (*E. hellem*, *E. intestinalis*, *E. cuniculi*, and *E. romaleae*) (Katinka et al. 2001; Pombert et al. 2012; Pombert et al. 2015). The *S. perivermis* genome survey resulted in the assembly of 679 contigs encoding over 2.2 Mbp (Chapter 5). In total, there were 1533 *S. perivermis* ORFs, of which 1479 (>95%) had a top BLAST hit (NCBI database) that was either an *Encephalitozoon* or an *O. colligata* ortholog (Chapter 5). *S. perivermis* shared high levels of synteny with *O. colligata* and *Encephalitozoon*, but *S. perivermis* was most similar to *O. colligata* (Chapter 5). One of the most significant rearrangements is a chromosomal breakage between chromosomes 5 and 10 in *Encephalitozoon* that is absent in *O. colligata* and *S. perivermis*, and could be related to chromosome number (Chapter 5). However, the genome size of *S. perivermis* is predicted to be greater than that of *O. colligata* (3 Mbp) and *Encephalitozoon* (2.3-2.9 Mbp) genomes. This is

because even though *S. perivermis* shares over 90% of its annotated ORFs with its closest relatives, and that the shared ORFs are similar in size, there were 37 *S. perivermis* ORFs that were not present in *O. colligata* and *Encephalitozoon* (Chapter 5). This suggests the *S. perivermis* could contain more ORFs than *O. colligata* and *Encephalitozoon* (Chapter 5). In addition, *S. perivermis* contains intergenic regions that on average (192 bp) are longer than the intergenic regions of *O. colligata* (166 bp) and *Encephalitozoon* species (106-166 bp) (Chapter 5).

6.2 Significance and future directions

Microsporidian parasites are a monophyletic group of fungal organisms that are ubiquitous in the environment and are suspected to be as diverse (~1 million species) as their hosts (mainly animals). Characterization of microsporidian diversity in the environment has often focused on screening a small number of species, often human-infecting species in water bodies. In Chapter 1, I showed that screening of microsporidian parasites in environmental sources that are poorly sampled (soil, sand, compost) revealed that there is a wide diversity of microsporidian parasites in these sources, and that most remain undescribed. These data indicate that future research assessing microsporidian diversity in the environment should not focus on screening a small number of species in water, but should screen more broadly for the presence of microsporidia and include possible reservoirs that are poorly sampled such as soil, sand, and compost. This will certainly expand our understanding of microsporidian diversity, it will assess the presence/absence of known and "important" microsporidians, and it could reveal undescribed species, such as *Sporanauta perivermis* (characterized in this thesis), which can provide valuable

insights into the nature of host-parasite interactions and evolutionary history of microsporidian parasites.

S. perivermis was the first confirmed case of a microsporidian infection in a free-living marine nematode (Chapter 3) and a second microsporidian infecting this group was reported more recently, *Nematocenator marisprofundi* (Sapir et al. 2014). *S. perivermis* and *N. marisprofundi* as well as their respective hosts are distantly related phylogenetically (Sapir et al. 2014). Having only two microsporidian species infecting one of the most diverse and abundant animal groups on the planet calls for a targeted approach to expand this number since marine nematodes could harbor an important fraction of the diversity of microsporidian parasites. Perhaps the most challenging aspect of this endeavor will be to find a microsporidian infection in a marine nematode that can be cultivated in the laboratory. This would allow for a thorough characterization of the host-parasite interactions that take place in different life stages of the host, as has been performed in a lab strain of *Caenorhabditis elegans* inoculated with *Nematocida parisii* (Troemel et al. 2008). Efforts to characterize nematode-infecting microsporidia should not be restricted to marine nematodes only, but should be expanded to include all nematodes, free-living and parasitic, since the total number of microsporidian parasites that have been reported to infect nematodes is tiny (eight), when compared to the total number of species known to infect humans (15) or insects (hundreds).

In this thesis, *S. perivermis* infection of *O. rectangula* nematodes was characterized by transmission electron microscopy (TEM) and fluorescent *in situ* hybridization (FISH) in adults, and by FISH in *O. rectangula* eggs and juveniles. TEM characterization of the infection in eggs

and juvenile *O. rectangula* could provide detailed descriptions of the life cycle of *S. perivermis* throughout the development of *O. rectangula*. It would be of particular importance to characterize the ultrastructure of the hypodermis in juveniles and examine whether or not *S. perivermis* sporogony is linked to structural rearrangements of this tissue.

Phylogenetic analyses showed that *S. perivermis*, the *Daphnia*-infecting microsporidian *Ordospora colligata*, and the *Encephalitozoon* group (five species) form a monophyletic clade with strong support (Chapter 2 and 5). The positioning of *S. perivermis* is of particular interest because there are three *Encephalitozoon* species (*E. hellem*, *E. intestinalis*, and *E. cuniculi*) that often cause acute infections in immuno-deficient individuals (e.g. AIDS patients). Multi-gene phylogenetic analyses showed that *S. perivermis* is sister to *O. colliga* and *Encephalitozoon* and that *O. colligata* is the closest known relative of *Encephalitozoon*. However, the multi-gene phylogenetic analyses performed in this thesis did not include the microsporidian *Mockfordia xanthocaeciliae* (host: bark-lice) (Sokolova et al. 2010) because there are no genomic sequences available for *M. xanthocaeciliae.* A genomic survey or whole-genome sequencing of *M. xanthocaeciliae* could serve to improve our understanding of the phylogenetic relationships in *Sporanauta–Ordospora–Encephalitozoon* clade and it could aid genome wide comparisons to better characterize the evolution of this clade at the genome level.

The genomic survey of *S. perivermis* served to make a preliminary comparison of the genetic content and structure of *S. perivermis* with that of *O. colligata* (Pombert et al. 2015) and the four sequenced *Encephalitozoon* genomes (*E. hellem*, *E. intestinalis*, *E. cuniculi*, and *E. romaleae*) available to date. There were over 2.2 Mbp assembled for *S. perivermis* that were fragmented in

678 contigs. To improve the assembly of the *S. perivermis* genome, I will attempt to connect the 251 *S. perivermis* ORFs that were fragmented in more than one contig reducing the number of contigs by approximately one third. I will attempt to connect all the other contigs by predicting their order on the *S. perivermis* genome using the *O. colligata* and the *Encephalitozoon* genomes as references. Over 90% of *S. perivermis* genes had an *O. colligata* or *Encephalitozoon* ortholog and the arrangement of the *S. perivermis* ORFs indicated that the *S. perivermis* genome maintains high synteny with *O. colligata* and *Encephalitozoon*. It is likely that the entire *S. perivermis* genome will not assemble completely, but improving its assembly could serve to define the number of *S. perivermis* chromosomes (10 vs 11), and will certainly improve our understanding of the evolution of the highly reduced genomes that characterize the members of this clade.

Overall, my PhD research has shed light on the importance of conducting a broad and integrative approach to characterize the diversity of microsporidian parasites in the environment. This approach can lead to discovering novel microsporidian species (such as *S. perivermis*) that infect poorly sampled groups of animals (marine nematodes) while provide novel insights on the biology, host-parasite interactions, and genome evolution of microsporidian parasites as a whole.

Bibliography

Agnew, P. and Koella, J. C. 1999. Life history interactions with environmental conditions in a host-parasite relationship and the parasite's mode of transmission. Evol. Ecol. 13:67–89.

Andreadis, T. G. and Hanula, J. L. 1987. Ultrastructural-study and description of *Ovavesicula popilliae* n.g., n. sp. (Microsporida, Pleistophoridae) from the Japanese-beetle, *Popillia japonica* (Coleoptera, Scarabaeidae). J. Protozool. 34:15–21.

Andreadis, T. G. 2007. Microsporidian parasites of mosquitoes. J. Am. Mosq. Control Assoc. 23:3–29.

Becnel, J. J. and Andreadis, T. G. 1999. Microsporidia in insects. In: Wittner, M. and Weiss, L.M. (ed.). The microsporidia and microsporidiosis. ASM Press, Washington, DC. 447–501.

Bhadury, P. and Austen, M. C. 2010. Barcoding marine nematodes: an improved set of nematode 18S rRNA primers to overcome eukaryotic co-interference. Hydrobiologia. 641:245–251.

Bhadury, P., Bik, H., Lambshead, J. D. Austen, M. C., Smerdon, G. R., and Rogers, A. D. 2011. Molecular diversity of fungal phylotypes co-amplified alongside nematodes from coastal and deep-sea marine environments. Plos One 6:e26445 doi:10.1371/journal.pone.0026445.

Bhadury, P., Bridge, P. D., Austen, M. C., Bilton, D. T., Smerdon, G. R. 2009. Detection of fungal 18S rRNA sequences in conjunction with marine nematode 18S rRNA amplicons. Aquat. Biol. 5:149–155.

Bird, A. F. The structure of nematodes. 1971. Academic press, New York.

Bird, A. F. and Bird, J. 1991. The structure of nematodes (2nd edition). Academic Press, San Diego, CA.

Bohne, W., Böttcher, K., and Groß, U. 2011. The parasitophorous vacuole of *Encephalitozoon cuniculi*: biogenesis and characteristics of the host cell-pathogen interface. Int. J. Med. Microbiol. 301(5):395–399.

Bongers, T. and Bongers, M. 1998. Functional diversity of nematodes. Appl. Soil Ecol. 10:239–251.

Brian, T. R. and Schwartz, D. A. 1999. Epidemiology of microsporidiosis. In: Wittner, M. and Weiss, L.M. (ed.). The microsporidia and microsporidiosis. AMS Press, Washington, DC. p. 502.

Briano, J. A., Patterson, R. S. and Cordo, H. A. 1995. Long-term studies of the black imported fire ant (Hymenoptera, Formicidae) infected with a microsporidium. Environ. Entomol. 241:328–1332.

Burri, L., Williams, B. A., Bursac, D., Lithgow, T., and Keeling, P. J. 2006. Microsporidian mitosomes retain elements of the general mitochondrial targeting system. Proc. Natl. Acad. Sci. USA. 103:15916–15920.

Cali, A. and Takvorian, P. M. 1999. Developmental morphology and life cycles of the microsporidia. In: Wittner, M. & Weiss, L. M. (ed.), The microsporidia and microsporidiosis. AMS Press, Washington, DC. p. 85–128.

Cali, A., Neafie, R., Weiss, L. M., Ghosh, K., Vergara, R. B., Gupta, R., and Takvorian, P. M. 2010. Human vocal cord infection with the microsporidium Anncaliia algerae. J. Eukaryot. Microbiol. 57:562–567.

Campbell, C., van Frankenhuyzen, K., and Smith, S. 2007. Incubation period, spore egestion and horizontal transmission of *Nosema fumiferanae* (Microsporidia: Nosematidae) in spruce budworm (*Choristoneura* sp., Lepidoptera: Tortricidae): The role of temperature and dose, J. Invertebr. Pathol. 94(3):204–210. doi:10.1016/j.jip.2006.11.005.

Canning, E. U. 1981. *Encephalitozoon lacertae* n. sp., a microsporidian parasite of the lizard *Podarcis muralis*. In: Parasitological Topics. Society of Protozoologists Special Publication 1. Allen Press, Lawrence, KS. p. 57–64.

Canning, E. U., Barker, R. J., Nicholas, J. P., and Page, A. M. 1985. The ultrastructure of 3 microsporidia from winter moth, *Operophtera brumata* (L.), and the establishment of a new genus *Cystosporogenes* n.g for *Pleistophora operophterae* (Canning, 1960). Syst. Parasitol. 7:213–225.

Canning, E. U., Curry, A., Cheney, S. A., Lafranchi-Tristem, N. J., Ebert, D., et al. 2001. *Flabelliforma montana* (Phylum Microsporidia) from *Phlebotomus ariasi* (Diptera, Psychodidae): ultrastructural observations and phylogenetic relationships. Eur. J. Protistol. 37:207–221.

Capella-Gutierrez, S., Marcet-Houben, M., and Gabaldon, T. 2012. Phylogenomics supports microsporidia as the earliest diverging clade of sequenced fungi. BMC Biol. 10:47 doi:10.1186/1741-7007-10-47.

Cavalier-Smith, T. 1983. Endosymbiotic origin of the mitochondrial envelope. In: Endocytobiology II. W. Schwemmler and H. E. A. Schenk. (ed.). Berlin: de Gruyter. p. 265–279.
Chen, Z. X., Chen, S. Y., and Dickson, D. W. 2004. Nematology advances and perspectives: nematode morphology, physiology and ecology. Vol 1. CAB International, UK.

Choudhary, M. M., Metcalfe, M. G., Arrambide, K., Bern, C., Visvesvara, G. S., et al. 2011. *Tubulinosema* sp. microsporidian myositis in immunosuppressed patient. Emerg. Infect. Dis. 17:1727–1730.

Corradi, N. and Keeling, P. J. 2009. Microsporidia: a journey through radical taxonomical revisions. Fungal Biol. Revs. 23:1–8.

Corradi N., Pombert, J. F., Farinelli, L., Didier, E., and Keeling, P. J. 2010.The complete sequence of the smallest known nuclear genome from the microsporidian *Encephalitozoon intestinalis*. Nat. Commun. 1:77. doi: 10.1038/ncomms1082.

Corradi N. and Selman, M. 2013. Latest progress in microsporidian genome research. J. Eukaryot. Microbiol. 60:309–312.

Coyle, C. M., Weiss, L. M., Rhodes, L. V., Cali, A., Takvorian, P. M. et al. 2004. Fatal myositis due to the microsporidian *Brachiola algerae*, a mosquito pathogen. N. Engl. J. Med. 351(1):42–7.

Criscuolo, A. and Gribaldo, S. 2010. BMGE (block mapping and gathering with entropy): a new software for selection of phylogenetic informative regions from multiple sequence alignments. BMC Evol. Biol. 10:210. doi:10.1186/1471-2148-10-210.

Cuomo, C. A., Desjardins, C. A., Bakowski, M. A., Goldberg, J., Ma, A. T., Becnel, J. J., Didier, E. S., Fan, L., Levin, J. Z., Young, S., Zeng, Q., Troemel, E. R. 2012. Microsporidian genome analysis reveals evolutionary strategies for obligate intracellular growth. Genome Res. 12: 2478–2488 doi:10.1101/gr.142802.112.

Dado, D., Izquierdo, F., Vera, O., Montoya, A., Mateo, M., Fenoy, S., Galvan, A. L., Garcia, S., Garcia, A., Aranguez, E., Lopez, L., del Aguila, C. & Miro, G. 2012. Detection of zoonotic intestinal parasites in public parks of Spain. Potential epidemiological role of microsporidia. Zoonoses Public Health. 59:23–28.

Delbac, F. and Polonais, V. 2008. The microsporidian polar tube and its role in invasion. In: Molecular mechanisms of parasite invasion. Burleigh, B.A. (ed.). 47:208–220.

Didier, E. S., Didier, P. J., Friedberg, D. N., Stenson, S. M., Orenstein, J. M., et al. 1991. Isolation and characterization of a new human microsporidian, *Encephalitozoon hellem* (n. sp.), from 3 AIDS patients with keratoconjunctivitis. J. Infect. Dis. 163:617–621.
Didier, E. S., Varner, P. W., Didier, P. J., Aldras, A. M., Millichamp, N. J., et al. 1994. Experimental microsporidiosis in immunocompetent and immunodeficient mice and monkeys. Folia Parasitol. 41:1–11.

Didier, E. S. and Bessinger, G. T. 1999. Host-parasite relationships in microsporidiosis: animal models in immunology. In: Wittner M. and Weiss L. M. (ed). The microsporidia and microsporidiosis. ASM Press, Washington, DC. p. 225.

Didier, E. S., Stovall, M. E., Green, L. C., Brindley, P. J., Sestak, K., and Didier, P. 2004. Epidemiology of microsporidiosis: sources and modes of transmission. Vet. Parasitol. 126:145–166.

Didier, E. S., Maddry, J. A., Brindley, P. J., Stovall, M. E. and Didier, P. J. 2005. Therapeutic strategies for human microsporidia infections. Expert. Rev. Anti. Infect. Ther. 3:419–434.

Didier, E. S. and Weiss, L. M. 2011. Microsporidiosis not just in AIDS patients. Curr. Opin. Infect. Dis. 24:490–495.

Dunn, A. M. and Smith, J. E. 2001. Microsporidian life cycles and diversity: the relationship between virulence and transmission. Microb. Infect. 3:381–388.

Estes, K. A., Szumowski, S. C., and Troemel, E. R. 2011. Non-lytic, actin-based exit of intracellular parasites from *C. elegans* intestinal cells. PLoS Pathog. 7:e1002227 doi:10.1371/journal.ppat.1002227.

Fischer, W. M. and Palmer, J. D. 2005. Evidence from small-subunit ribosomal RNA sequences for a fungal origin of Microsporidia. Mol. Phylogenet. Evol. 36:606–622.

Fonseca, V.G., Carvalho, G. R., Sung, W., Johnson, G. R., Power, D. M. et al. 2010. Second-generation environmental sequencing unmasks marine metazoan biodiversity. Nat. Commun. 1:98 doi:10.1038/ncomms1095.

Franzen C. 2004. Microsporidia: how can they invade other cells? Trends Parasitol. 20: 275–279.

Geer, L.Y., Marchler-Bauer, A., Geer, R. C., Han, L., He, J., He, S., Liu, C., Shi, W., and Bryant, S.H. 2010. The NCBI BioSystems database. Nucleic Acids Res. 38:D492-6. http://www.ncbi.nlm.nih.gov/biosystems.

Giere O. 2009. Meiobenthology: the microscopic motile fauna of aquatic sediments. Springer-Verlag, Berlin, Germany.

Goertz, D. and Hoch, G. 2008. Vertical transmission and overwintering of microsporidia in the gypsy moth, *Lymantria dispar*. J. Invertebr. Pathol. 99(1):43–48. doi:10.1016/j.jip.2008.03.008.

Gouy, M., Guindon, S. and Gascuel, O. 2010. SeaView version 4: a multiplatform graphical user interface for sequence alignment and phylogenetic tree building. Mol. Biol. Evol. 27:221–224.

Graczyk, T. K., Majewska, A. C. and Schwab, K. J. 2008. The role of birds in dissemination of human waterborne enteropathogens. Trends. Parasitol. 24:55–59.

Guindon, S. and Gascuel, O. 2003. A simple, fast and accurate algorithm to estimate large phylogenies by maximum likelihood. Syst. Biol., 52:696–704.

Hazard, E. I., Fukuda, T. and Becnel, J. J. 1985. Gametogenesis and plasmogamy in certain species of microspora. J. Invertebr. Pathol. 46:63–69.

Heinz, E., Williams, T. A., Nakjang, S., Noël, C. J., Swan, D. C. et al. 2012. The genome of the obligate intracellular parasite *Trachipleistophora hominis*: new insights into microsporidian genome dynamics and reductive evolution. PLoS Pathog. 8(10):e1002979 doi: 10.1371/journal.ppat.1002979.

Hirt R. P., Logsdon, J. M. Jr., Healy, B., Dorey, M. W., Doolittle, W. F., and Embley, T. M. 1999. Microsporidia are related to Fungi: Evidence from the largest subunit of RNA polymerase II and other proteins. Proc. Natl. Acad. Sci. USA. 96: 580–585.

Hopper, B. E., Meyers, S. P., and Cefalu, R. 1970. Microsporidian infection of a marine nematode *Metoncholaimus scissus*. J. Invertebr. Pathol. 16:371–377.

Hu, P. J. 2007. Dauer. In: WormBook, ed. The C. elegans Research Community, WormBook, doi/10.1895/wormbook.1.144.1, http://www.wormbook.org.

Hurst, L. D. 1991. The incidences and evolution of cytoplasmic male killers. Proc. R. Soc. Lond. Ser. B Biol. Sci. 244:91–99.

Hyde, K. D., Gareth Jones, E. B., Leaño, E., Pointing, S. B. Poonyth, A. D., and Vrijmoed, L. L. P. 1998. Role of fungi in marine ecosystems. Biodivers. Conserv. 7:1147–1161.

Ironside, J. E., Smith, J. E., Hatcher, M. J., Sharpe, R. G., Rollinson, D., and Dunn, A. M. 2003. Two species of feminizing microsporidian parasite coexist in populations of *Gammarus duebeni*. J. Evol. Biol. 16, 467–473.

Izquierdo, F., Castro Hermida, J. A., Fenoy, S., Mezo, M., Gonzalez-Warleta, M. and del Aguila, C. 2011. Detection of microsporidia in drinking water, wastewater and recreational rivers. Water. Res. 45:4837–4843.

James, T. Y., Pelin, A., Bonen, L., Ahrendt, S., Sain, D., Corradi, N., and Stajich, J. E. 2013. Shared signatures of parasitism and phylogenomics unite Cryptomycota and Mucrosporidia. Curr. Biol. 23:1548–1553.

Jamshidi, S., Tabrizi, A. S., Bahrami, M. and Momtaz, H. 2012. Microsporidia in household dogs and cats in Iran; a zoonotic concern. Vet. Parasitol. 185:121–123.

Jahnke, M., Smith, J. E., Dubuffet, A. and Dunn, A. M. 2013. Effects of feminizing microsporidia on the masculinizing function of the androgenic gland in *Gammarus duebeni*. J. Invertebr. Pathol. 112(2):146–151.

Johnston W. L. and Dennis J. W. 2012. The eggshell in the *C. elegans* oocyte-to-embryo transition. Genesis 50:333–349.

Katinka, M. D., Duprat, S., Cornillot, E., Metenier, G., Thomarat, F., et al. 2001. Genome sequence and gene compaction of the eukaryote parasite *Encephalitozoon cuniculi*. Nature. 414:450-453.

Keeling P. J. 2009. Five questions about microsporidia. PLoS Pathog. 5:e1000489 doi:10.1371/journal.ppat.1000489.

Keeling P. J. 2014. Phylogenetic place of microsporidia in the tree of eukaryotes. In: Microsporidia: pathogens of opportunity. Weiss, L.M. and Becnel, J.J. (ed). John Wiley & Sons, Inc., Chichester, UK. doi: 10.1002/9781118395264.ch5

Keeling, P. J. and Fast, N. M. 2002. Microsporidia: biology and evolution of highly reduced intracellular parasites. Annu. Rev. Microbiol. 56:93–116.

Keeling, P. J. and Corradi, N. 2011. Shrink it or loose it: balancing loss of function with shinking genomes in the microsporidia. Virulence 1:67–70.

Kelly, A., Hatcher, M. J., and Dunn, A. M. 2003. The impact of a vertically transmitted microsporidian, *Nosema granulosis* on the fitness of its *Gammarus duebeni* host under stressful environmental conditions. Parasitology. 126:119–124.

Keohane, E. M. and Weiss, L. M. 1998. Characterization and function of the microsporidian polar tube: a review. Folia Parasitol. 45(2):117–127.

Knell, J. D., Allen, G. E. and Hazard, E. I. 1977. Light and electron-microscope study of *Thelohania solenopsae* n.sp. (Microsporida: Protozoa) in red imported fire ant, *Solenopsis invicta*. J. Invertebr. Pathol. 29:192–200.

Kotler, D. P. and Orenstein, J. M. 1998. Clinical syndromes associated with microsporidiosis. Adv. Parasitol. 40:321–349.

Kudo, R., and Hetherington, D.C. 1922. Notes on a microsporidian parasite of a nematode. J. Parasitol. 8:129–132.

Kullman, B., Tamm, H., and Kullman, K. 2005. Fungal Genome Size Database. http://www.zbi.ee/fungal-genomesize/

Lahl, V., Sadler, B., and Schierenberg, E. 2006. Egg development in parthenogenetic nematodes: variations in meiosis and axis formation. Int. J. Dev. Biol. 50:393–398.

Lambshead P.J.D. and Boucher G. 2003. Marine nematode deep-sea biodiversity - hyperdiverse or hype?. J. Biogeogr. 30:475–485.

Lange, C. E., Johny, S., Baker, M. D., Whitman, D. W., and Solter, L. F. 2009. A new *Encephalitozoon* species (Microsporidia) isolated from the lubber grasshopper, *Romalea microptera* (Beauvois) (Orthoptera: Romaleidae). J. Parasitol. 95:976–986.

Larsson, J. I. R., Ebert, D., and Vávra, J. 1997. Ultrastructural study and description of *Ordospora colligata* gen. et sp. nov. (Microspora, Ordosporidae fam. nov.), a new microsporidian parasite of *Daphnia magna* (Crustacea, Cladocera). Eur. J. Protistol. 33:432–443.

Lartillot, N., Lepage, T., and Blanquart ,S. 2009. PhyloBayes 3: a Bayesian software package for phylogenetic reconstruction and molecular dating. Bioinformatics. 25: 2286–2288.

Le Goff, O., Bru-Adan, V., Bacheley, H., Godon, J., and Wery, N. 2010. The microbial signature of aerosols produced during the thermophilic phase of composting. J. Appl. Microbiol. 108:325–340.

Lee, D.L. 2002. The biology of nematodes. CRC Press. Boca Raton, FL

Lee, S., Lee, S., Lyoo, Y. S., and Park, H. 2011. DNA detection and genotypic identification of potentially human-pathogenic microsporidia from asymptomatic pet parrots in South Korea as a risk factor for zoonotic emergence. Appl. Environ. Microbiol. 77:8442–8444.

Loh, R. S., Chan, C. M. L., Ti, S. E., Lim, L., Chan, K. S., and Tan, D. T. H. 2009. Emerging prevalence of microsporidial keratitis in Singapore epidemiology, clinical features, and management. Ophthalmology. 116:2348–2353.

Lorenzen S. 1971. Die Nematodenfauna im Verklappundsgebiet fur Industrieabwasser nordwestlich von Helgoland: I. Araeolaimida und Monhysterida. Zool. Anz. Leipzig. 187:223–248.

Lucy, F. E., Graczyk, T. K., Tamang, L., Miraflor, A., and Minchin, D. 2008. Biomonitoring of surface and coastal water for Cryptosporidium, Giardia, and human-virulent microsporidia using molluscan shellfish. Parasitol. Res. 103:1369–1375.

Magalhaes, N., Lobo, M. L., Antunes, F., and Matos, O. 2006. Birds and dogs as potencial sources of zoonotic infections by microsporidia. Rev. Port. Ciênc. Vet. 101:69–75.

Maggenti, A. 1981. Nematode intergument. In: General nematology. Springer-Verlag New York, Inc.

Mathis, A., Weber, R., and Deplazes, P. 2005. Zoonotic potential of the microsporidia. Clin. Microbiol. Rev. 18:423–445.

Meissner, E. G., Bennett, J. E., Qvarnstrom, Y., da Silva, A., Chu, E. Y., Tsokos, M., and Gea-Banacloche, J. 2012. Disseminated microsporidiosis in an immunosuppressed patient. Emerg. Infect. Dis., 18:1155–1158.

Microsporidian Comparative Database. 2010. Broad Institute. http://www.broadinstitute.org/annotation/genome/microsporidia_comparative/MultiHome.html

Morris, D. J. and Freeman, M. A. 2010. Hyperparasitism has wide-ranging implications for studies on the invertebrate phase of myxosporean (Myxozoa) life cycles. Int. J. Parasitol. 40:357–359.

Mota, P., Rauch, C., and Edberg, S. C. 2000. Microsporidia and Cyclospora: epidemiology and assessment of risk from the environment. Crit. Rev. Microbiol. 26:69–90.

Murray, W. & Weiss, L. M. 1999. The microsporidia and microsporidiosis. AMS Press, Washington, DC.

Nakjang, S., Williams, T., Heinz, E., Watson, A., Foster, P., Sendra, K., et al. 2013. Reduction and expansion in microsporidian genome evolution: new insights from comparative genomics. Genome Biol. Evol. 5(12): 2285. doi:10.1093/gbe/evt184.
Nägeli KW, 1857. Uber die neue Krankheit der Seidenraupe und verwandte Organismen. Bot. Z. 15:760–761.

Nicholas, W. L. 1984. The biology of free-living marine nematodes (2end edition). Claredon Press, Oxford.

Platt, H. M, and Warwick, R. M. 1988. Part II: British chromadorids. In: Brill EJ, Backuys W, editors. (ed), Free living marine nematodes. The Linnean Society of London and The Estuarine and Brackish-Water Science Association, Avon, Great Britain. p. 58–59.

Peyretaillade, E., Parisot, N., Polonais, V., Terrat, S., Denonfoux, J., *et al.* 2012. Annotation of microsporidian genomes using transcriptional signals. Nat. Commun. 3: 1137 doi: 10.1038/ncomms2156.

Poinar, G. O. and Hess, R. 1986. *Microsporidium rhabdophilum* sp. n. (Microsporida: Pansporoblastina), a parasite of the nematode, *Rhabditis myriophila* (Rhabditina: Rhabditidae). Rev. Nematol. 9:369–375.

Poinar, G. O. 1988. A microsporidian parasite of *Neoplectana glaseri* (Steinernematidae: Rhabditida). Rev. Nematol. 11:359–361.

Pombert, J.F., Selman, M., Burki, F., Bardell, F.T., Farinelli, L., et al. 2012. Gain and loss of multiple functionally related, horizontally transferred genes in the reduced genomes of two microsporidian parasites. Proc. Natl. Acad. Sci. USA. 109:12638–12643.

Pombert, J.F., Haag, K. L., Beidas, S., Ebert, D., and Keeling, P. J. 2015. The *Ordospora colligata* genome: evolution of extreme reduction in microsporidia and host-to-parasite horizontal gene transfer. mBio 6(1):e02400-14. doi:10.1128/mBio.02400-14.

Refardt, D., Canning, E. U., Mathis, A., Cheney, S.A., Lafranchi-Tristem, N.J., and Ebert. D. 2002. Small subunit ribosomal DNA phylogeny of microsporidia that infect *Daphnia* (Crustacea: Cladocera). Parasitology. 124:381–389.

Rodgers-Gray, T.P., Smith, J.E., Ashcroft, A.E., Isaac, R.E., and Dunn, A.M. 2004. Mechanisms of parasite-induced sex reversal in *Gammarus duebeni*. Int J Parasitol 34: 747–753.

Rönnebäumer, K., Gross, U., and Bohne, W. 2008. The nascent parasitophorous vacuole membrane of *Encephalitozoon cuniculi* is formed by host cell lipids and contains pores which allow nutrient uptake. Eukaryot. Cell. 7:1001–1008.

Ronquist, F., Teslenko, M., van der Mark, P., Ayres, D., Darling, A., Höhna, et al. 2011. MrBayes 3.2: efficient Bayesian phylogenetic inference and model choice across a large model space. Syst. Biol., 61:539–542.

Sánchez, R., Serra, F., Tárraga, J., Medina, I., Carbonell, et al. 2011. Phylemon 2.0: a suite of web-tools for molecular evolution, phylogenetics, phylogenomics and hypotheses testing. Nucleic Acids Res., 39:W470–W474.

Rodgers-Gray, T. P., Smith, J. E., Ashcroft, A. E., Isaac, R. E., and Dunn, A. M. 2004 Mechanisms of parasite-induced sex reversal in *Gammarus duebeni*. Int. J. Parasitol. 34, 747–753.

Sak, B., Kasickova, D., Kvac, M., Kvetonova, D. and Ditrich, O. 2010. Microsporidia in exotic birds: intermittent spore excretion of *Encephalitozoon* spp. in naturally infected budgerigars (*Melopsittacus undulatus*). Vet. Parasitol. 168:196–200.

Sapir, A., Dillman, A. R., Connon, S. A., Grupe, B. M., Ingels, J., Mundo-Ocampo, M., et al. 2014. Microsporidia-nematode associations in methane seeps reveal basal fungal parasitism in the deep sea. Front. in Microbiol. 5:43. doi:10.3389/fmicb.2014.00043.

Scanlon, M., Leitch, G. J., Visvesvara, G. S., and Shaw, A. P. 2004. Relationship between the host cell mitochondria and the parasitophorous vacuole in cells infected with *Encephalitozoon* microsporidia. J. Eukaryot. Microbiol. 51:81–87.

Sharma, S., Das, S., Joseph, J., Vemuganti, G. K. & Murthy, S. 2011. Microsporidial keratitis: need for increased awareness. Surv. Ophthalmol. 56:1–22.

Schottelius J, Schmetz, C., Kock, N. P., Schüler, T., Sobottka, I., and Fleischer, B. 2000. Presentation by scanning electron microscopy of the life cycle of microsporidia of the genus *Encephalitozoon*. Microb. Infect. 2:1401–1406.

Slamovits, C. H., Williams, B. A. P. & Keeling, P. J. 2004. Transfer of *Nosema locustae* (Microsporidia) to *Antonospora locustae* n. comb. based on molecular and ultrastructural data. J. Eukaryot. Microbiol., 51:207–213.

Stamatakis, A. 2014. RAxML version 8: A tool for phylogenetic analysis and post-analysis of large phylogenies. 30(9):1312-1313. doi: 10.1093/bioinformatics/btu033.

Soanes, D. M., Alam, I., Cornell, M., Wong, H. M., Hedeler, C. et al. 2008. Comparative genome analysis of filamentous fungi reveals gene family expansions associated with fungal pathogenesis. PLoS ONE. 3(6): e2300. doi: 10.1371/journal.pone.0002300.

Sokolova, Y. Y., Lange, C. E., Mariottini, Y., and Fuxa, J. R. 2009. Morphology and taxonomy of the microsporidium *Liebermannia covasacrae* n. sp. from the grasshopper *Covasacris pallidinota* (Orthoptera, Acrididae). J. Invertebr. Pathol. 101:34–42.

Sokolova ,Y.Y., Sokolov, I.M., and Carlton, C.E. 2010. New microsporidia parasitizing bark-lice (Insecta: Psocoptera). J. Invertebr. Pathol. 104:186–194.

Stanke, M., Diekhans, M., Baertsch, R., and Haussler, D. 2008. Using native and syntenically mapped cDNA alignments to improve de novo gene finding. Bioinformatics. 24:637–644. doi: 10.1093/bioinformatics/btn013. http://bioinf.uni-greifswald.de/augustus/

Stentiford, G.D., Feist, S.W., Stone, D.M., Bateman, K.S., and Dunn, A.M. 2013. Microsporidia: doverse, dynamic, and emergent pathogens in aquatic systems. Trends Parasitol. 29(11):567–578.

Stine, S. W., Vladich, F. D., Pepper, I. L. and Gerba, C. P. 2005. Development of a method for the concentration and recovery of microsporidia from tap water. J. Environ. Sci. Health A. Toxi. Hazard. Subst. Environ. Eng. 40:913–925.

Terry, R. S., Smith, J. E., Sharpe, R. G., Rigaud, T., Littlewood, D. T. J., et al. 2004. Widespread vertical transmission and associated host sex–ratio distortion within the eukaryotic phylum Microspora. Proc. R. Soc. Lond. B. 27:1783-1789. doi: 10.1098/rspb.2004.2793.

Troemel, E. R., Felix, M. A, Whiteman, N. K., Barriere, A., and Ausubel, F. M. 2008. Microsporidia are natural intracellular parasites of the nematode *Caenorhabditis elegans*. PLoS Biol. 6:2736–2752 doi: 10.1371/journal.pbio.0060309.

Vávra, J. and Undeen, A. H. 1970. Nosema Algerae N. Sp. (Cnidospora, Microsporida) a pathogen in a laboratory colony of *Anopheles stephensi* Liston (Diptera, Culicidae). J. Protozool. 17:240–249.

Vávra, J. and Larsson, J. I. R. 1999. Structure of the microsporidia. In: Wittner, M. & Weiss, L. M. (ed.), The microsporidia and microsporidiosis. AMS Press, Washington, DC. p. 7–84.

Vávra, J. and Lukeš, L. 2013. Microsporidia and 'The Art of Living Together', In: Advances in Parasitology. D. Rollinson. (ed.). Academic Press. 82: 253–319, doi: 10.1016/B978-0-12-407706-5.00004-6.

Veremchuk, G. V. and Issi, I. V. 1970. The development of microsporidians of insects in the entomopathogenic nematode *Neoaplectana agriotos* (Nematoda: Steinernematidae) Parazitologiya. 4:3–7.

Vizoso, D. B. and Ebert, D. 2005. Phenotypic plasticity of host-parasite interactions in response to the route of infection. J. Evol. Biol. 28:911–921. doi:10.1111/j.1420-9101.2005.00920.x.

Vizoso, D. B., Lass, S., and Ebert, D. 2005. Different mechanisms of transmission of the microsporidium *Octosporea bayeri*: A cocktail of solutions for the problem of parasite permanence. Parasitology. 130:501–509.

Visvesvara, G. S., Belloso, M., Moura, H., Da Silva, A. J., Moura, I. N. S. et al. 1999. Isolation of Nosema algerae from the cornea of an immunocompetent patient. J. Eukaryot. Microbiol. 46:10S.

Vossbrinck, C. R., Baker, M. D., Didier, E. S., Debrunner-Vossbrinck, B. A, Shadduck, J. A. 1993. Ribosomal DNA sequences of *Encephalitozoon hellem* and *Encephalitozoon cuniculi*: species identification and phylogenetic construction. J. Eukaryot. Microbiol. 40:354–362.

Vossbrinck, C. R. and Debrunner-Vossbrinck, B. A. 2005. Molecular phylogeny of the Microsporidia: ecological, ultrastructural and taxonomic considerations. Folia. Parasitol. 52:131–142.

Vossbrinck, C. R., Baker, M. D., and Andreadis, T. G. 2010. Phylogenetic position of Octosporea muscaedomesticae (Microsporidia) and its relationship to *Octosporea bayeri* based on small subunit rDNA analysis. J. Invertebr. Pathol. 105:366–370.

Weber, R., Bryan, R.T., Schwartz, D.A., Owen, R.L. 1994. Human microsporidial infections. Clin. Microbiol. Rev. 7:426–461

Weiss, L. M. and Vossbrinck, C. R. 1998. Microsporidiosis: molecular and diagnostic aspects. Adv. Parasitol. 40:351–395.

Weiss, L. M. and Vossbrinck, C. R. 1999. Molecular biology, molecular phylogeny, and molecular diagnostic approaches to the microsporidia. In: Wittner, M. & Weiss, L. M. (ed.), The microsporidia and microsporidiosis. AMS Press, Washington, DC. p. 129.

Williams, B. A. P., Cali, A., Takvorian, P. M., and Keeling, P. K. 2008. Distinct localization patterns of two putative mitochondrial proteins in the microsporidian *Encephalitozoon cuniculi*. J. Eukaryot. Microbiol. 55(2):131–133.

Wittner, M. and Weiss, L. M. 1999. The microsporidia and microsporidiosis. ASM Press, Washington, DC.

WormAtlas. Altun, Z. F., Herndon, L. A., Croker, C., Lints, R., and Hall, D.F. (ed). 2002–2015. http://www.wormatlas.org

Xu, Y. J. and Weiss, L. M. 2005. The microsporidian polar tube: a highly specialised invasion organelle. Int. J. Parasitol. 35:941–953.

Xu, X., Shen, Z., Zhu, F., Tao, H., Tang, X. & Xu, L. 2012. Phylogenetic characterization of a microsporidium (*Endoreticulatus* sp. Zhenjiang) isolated from the silkworm. *Bombyx mori*. Parasitol. Res. 110:815–819.

Zhang, Z.Q. 2013. Animal Biodiversity: An outline of higher-level classification and survey of taxonomic richness. Zootaxa. 3703:1–82.